Distribution Agreement

In presenting this thesis or dissertation as a partial fulfillment of the requirements for an advanced degree from Emory University, I hereby grant to Emory University and its agents the non-exclusive license to archive, make accessible, and display my thesis or dissertation in whole or in part in all forms of media, now or hereafter known, including display on the world wide web. I understand that I may select some access restrictions as part of the online submission of this thesis or dissertation. I retain all ownership rights to the copyright of the thesis or dissertation. I also retain the right to use in future works (such as articles or books) all or part of this thesis or dissertation.

Signature:

_____ _____

Sara Marie Fielder Date

Meiotic Synapsis: a Novel Role for Dynein Light Chain 1 in Synapsis Regulation and Sex-specific Processes in Meiotic Prophase I

By

Sara Marie Fielder
Doctor of Philosophy

Graduate Division of Biological and Biomedical Science
Genetics and Molecular Biology

_____
William G. Kelly, Ph.D.
Advisor

_____
Roger B. Deal, Ph.D.
Committee Member

_____
David J. Katz, Ph.D.
Committee Member

_____
Stephanie L. Sherman, Ph.D.
Committee Member

_____
Paula M. Vertino, Ph.D.
Committee Member

Accepted:

_____
Lisa A. Tedesco, Ph.D.
Dean of the James T. Laney School of Graduate Studies

_____
Date

Meiotic Synapsis: a Novel Role for Dynein Light Chain 1 in Synapsis Regulation and Sex-specific Processes in Meiotic Prophase I

By

Sara Marie Fielder

B.A., Bryn Mawr College, 2013

Advisor: William G. Kelly, Ph.D.

An abstract of

A dissertation submitted to the Faculty of the

James T. Laney School of Graduate Studies of Emory University

in partial fulfillment of the requirements for the degree of

Doctor of Philosophy

in Genetics and Molecular Biology

2020

Abstract

Meiotic Synapsis: a Novel Role for Dynein Light Chain 1 in Synapsis Regulation and Sex-specific Processes in Meiotic Prophase I

By Sara Marie Fielder

Meiotic synapsis is an essential process of connecting homologous chromosomes and holding them in close proximity for recombination. As *C. elegans* chromosomes search for their homologous partner, one end of each chromosome attaches to nuclear membrane proteins and movements at the periphery are driven by cytoplasmic dynein motors to aid the search. The dynein motor has been proposed to generate tension between homolog pairs that tests the matches and signals for synapsis initiation. The central element of the synaptonemal complex is composed of six synapsis proteins (SYPs 1-6) that form a physical, phase-separated, zipper-like bridge between homologs. Chromosomes that fail to synapse are targeted for enrichment of the heterochromatin mark Histone H3 Lysine 9 dimethylation (H3K9me2).

We have discovered that the dynein light chain 1 (DLC-1) has a potential additional chaperone-like role in aiding SYP protein folding at slightly elevated temperatures. Knockdown of *dlc-1* results in aggregation of SYP proteins, and this phenotype increases in frequency at higher growth temperatures. DLC-1 interacts with SYP-2 through a binding motif, and elimination of the binding motif partially, but not completely, eliminates the interaction. This work adds to the understanding of the roles of DLC-1 in meiosis, and motor-independent roles of the light chain.

Additionally, we have identified several sex-specific differences in meiotic regulation, including a new sex-specific mechanism that senses the initiation of synapsis. If synapsis is unable to initiate, H3K9me2 enrichment in hermaphrodite chromatin is not observed. However, mutants that are able to partially synapse their chromosomes display widespread H3K9me2 enrichment. In contrast, widespread H3K9me2 enrichment is observed in males when synapsis is prevented. This indicates that there may be a hermaphrodite/female-specific checkpoint-like mechanism that stalls meiosis when synapsis does not initiate, and this arrest precedes H3K9me2 targeting. Additionally, whereas hermaphrodite synapsis is temperature-sensitive and will form un-recoverable SYP protein aggregates at temperatures above 26.5°, males still synapse their chromosomes even when raised at 27.8°. Furthermore, the SYP aggregates that occur when DLC-1 is depleted in hermaphrodites are not observed in males. These differences indicate that studying male meiosis could reveal as yet undiscovered mechanisms regulating meiosis.

Meiotic Synapsis: a Novel Role for Dynein Light Chain 1 in Synapsis Regulation and Sex-specific Processes in Meiotic Prophase I

By

Sara Marie Fielder

B.A., Bryn Mawr College, 2013

Advisor: William G. Kelly, Ph.D.

A dissertation submitted to the Faculty of

James T. Laney School of Graduate Studies of Emory University

in partial fulfillment of the requirements for the degree of

Doctor of Philosophy

in Genetics and Molecular Biology

2020

Acknowledgements

I would like to thank my advisor, Bill Kelly, for the wealth of knowledge you always shared, and your amazing ability to come up with an insane amount of alternate experimental starting points. Thank you as well for allowing me the freedom to grow as a scientist and largely control my own direction of study. Thank you to my committee Roger, Paula, Stephanie, and Dave for helpful suggestions on how to focus my experiments. Thank you to my undergraduate advisor Tamara Davis for encouraging my excitement for research. To my current and former lab members, thank you to John Ahn for training me in my rotation, thank you to Quincey Caylor and Tori McKinney Kent for always having my back in helping me make and acquire reagents, and thank you to Christine Doronio for helpful suggestions on protocols and data analysis. I would also like to thank Teresa Lee and Brandon Carpenter in the Katz lab for help with protocols when I was struggling with new experiments. To the members of my cohort, especially Cristina Trevino, Chris Rounds, Stephanie Jones, and Mike Nichols, thank you for the weekly cohort dinners to look forward to as a time to commiserate, support, and good company. Thank you to Cristina Trevino for being my writing buddy late nights at cafes.

I would like to thank my amazing fiancé, Julie Oliver, for always being there for me while I was working weekends, writing in the evenings, and for always being so patient when I was unable to go out, or had to say no to trips because of worms that needed constant attention. I could not have done this without your sweet, kind-hearted support, and I can't wait to begin our lives together. Thank you to my parents who have always encouraged my inquisitive mind, I wouldn't have made it this far without you both as role models of hard work and to never stop asking questions and finding answers.

Table of Contents

CHAPTER 1: INTRODUCTION 1

1.1 Chromosome movement and homolog pairing 2

1.2 Synaptonemal complex axis formation 4

1.3 Central element assembly and synapsis 6

1.4 Meiotic silencing of unsynapsed chromatin 8

1.5 Meiotic checkpoints 9

1.6 Differences in male meiosis 10

1.7 Dynein light chain 11

1.8 Scope of this dissertation 12

1.9 Figures 15

CHAPTER 2: A MOTOR-INDEPENDENT REQUIREMENT FOR DYNEIN LIGHT CHAIN IN *C. ELEGANS* MEIOTIC SYNAPSIS 18

2.1 Abstract 18

2.2 Introduction 19

2.3 Methods 21

2.4 Results 26

2.4.1 Knockout of dynein heavy chain and/or dynactin does not induce SYP foci formation 26

2.4.2 SYP proteins form foci in a temperature sensitive manner with knockdown of DLC-1 27

2.4.3 SYPs form insoluble foci with knockdown of DLC-1 27

2.4.4 SYP-2 interacts with DLC-1 in vivo through a conserved binding motif 28

2.4.5 Mutation of the putative DLC-1 binding site in SYP-2 results in temperature sensitive meiotic defects 30

2.5 Discussion 32

2.6 Acknowledgements 37

2.7 Figures 38

2.8 Tables 51

2.9 Supplemental Material 55

CHAPTER 3: MULTIPLE SEX-SPECIFIC DIFFERENCES EXIST IN THE REGULATION OF SYNAPSIS IN *C. ELEGANS* MEIOSIS 59

3.1 Abstract 59

3.2 Introduction 60

3.3 Methods 65

3.4 Results 68

3.4.1 H3K9me2 targeting to unsynapsed chromosomes differs between sexes ... 68

3.4.2 PCH-2 is not required for adult hermaphrodite- specific prevention of H3K9me2 enrichment with disrupted synapsis 70

3.4.3 Initiation of synapsis is required for H3K9me2 enrichment of unsynapsed chromosomes in adult hermaphrodite meiosis 71

3.4.4 Dynein is not required for males to correctly pair and synapse chromosomes. 72

3.4.5 Male synapsis is not as sensitive to heat as hermaphrodite synapsis 74

3.4.6 Spindle assembly checkpoint proteins in males. 75

3.5 Discussion 76

3.6 Figures 85

3.7 Tables 97

3.8 Supplemental Figures 98

Chapter 4. Discussion and Future Directions 101

4.1 Summary of Dissertation 101

4.2 A screen for components in the synapsis initiation "checkpoint" 103

4.3 Post-translational modification of axial elements and the synapsis initiation failure response 104

4.4 Male *C. elegans* evolution favors less stringent meiosis 105

4.5 Dynein light chain's myriad of functions 107

4.6 Ability of males to complete synapsis without DLC-1 107

4.7 Future directions for study of interactions of DLC-1 with SYP proteins 108

4.8 Future study required into CRL4 and DLC-1 similarities 109

4.9 MPK-1 as a potential player in early meiosis 110

4.10 Future direction of study of SYP-2 in late meiosis 111

4.11 Final Conclusions 111

REFERENCES 113

List of Figures

1.1: *C. elegans* meiotic progression

1.2: Meiotic Synaptonemal Complex

2.1: DLC-1 but not other dynein complex components are required for synapsis

2.2: Synapsis defect in *dlc-1(RNAi)* is temperature sensitive.

2.3: SYP foci formed with DLC-1 reduction or exposure to elevated temperature are resistant to hexanediol.

2.4: DLC-1 and SYP-2 interact in vivo.

2.5: Mutation of the putative DLC-1 binding site in SYP-2 results in meiotic defects in the gonad.

2.6: Mutation of the putative DLC-1 binding site in SYP-2 causes temperature-sensitive embryonic lethality and hallmarks of increased aneuploidy.

2.7: Model of DLC-1's role in pre-synapsis meiosis.

2.S1. Heat induced foci are partially susceptible to 1,6-hexanediol.

2.S2. SYP-2 and SYP-1 co-localize in foci formed under various conditions.

2.S3. Mutation of putative binding site in SYP-2 results in meiotic defects.

2.S4. Anti-GFP IP less efficient in the mutant line.

3.1: Germline sex-specific H3K9me2 enrichment in response to meiotic synapsis defects

3.2: *pch-2* hermaphrodites do not have widespread enrichment of H3K9me2 with absence of synapsis.

3.3: Partial initiation of synapsis is sufficient to trigger widespread H3K9me2 enrichment in hermaphrodite germ cells.

3.4: Dynein depletion dramatically affects adult hermaphrodites, but not male synapsis.

3.5: Pairing rates remain unchanged in *dlc-1(RNAi)* males.

3.6: Synaptonemal complex stability is unaffected by increased temperature in male germ cells.

3.7: MDF-2 localization in early meiosis changes in males.

3.8: Loss of MDF-2 or MDF-1 does not increase rate of synapsis in male germ cells.

3.9: Timing of newly proposed mechanism.

3.S1: Both WT and syp-1 hermaphrodites have widespread enrichment of H3K9me2 in late pachytene, early diplotene

3.S2: H3K9me2 stays low with depletion of HTP-3 with occasional exceptions in hermaphrodites

List of Tables

2.1: sgRNA sequences used for transgenic strain construction

2.2: Repair templates used for transgenic strain construction

2.3: Primers used to amplify regions of genes from genomic DNA to insert into L4440.

2.4: Less FLAG::DLC-1 pulls down with SYP-2::GFP(AMTA) than WT SYP-2::GFP

3.1 *zim-2* has over ten times as high total amount of H3K9me2 in each nucleus as in a synapsis mutant

CHAPTER 1: INTRODUCTION

Meiosis is a complex and highly regulated process of sexual reproduction, requiring precise timing and the coordinated activities of many players to ensure proper inheritance of genetic information by subsequent generations. *Caenorhabditis elegans*, a small nematode, is an excellent model system for studying meiosis, as they are transparent at all stages and continually undergo meiosis during adulthood. Gonads contain a germline stem cell pool at the distal end that mitotically divide and nuclei advance proximally as they enter and progress through meiosis (reviewed in (LUI AND COLAIACOVO 2013)). In this way, each meiotic stage is visible sequentially in the *C. elegans* gonad, allowing a snapshot of each stage at any point in time (Fig. 1.1). Meiotic prophase I has two key initial steps that set the stage for distributing genetic material to the next generation: leptotene and zygotene, in which homologous chromosome pairing and meiotic synapsis occurs; followed by pachytene, in which recombination occurs. The central element (CE) of the synaptonemal complex (SC; described below) keeps homologs in close proximity to aid in recombination. Additionally, the SC plays a role in the timing of steps in recombination (NADARAJAN *et al.* 2017; SATO-CARLTON *et al.* 2018). In *C. elegans*, synapsis is decoupled from double strand break initiation, which is not the case in most organisms (DERNBURG *et al.* 1998).

This Introduction will mainly focus on early meiotic processes including leptotene and zygotene, which in *C. elegans* results in a clustered chromosome configuration that is collectively termed the Transition Zone (TZ)(Fig. 1.1). I will also focus on early steps in pachytene.

1.1 Chromosome movement and homolog pairing

In *C. elegans*, four Zinc finger In Meiosis (ZIM) proteins bind to specific, unique DNA sequences enriched on one end of each chromosome, called pairing centers (PC) (McKim *et al.* 1988; Phillips and Dernburg 2006; Phillips *et al.* 2009). These proteins are essential for the pairing of homologous chromosomes, and each ZIM protein drives the pairing of one or two specific chromosome sets. For example, ZIM-2 binds to chromosome V, and HIM-8 binds to the X chromosome (Phillips *et al.* 2005; Phillips and Dernburg 2006). Two sets of two chromosomes share a ZIM protein for pairing; for example, ZIM-1 binds to chromosomes II and III, indicating that there is a secondary mechanism for correct homologous chromosome identification (Phillips and Dernburg 2006). The chromo-domain protein MRG-1 appears to aid in alignment of homologs in non-PC areas of chromosomes, and absence of this protein results in mispairing and non-disjunction that is usually caught and eliminated by meiotic checkpoints (Dombecki *et al.* 2011; Mei *et al.* 2015).

After ZIM proteins bind to the appropriate chromosome end, this end localizes to the nuclear envelope near the inner nuclear membrane protein, SUN-1 (Sato *et al.* 2009). ZIM proteins are phosphorylated by CHK-2, which allows recruitment and phosphorylation by PLK-2: without these phosphorylations, full synapsis is delayed and pairing is defective (Harper *et al.* 2011; Kim *et al.* 2015). ZIM proteins are still able to localize to the nuclear envelope without SUN-1, indicating that they must interact with another nuclear envelope component for their localization to the periphery (Sato *et al.* 2009). SUN-1 is phosphorylated first by CHK-2, and then phosphorylated again by PLK-2, both of which are required for proper, efficient pairing (MacQueen and Villeneuve

2001; HARPER *et al.* 2011; LABELLA *et al.* 2011; MACHOVINA *et al.* 2016). After phosphorylation, SUN-1 proteins then come together to form patches around the nuclear envelope, close to the ZIM-bound chromosome ends (Fig. 1.2A) (PENKNER *et al.* 2007; PENKNER *et al.* 2009; SATO *et al.* 2009). ZIM protein localization to the nuclear envelope is required for SUN-1 phosphorylation at Serine 12 (S12) by PLK-2, SUN-1/ZYG-12 patch formation, and for clustered chromosome configuration seen in the transition zone (TZ) (PENKNER *et al.* 2009; HARPER *et al.* 2011; LABELLA *et al.* 2011). SUN-1 can still form patches without phosphorylation, but these patches are much smaller than normal and the TZ is lengthened (WOGLAR *et al.* 2013). SUN-1 connects to ZYG-12 between the two nuclear membranes, and then ZYG-12 attaches to the dynein motor complex in the cytoplasm (Fig. 1.2A) (MALONE *et al.* 2003; MINN *et al.* 2009). Dynein motor driven movements aid the search for homologous pairing partners (SATO *et al.* 2009; WYNNE *et al.* 2012). Without the dynein motor, movements decrease greatly, pairing does not always complete, and the central element is unable to assemble onto chromosomes (SATO *et al.* 2009; WYNNE *et al.* 2012). However, 60% of nuclei are able to correctly pair chromosome V correctly, indicating the ZIM-mediated pairing system is fairly robust even without dynein driven movements (SATO *et al.* 2009). Dephosphorylation of S12 of SUN-1 is required for nuclei to disperse from the clustered TZ conformation (PENKNER *et al.* 2009). If no recombination intermediates form, CHK-2 and PLK-2 will remain at PCs, and will continue to phosphorylate ZIM proteins and SUN-1, keeping nuclei in the TZ conformation (KIM *et al.* 2015)

Interestingly, while HIM-8 associates with SUN-1 patches in males, these patches are not phosphorylated at S12 even though they recruit PLK-2 (WOGLAR *et al.*

2013). Constitutive phosphorylation (i.e. S12E) results in a minor triggering of the synapsis checkpoint, as evidenced in a short delay in meiotic progression, but not nearly to the extent that an unsynapsed autosome would cause (WOGLAR *et al.* 2013). Male *C. elegans* only have one X chromosome that will remain unpaired and unsynapsed throughout prophase I. This would normally set off meiotic checkpoints in hermaphrodites, so the absence of SUN-1 phosphorylation at the HIM-8 of males implies that this helps shield the lone X from checkpoint machinery (WOGLAR *et al.* 2013).

1.2 Synaptonemal complex axis formation

The axis of the synaptonemal complex (SC) is composed of four HORMA domain containing proteins (HTP-1, HTP-2, HTP-3, and HIM-3) that assemble onto sister-chromatid cohesin complex, and is required for the central elements of the SC to assemble between and synapse homologous chromosomes (ZETKA *et al.* 1999; COUTEAU *et al.* 2004; COUTEAU AND ZETKA 2005; MARTINEZ-PEREZ AND VILLENEUVE 2005; GOODYER *et al.* 2008). HTP-3 is the first axis protein to load onto DNA-associated cohesins, and stabilizes the sister chromatid cohesin complex on chromosomes throughout meiosis (GOODYER *et al.* 2008; SEVERSON *et al.* 2009; KIM *et al.* 2014; KOHLER *et al.* 2017). HTP-1 and HTP-2 have high sequence similarity, and are partially redundant. The absence of HTP-1 leads to an increase in non-homologous synapsis, and a delay in pairing at the pairing center (COUTEAU AND ZETKA 2005; MARTINEZ-PEREZ AND VILLENEUVE 2005). Knockdown of HTP-2 in *htp-1* mutants further reduces pairing at the pairing centers at later stages in meiosis, yet initially has a higher pairing rate than even WT, and this is not observed in *htp-1* single mutants (COUTEAU AND ZETKA 2005).

The axial elements HTP-1, HTP-2, and HIM-3 all have a “closure motif” at their C-terminus; as in other HORMA proteins, these undergo conformational changes upon binding of heterodimers (LUO *et al.* 2002; SIRONI *et al.* 2002). HTP-3 has six of these closure motifs in the C-terminal half of the protein. The HORMA domain of HIM-3 interacts with four of the HTP-3 closure motifs, and mutation of all four domains abolishes HIM-3 localization to chromosome axes. HTP-1/2 HORMA domains bind to the other two closure motifs in HTP-3, as well as to the closure motif at the C-terminal of HIM-3, increasing the robustness of axis formation (see Fig. 1.2B for a schematic) (KIM *et al.* 2014).

Homolog pairing has been reported to occur after loading of HIM-3 onto the axis, however, this study might have been incomplete. In *syp-1* mutants, that completely lack synapsis, homologs still pair correctly at the pairing center, but the opposite end of each chromosome remain unaligned (MACQUEEN *et al.* 2002). In another study using a *him-3* mutant, one end of each chromosome was examined, and it was reported that pairing did not occur for autosomes but the X chromosomes looked to be paired (COUTEAU *et al.* 2004). However, they used a DNA probe on the pairing center end of the X chromosome, and probe(s) targeting the non-pairing center end of the other chromosomes, which would only assess if the autosome homologs failed to completely align. Therefore, it is possible that pairing could occur before HIM-3 loads onto chromosome axes, or that pairing is independent of axis formation. It is possible that the X chromosome is an exception, and indeed the X chromosome has unique characteristics during meiosis. For example, its pairing protein HIM-8 remains associated with the X’s throughout much of meiosis, whereas the autosomal ZIM fall off

in early pachytene, and the X is the last chromosome to both replicate and synapse (PHILLIPS *et al.* 2005; PHILLIPS AND DERNBURG 2006; MLYNARCZYK-EVANS AND VILLENEUVE 2017). Another study focusing on HTP-3 also only examined one end of each chromosome, but in this case the X pairing centers were not aligned, indicating that pairing requires HTP-3, and further implying that the X chromosome is not an exception to pairing before the AE (axial element) assembles (GOODYER *et al.* 2008). If the X chromosome does pair in the same conditions as the other chromosomes, then this could indicate that HTP-3 loads onto chromosomes either before or as pairing begins, and then HIM-3 loads onto the axial element. HTP-3 is required to stabilize sister chromatid cohesin, thus it would make sense that it needs to load onto chromosomes before the axial element of the synaptonemal complex (SEVERSON *et al.* 2009).

1.3 Central element assembly and synapsis

Before central element assembly is allowed, SYP proteins will still self-assemble into small presumably dynamic “polycomplexes” that resemble the ladder-like structure of the Central Element (CE) in the synaptonemal complex, but less organized and unassociated with the chromosomes (MACQUEEN *et al.* 2002; ROG *et al.* 2017). If CE assembly is unable to occur, such as if the Axial Element (AE) cannot or does not form, these polycomplexes will grow, stabilize throughout the rest of prophase I, and meiosis is arrested (COUTEAU *et al.* 2004; GOODYER *et al.* 2008).

Synapsis initiation is closely monitored, with apparent delays incorporated to ensure enough time for pairing to properly complete, such as by the spindle assembly complex located at the nuclear envelope and inhibition of synapsis progression by the pachytene checkpoint factor PCH-2 (DESHONG *et al.* 2014; BOHR *et al.* 2015). Absence

of the spindle assembly checkpoint complex (SAC), composed of the proteins MDF-1, MDF-2, BUB-3, and BUB-1, at the nuclear envelope results in faster synapsis than normal, although without an obvious increase in mis-pairing events. Time course analyses have confirmed that initiation takes much longer than synapsis itself, as once SYP assembly begins, it proceeds quickly from the pairing centers down the lengths of the homologs (ROG AND DERNBURG 2015).

After chromosomes have been determined to be paired correctly, SYP proteins assemble between homologs. CE element assembly onto chromosomes can still occur without proper pairing, such as in mutants lacking all ZIM proteins or in SUN-1 missense mutants, but it is usually non-homologous and/or fold-back synapsis that proceeds much slower than normal synapsis (PENKNER *et al.* 2007; HARPER *et al.* 2011; ROG AND DERNBURG 2015). Six SYP proteins have been identified thus far (SYP-1,-2,-3,-4,-5,-6), two of which (SYP-5 and SYP-6) appear to have redundant functions (Fig. 1.2C)(MACQUEEN *et al.* 2002; COLAIACOVO *et al.* 2003; SMOLIKOV *et al.* 2007; SMOLIKOV *et al.* 2009; SCHILD-PRUFERT *et al.* 2011; HURLOCK *et al.* 2020). CE proteins of the synaptonemal complex do not have a high amount of sequence conservation, yet the ladder/zipper-like structure with approximately 100nm distance between homologs is conserved (PAGE AND HAWLEY 2001; MACQUEEN *et al.* 2002). These proteins appear to phase separate when loading onto chromosomes into a “liquid crystal”, which can be disrupted with addition of an amphiphilic solvent (ROG *et al.* 2017). SYP-1 spans across the middle of the CE, and its N terminus forms a homodimer with the N-terminus of other SYP-1 proteins across the length (Fig. 1.2C)(SCHILD-PRUFERT *et al.* 2011). SYP-1 is N-terminally acetylated in early meiosis by the NatB complex, and this modification

appears to facilitate this head to head homodimerization of SYP-1 between homologs (GAO *et al.* 2016). Even though the CE essentially "glues" homologs together, it is not a solid, static structure. SYP proteins diffuse along the SC during meiosis, as demonstrated by FRAP experiments (ROG *et al.* 2017).

Once homologs have been synapsed, PLK-2 spreads from the pairing center down the length of the CE, and phosphorylates SYP-4 as double stranded breaks begin to form (LABELLA *et al.* 2011; NADARAJAN *et al.* 2017; PATTABIRAMAN *et al.* 2017). When SYP-4 is mutated so that it is unable to be phosphorylated by PLK-2, RAD-51 foci (an indicator of double stranded breaks made for recombination (TAKANAMI *et al.* 1998; ALPI *et al.* 2003)), increase, indicating that either double stranded breaks occur for an extended period of time, or that double stranded breaks are not being repaired (NADARAJAN *et al.* 2017). After SYP-4 phosphorylation, the mobility of SYP proteins within the SC is reduced but not completely abolished (NADARAJAN *et al.* 2017). Additionally, SYP-1 is phosphorylated at several residues on the C-terminus in the TZ, and phosphorylation at T452 is required for PLK-2 to leave the PC and distribute along the SC. In mutants unable to phosphorylate these residues, pairing still occurs normally, but meiotic progression is delayed in the TZ and during early pachytene, allowing more than normal RAD-51 foci to occur, and ultimately results in reduced fertility and a High Incidence of Males (Him) phenotype (SATO-CARLTON *et al.* 2018).

1.4 Meiotic silencing of unsynapsed chromatin

Chromosomes that do not get synapsed, such as the lone male X chromosome, are targeted for Histone H3 Lysine 9 dimethylation (H3K9me2)(BEAN *et al.* 2004). This is a phenomenon that also occurs in mammals, and is called meiotic silencing of

unsynapsed chromosomes (MSUC) (reviewed in (TURNER 2007)). A ChIP-chip study investigating the increase of H3K9me2 on both X chromosomes in *him*-8 mutants, in which X chromosomes do not synapse, showed that there was little if any *de novo* H3K9me2 accumulation, but rather the enrichment was largely in regions where it normally occurs in WT animals (GUO *et al.* 2015). It is thus not clear that the enrichment is increased "silencing" per se. This mechanism has been proposed to potentially shield the lone male X from checkpoint machinery (described below)(CHECCHI AND ENGEBRECHT 2011). However, this study was conducted in *fem-3* sex-determination mutants, which undergo oogenesis despite having one X-chromosome. As my work has illuminated, males can have very different mechanisms in meiosis (described below), so there is a possibility that H3K9me2 only shields the unsynapsed X in oogenesis and this is not its function in males.

1.5 Meiotic checkpoints

To ensure that all chromosomes synapse, there is a checkpoint in pachytene that monitors whether synapsis occurs and is completed. In this checkpoint, PCH-2 senses any chromosomes with unsynapsed pairing centers and activates apoptosis to prevent the resulting aneuploidy that would occur in progeny (BHALLA AND DERNBURG 2005). *syp-1* and *syp-2* mutants will activate this pachytene checkpoint, but *syp-3* mutants will not, indicating that SYP-3 is required for this checkpoint (BOHR *et al.* 2016). Additionally, axis components HTP-1, HTP-3, and HIM-3 are required to activate the synapsis checkpoint (BOHR *et al.* 2016). Additionally, the two histone methyltransferases for histone H3 Lysine 36, MET-1 and MES-4, are required to activate the pachytene checkpoint when a chromosomal duplication with a PC is present (DESHONG *et al.* 2014). PCH-2 is

located along the SC in pachytene, until the recombination factor COSA-1 binds to recombination sites, and its presence slows recombination rates (DESHONG *et al.* 2014). PCH-2 is not always required to activate the synapsis checkpoint: *syp-4* mutants will activate apoptosis through components of the spindle assembly complex instead of using PCH-2 (BOHR *et al.* 2016).

The other main early meiotic checkpoint is the DNA damage checkpoint. In response to DNA damage or unrepaired recombination intermediates, the 9-1-1 complex (containing RAD-9, RAD-1, and HUS-1) signals to activate the apoptotic program in hermaphrodites (VOLKMER AND KARNITZ 1999; GARTNER *et al.* 2000; HOFMANN *et al.* 2002). This activation of this checkpoint is detected by phosphorylation of CHK-1(JARAMILLO-LAMBERT *et al.* 2010)(and reviewed in (NOJIMA 2006)). This checkpoint ensures that if there are excessive double stranded breaks, or DNA damage through other means that cannot be repaired, a broken genome is not transmitted into gametes and hence into the next generation.

1.6 Differences in male meiosis

Even though the initial goal of meiotic prophase I is the same in both males and hermaphrodites, there are surprising differences between the two sexes. For example, male *C. elegans* complete meiotic prophase 2.5-3 times faster than hermaphrodites (JARAMILLO-LAMBERT *et al.* 2007). Additionally, while hermaphrodites undergo programmed cell death during oogenesis normally and in response to activated checkpoints, males do not (GUMIENNY *et al.* 1999; GARTNER *et al.* 2000). Males still delay meiotic progression in response to meiotic checkpoints, but instead attempt to repair the damage instead of engaging apoptosis (JARAMILLO-LAMBERT *et al.* 2010).

Recombination begins earlier in males than in hermaphrodites, as males display recombination intermediates at an earlier stage (in the transition zone) than their hermaphrodite/female counter parts (early to mid pachytene)(JARAMILLO-LAMBERT AND ENGEBRECHT 2010). Additionally, whereas the loss of the meiotic cohesion complex component REC-8 in males results in a great reduction in fertility, its loss in hermaphrodites causes only a minor effect on fertility (SEVERSON *et al.* 2009).

Sex differences in early meiosis are seen in other organisms besides *C. elegans*. For example, in *Drosophila*, females undergo meiotic synapsis and recombination, while males do not undergo either process (MORGAN 1914). Similar to *C. elegans, Drosophila* males also complete meiosis faster than females (5 days in males as compared to 12 days in females)(GYURICZA *et al.* 2016). Additionally, in mammals, it appears that females have less stringent checkpoints and responses to checkpoints than males do. For example, male mice with axis protein mutants (HORMAD1) undergo meiotic arrest at pachytene and undergo apoptosis, while female mice still produce oocytes, albeit ones with increased aneuploidy (KURAHASHI *et al.* 2012).

1.7 Dynein light chain

Dynein light chain is a small subunit of the dynein motor complex that moves cellular cargo along microtubules in the cytoplasm. However, dynein light chain interacts with many proteins outside of the function of the dynein motor complex (reviewed in (RAPALI *et al.* 2011)). It has been shown to aid in dimer interactions, yet is also hypothesized to interfere with and/or regulate protein interactions. In fact, even in its canonical interaction with dynein intermediate chain, the light chain influences structure by aiding in folding and increasing α-helical content of the intermediate chain (MAKOKHA

et al. 2002; NYARKO *et al.* 2004). The light chain can bind to two different motifs (($K_{-3}X_{-2}T_{-1}Q_0T_1X_2$) and ($X_{-3}G_{-2}I/V_{-1}Q_0V_1D_2$)), but has been shown to bind proteins without either one of these motifs (RODRIGUEZ-CRESPO *et al.* 2001; WANG *et al.* 2016).

Dynein light chain 1 (DLC-1) has been previously shown to play multiple roles in *C. elegans* meiosis. FBF-2, a translation inhibitor of meiotic mRNAs, needs to bind to DLC-1 to localize to P-granules and to maintain the germline stem cell pool (WANG *et al.* 2016). Next, DLC-1 binds to GLD-1 and this binding also helps to suppress translation of germline stem cell genes (ELLENBECKER *et al.* 2019). The methyltransferase METT-10 that is needed to inhibit germline stem cell proliferation also requires binding to DLC-1 to localize to the nucleus and to function correctly (DORSETT AND SCHEDL 2009). After meiosis has begun, as discussed above, DLC-1 aids the dynein motor complex in moving chromosomes along the nuclear envelope to help find their homologs for meiotic synapsis (SATO *et al.* 2009).

1.8 Scope of this dissertation

In chapter two, this dissertation identifies an additional role for a component of the dynein motor complex in meiosis apart from aiding movement of chromosomes during pairing. Depletion of the dynein light chain (DLC-1) in dynein heavy chain (DHC-1) mutants has been reported to result in aggregates of SYP proteins away from chromosomes; however, *dhc-1* mutants still synapse chromosomes, and depletion of DLC-1 alone results in these aggregates in a temperature-dependent manner (Chapter 2)(SATO *et al.* 2009). These aggregates do not behave like polycomplexes observed in axial element mutants, as they do not dissolve with addition of amphiphilic solvent (Chapter 2). This is characteristic of heat induced SYP protein aggregates, which are

hypothesized to result from misfolding of the SYP proteins (ROG *et al.* 2017). Additionally, DLC-1 interacts with SYP-2 at elevated temperatures *in vivo* through a conserved binding motif, although interaction is not completely abolished with mutation of two residues in this motif (Chapter 2). This indicates that DLC-1 could be acting as a protein chaperone to aid in folding of SYP proteins before they assemble between homologs.

In chapter three, this dissertation examines differences in early meiotic prophase I between *C. elegans* hermaphrodites and males, and identifies a mechanism for sensing initiation of synapsis in hermaphrodites that does not exist in males. Adult hermaphrodite meiosis is sensitive to temperatures above 26.5°, and will form aggregates of SYP proteins that do not interact in the same way as polycomplexes formed in the absence of the synaptonemal complex axis, but male SYP proteins do not show this temperature sensitivity (Chapter 3) (BILGIR *et al.* 2013; ROG *et al.* 2017). Additionally, *dlc-1(RNAi)* males do not form SYP aggregates like their *dlc-1(RNAi)* hermaphrodite counterparts, and instead display apparently normal SC between chromosomes (Chapter 3). Chromosomes that remain unsynapsed are targeted for enrichment of the heterochromatin mark Histone H3 Lysine 9 dimethylation (H3K9me2), but if no synapsis occurs, hermaphrodites do not display enrichment of this heterochromatin mark (BEAN *et al.* 2004). This absence implies there is a mechanism that senses that synapsis has not initiated, and will stall meiosis before the methyltransferase adds heterochromatin marks to unsynapsed chromosomes. On the other hand, male *syp* mutants do display widespread enrichment of the heterochromatin mark, indicating this newly described mechanism is sex-specific (Chapter 3).

These studies 1) add to the growing data that show that dynein light chain function is not limited to its canonical role in dynein motors, 2) identify a novel role for DLC-1 in regulating meiotic synapsis in a temperature dependent manner, suggesting this role may be related to chaperone-like functions, and 3) identify significant differences in male and hermaphrodite meiotic regulation that are likely the evolved consequence of the XO sex chromosome situation in males. The absence of an X homolog in XO male meiosis, which could trigger monitoring checkpoints, requires the modification or absence of such checkpoints in males and these studies are the first to identify one such process in *C. elegans* males.

1.9 Figures

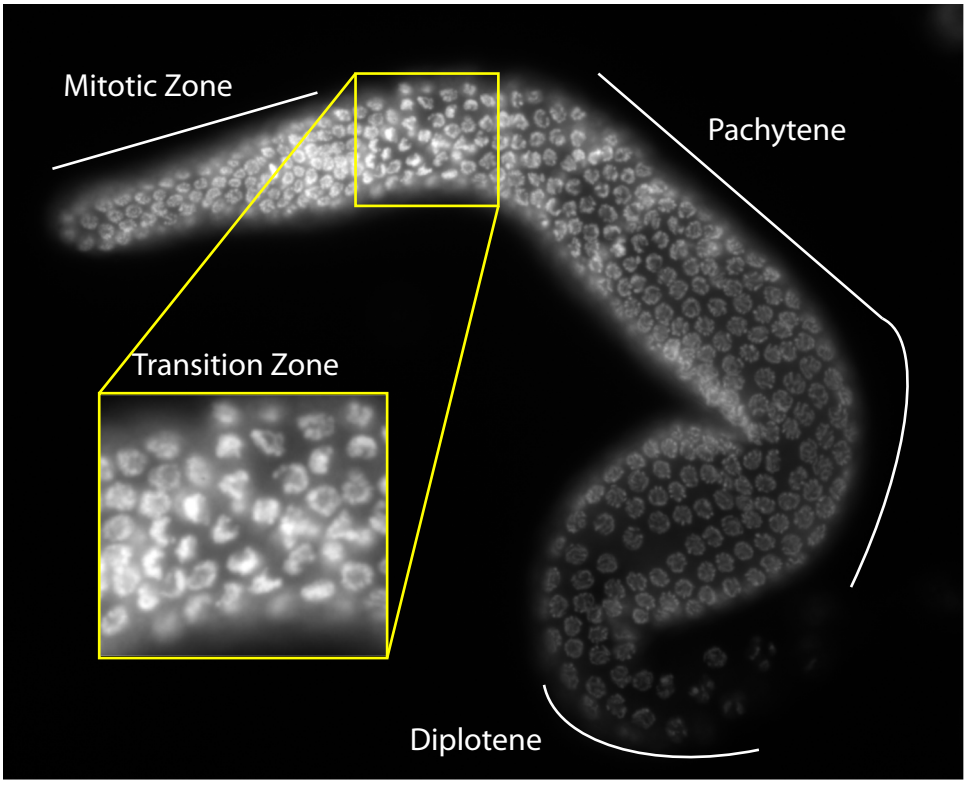

Figure 1.1 *C. elegans* meiotic progression. Whole mount fixed wild type gonad stained with DAPI. The germline stem cell pool resides in the distal tip, termed the Mitotic Zone. Nuclei enter meiosis in the Transition Zone, which contains leptotene I and zygotene I. In these stages, chromosomes condense and cluster together while searching for their homologous partner, and then synapse together. Nuclei then enter Pachytene, where recombination occurs. Recombination finishes, and chromosomes condense further in diplotene.

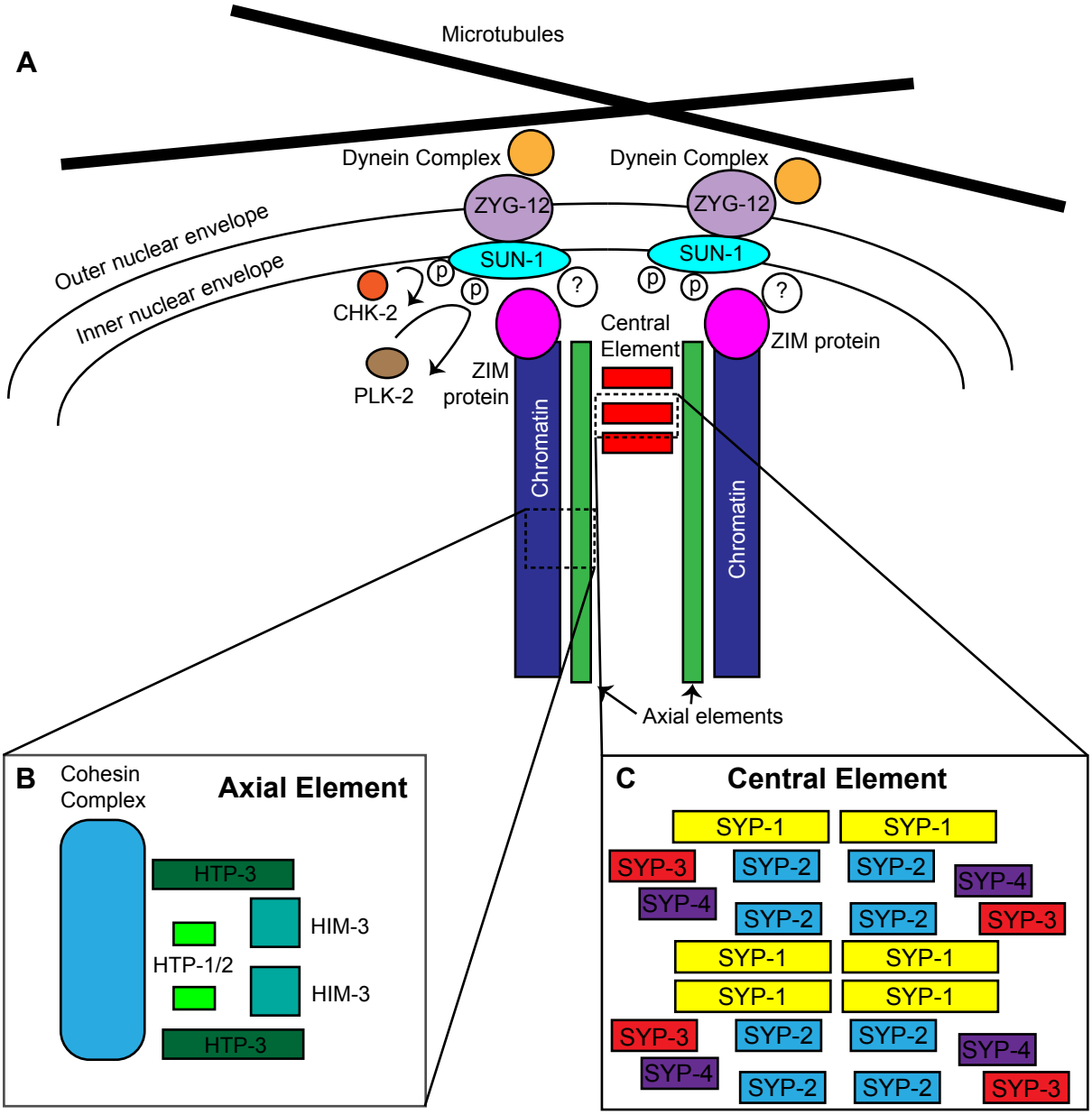

Figure 1.2 Meiotic Synaptonemal Complex. (A) ZIM proteins bind to one end of each chromosome, and localize to the nuclear envelope near SUN-1, through an unknown protein. SUN-1 is phosphorylated first by CHK-2 and then by PLK-2 that is required for pairing. SUN-1 binds to ZYG-12, which interacts with the dynein motor complex and microtubules in the cytoplasm. (B) The Axial element HTP-3 interacts with the cohesin complex keeping sister chromatids together. HIM-3 and HTP-1 and HTP-2 bind to HTP-

3 to form the axial element of the synaptonemal complex. (C) After pairing, the central element assembles. SYP-1 spans the gap in between homologous chromosomes, and directly interacts with SYP-3 and SYP-2. SYP-3 directly interacts with SYP-4. The placement of the newly discovered SYP-5 and SYP-6 is currently unknown. Adapted from model figures in (SCHILD-PRUFERT *et al.* 2011; KOHLER *et al.* 2017)

CHAPTER 2: A MOTOR-INDEPENDENT REQUIREMENT FOR DYNEIN LIGHT CHAIN IN *C. ELEGANS* MEIOTIC SYNAPSIS

Sara M. Fielder, Huiping Ling, Elizabeth J. Gleason, William G. Kelly

This work is under review for publication at the journal Genetics.

Sara Fielder performed all experiments and data analysis for this paper (Figures 2.1-2.6, and Supplemental Figures 2.S1-2.S4) except CRISPR strain design, which was primarily conducted by E. Gleason, and injections for CRISPR strains was performed by H. Ling. Model figure 2.7 was co-designed by Sara Fielder and W.G. Kelly

2.1 Abstract

The dynein motor complex is thought to aid in homolog pairing in many organisms by moving chromosomes around the nuclear periphery to promote and test homologous interactions. This precedes synaptonemal complex (SC) formation during homolog synapsis, which stabilizes homolog proximity during recombination. We observed that depletion of the dynein light chain (DLC-1) in *Caenorhabditis elegans* prevents synapsis, causing off-chromatin formation of SC protein foci with increasing frequency with rising temperature. This phenotype is independent of DLC-1 function in dynein motors, as SYP protein foci do not form with depletion of other motor components. In contrast to normal SC-related structures, foci formed upon DLC-1 depletion are resistant to dissolution with 1,6-hexanediol, similar to aggregates of SC proteins formed at high growth temperatures. Dynein light chains have been shown to act as hub proteins that interact with other proteins through a conserved binding motif.

We identified a similar DLC-1 binding motif in the *C. elegans* SC protein SYP-2 and demonstrate that SYP-2 co-immunoprecipitates with DLC-1 *in vivo*. Mutation of the putative DLC-1 binding motif causes meiotic defects resulting in reduced brood size, increased chromosome non-disjunction, and appears to decrease SYP-2's interaction with DLC-1. We propose that DLC-1 acts as a pre-synapsis chaperone for SYP proteins to help regulate their self-association prior to SC assembly, a role that is revealed by its increased essentiality at elevated temperatures and physical interaction.

2.2 Introduction

Meiotic synapsis is the process of physically connecting paired homologous chromosomes together during meiosis to aid in recombination and to ensure that subsequent generations inherit the correct chromosome complement. The synaptonemal complex (SC) is a conserved structure composed of an axis that assembles onto cohesion proteins on each chromosome, and a central element (CE) that physically connects two homologous chromosomes together (reviewed in (LUI AND COLAIACOVO 2013)). The CE in *C. elegans* consists of six SYP proteins that assemble onto the axial element of the SC after chromosomes have correctly paired (MACQUEEN *et al.* 2002; COLAIACOVO *et al.* 2003; SMOLIKOV *et al.* 2007; SMOLIKOV *et al.* 2009; SCHILD-PRUFERT *et al.* 2011; HURLOCK *et al.* 2020). SYP proteins will self-assemble even if they are unable to assemble onto chromosomes. For example, in mutants lacking either axial element HTP-3 or HIM-3, SYP proteins assemble into nucleoplasmic foci away from chromatin (COUTEAU *et al.* 2004; GOODYER *et al.* 2008). These foci, termed polycomplexes, are composed of clusters of ladder-like structures that resemble the normal SC structure that assembles between synapsed chromosomes when viewed

using electron microscopy (ROG *et al.* 2017). Both the normal SC and the polycomplexes formed in *htp-3* mutants can be disrupted by addition of an amphiphilic solvent, such as 1,6-hexanediol (ROG *et al.* 2017). SC protein foci are also observed in the nucleoplasm of animals grown at elevated temperatures above 26.5° (BILGIR *et al.* 2013), but these foci are more resistant to solvent (ROG *et al.* 2017). This suggests that a structural change in SC proteins occurs at elevated temperatures that prevent proper assembly onto chromatin or even into ladder-like structures.

In *C. elegans*, chromosomes initially pair using Zinc-finger In Meiosis proteins (ZIM) that bind specific sequence repeats located on one end of each chromosome (PHILLIPS *et al.* 2005; PHILLIPS AND DERNBURG 2006). This end of each chromosome localizes to the nuclear envelope and connects indirectly to the dynein motors in the cytoplasm through the nuclear membrane proteins SUN-1 and ZYG-12 (PENKNER *et al.* 2007; SATO *et al.* 2009). Dynein is thought to aid chromosomes in the search for their homologous pairing partners by moving chromosomes around the nuclear periphery and increasing their interactions (SATO *et al.* 2009; WYNNE *et al.* 2012). The current model is that potential homologous chromosome matches are tested through dynein-dependent forces that can disrupt non-homologous associations, with correct matches providing tension-dependent signals for synapsis initiation (SATO *et al.* 2009). However, mutants lacking dynein-dependent movement or all pairing center activity can still undergo non-homologous and fold-back synapsis, indicating that synapsis can still occur without dynein-dependent associations (PENKNER *et al.* 2007; HARPER *et al.* 2011; ROG AND DERNBURG 2015).

Despite its original identification as a critical component of the dynein motors, the dynein light chain has been shown to have numerous cellular roles in protein-protein interactions independent of the dynein motor complex (reviewed in (RAPALI *et al.* 2011)). Light chain dimers bind to two identified motifs on other proteins (RODRIGUEZ-CRESPO *et al.* 2001), which are frequently located adjacent to a coiled-coil domain. Light chain binding has been shown to facilitate protein-protein interactions and influence protein conformation of its targets (MAKOKHA *et al.* 2002; NYARKO *et al.* 2004; WAGNER *et al.* 2006) (and reviewed in (RAPALI *et al.* 2011)).

In this study, we have identified a dynein-independent role for the *C. elegans* dynein light chain (DLC-1) in meiotic synapsis. Depletion of DLC-1 alone causes amphiphilic solvent-resistant foci of SYP proteins, similar to aggregates induced by high temperature, whereas mutation or knockdown of other dynein components does not induce such aggregates. DLC-1 is dispensable for SC assembly at lower temperatures, but its absence causes the aggregate phenotype with increasing frequency as the temperature rises. We identify a possible DLC-1 interacting motif in the CE protein SYP-2 and show that DLC-1 physically interacts with SYP-2 *in vivo,* and mutations in this binding site cause chromosome segregation defects in meiosis. These results indicate that DLC-1 acts not only in the dynein complex moving chromosomes during pairing, but also acts as a protein chaperone during the regulation of SC assembly at elevated temperatures.

2.3 Methods

Strains

Strains used in this paper are jmntSi13 [pME4.1] II (WANG *et al.* 2016); *dlc-1*(tm3153) III, *syp-2*(ok307) V; wgIs227, *dhc-1(or195)* I, and *dnc-1(or676)* IV. Transgenic strains ck38 and ck39 were produced using CRISPR-Cas9 system, discussed below. Animals were grown at temperatures indicated in each figure. Some strains were provided by the CGC, which is funded by NIH Office of Research Infrastructure Programs (P40 OD010440).

Transgenic strain construction using CRISPR-Cas9 system

Strains ck38 (denoted WT *syp-2::GFP*) and ck39 (denoted *syp-2::GFP(AMTA)*) were constructed using the CRISPR-Cas9 system. gRNA was designed within 35 bp of site of integration using the IDT design custom gRNA online tool (Table 2.1). gBlock® Gene Fragment (Integrated DNA Technologies) was amplified using Platinum Super Fi PCR Master Mix (Invitrogen #12358010) with only 12 cycles of PCR to ensure lower chance of incorporation of a mutation into the HDR template. Nine PCR reactions were pooled and purified using the Zymo DNA Clean & Concentrator-5 kit (Zymo D4004). Each Alt-R® CRISPR-Cas9 sgRNA (Integrated DNA Technologies) was duplexed with an equal concentration of Alt-R® CRISPR-Cas9 tracrRNA (Integrated DNA Technologies #1072532) in duplex buffer (IDT #1072570). An injection mix consisting of 0.5 µM of each sgRNA duplex mix, 0.31 µM of Cas9 Nuclease V3 (IDT #1081058), 0.5 µM of Dpy10 sgRNA, 0.5 µM of Dpy10 ssDNA Oligo HDR template for positive selection (Table 2.2), and 0.115 µM of amplified and purified SYP-2::GFP gBlock (for generation of ck38 strain)(Table 2.2) or 5µM of Oligo HDR Syp2(AMTA) ssDNA template (for ck39 strain) (Table 2.2) was made and injected into young adult N2 animals. The ck39 allele was made by injecting the corresponding injection mix targeting the mutation site into

young adult ck38 animals. Both created strains were sequence verified and outcrossed to N2 5 times before phenotypic analysis.

Immunofluorescence

Measurements of aggregate frequency at different temperatures was performed using live imaging of *syp-2*(ok307) V; wgIs227 in the GFP channel at 48 hours after L4 stage, after being grown from larval stage L4 at 16° or 20°, or after being after growth at 20° and then shifted to 25° for 24 hours.

Immunofluorescence was performed as previously described (ref, in press). Primary antibodies used in this study: goat anti-SYP-1 (HARPER *et al.* 2011) (1:1500), chicken anti-GFP (1:300)(Aves Labs GFP-1020). The following secondary antibodies were used: donkey anti-goat (1:500)(Invitrogen A11055), and donkey anti-chicken (1:1000) (Jackson Immuno Research Laboratories 703-586-155)

RNA interference

Plasmids were transformed into HT115 cells, and grown in culture overnight for 12-15 hours with 100 µg/mL ampicilin, followed by an induction step with 1mM IPTG for 2 additional hours before plating on 100 µg/mL ampicillin-1mM IPTG NGM plates and grown at 25° for 2 days. Synchronized L1s were added to RNAi plates and grown to 24 hours past larval L4 stage at 20°C before being shifted to 25° for 24 hours before analysis. Knockdown of *dlc-1* was achieved by cloning a 700 base pair segment from *dlc-1's* genomic sequence (see Table 2.3 for primer pairs) and inserting this segment into the L4440 empty vector multi-cloning site. Knockdown of *htp-3* was achieved using the plasmid obtained from Source Bioscience clone (F57C9.5)(KAMATH *et al.* 2003). Empty vector control RNAi was performed using the L4440 plasmid.

Hexanediol treatment

1,6-hexanediol treatments performed essentially as described previously (ROG *et al.* 2017). Live animals were dissected on poly L-lysine coated slides in 1x egg buffer + 2.5mg/mL levamisole to immobilize animals. Slides were imaged immediately, and then 2x volume of 10% 1,6-hexanediol (dissolved in 1x egg buffer) was gently added underneath the coverslip, images were taken at 30 seconds and again 1 minute after addition of 1,6-hexanediol. Stage movement in the Z-axis occurred between before and first after picture.

Brood assays

Larval stage L4 animals were singled out to plates with a small OP50 lawn, and grown at the temperature specified, moving animals to fresh plates every 20-25 hours until the animal ceased producing embryos for 24 hours. 24 hours after removal of the adult, plates were scored for number of remaining unhatched embryos. When progeny reached young adult stage, each F1 animal was counted as male, hermaphrodite, or *Dpy*. Each temperature for each strain had 9-12 replicates.

Protein Co-Immunoprecipitation

Protein extraction and co-Immunoprecipitation was performed similarly as previously described (NADARAJAN *et al.* 2016), with some modifications generously suggested by the Colaiacovo lab (S. Nadajaran and M. Colaiacovo, personal communication). Modifications include using 20 synchronized, confluent 10 cm plates of young adult animals grown at 25° for each strain, and after freezing samples in liquid nitrogen, a 1.5x lysis buffer (75 mM Hepes pH 7.5, 1.5 mM $MgCl_2$, 150mM KCl, 0.1% NP-40, and 15% glycerol, with cOmplete EDTA free protease inhibitor cocktail (Roche

11836170001)) was used for lysing and freezing samples. To lyse animals, samples were sonicated for 15 seconds on, 45 seconds off for 18-25 minutes. After examination under the microscope to ensure animal bodies were broken up into small fragments, the concentration of KCl was brought up to 300mM in each sample. GFP-Trap magnetic beads (Chromotek gtma-20) were added to the lysates and samples were incubated with mixing at 4° overnight. Immunoprecipitates were washed with 1x PBS + cOmplete ETDA free protease inhibitor cocktail three times, followed by boiling beads with 2x Sample Buffer for 10 minutes to elute.

Western Blot

Following co-immunoprecipitation, each sample was loaded onto a precast 4-12% gradient Bis-Tris gel (Invitrogen NW04120BOX) and transferred onto a PVDF membrane using a Power Blotter (ThermoScientific 22834SPCL). Blots were blocked with 5% Bovine Serum Albumin in TBS + 0.1% Tween-20 (TBS-T) for two to three hours before incubation with primary antibody at 4° overnight. After three 10 minute washes with TBS-T, blots were incubated with secondary antibodies for three hours at room temperature, followed by the same wash procedure. Blots were incubated with Clarity Western ECL substrate (BioRad 170-5060) for five minutes and visualized using the Bio-Rad ChemiDoc Imaging System. Primary antibodies used for this study are goat anti-SYP-1 (1:2000), chicken anti-GFP (1:2000)(Aves Labs GFP-1020), mouse anti-flag (1:2000) (Sigma-Aldrich #F1804). Secondary antibodies used were donkey anti-goat HRP (1:2000) (Abcam ab97110), donkey anti-chicken peroxidase (1:2000) (Jackson #703-035-153), donkey anti-mouse HRP (1:2000) (Jackson 715-035-150). HRP visualized with Clarity Western ECL Substrate (Bio-Rad #170-5060).

2.4 Results

2.4.1 Knockout of dynein heavy chain and/or dynactin does not induce SYP foci formation

Previous reports indicated that RNAi-mediated knockdown of *C. elegans* dynein light chain (*dlc-1*) in combination with dynein heavy chain (*dhc-1*) temperature sensitive (ts) mutants raised at the restrictive temperature (25°) results in the formation of SYP protein foci not associated with chromatin in hermaphrodite meiosis (SATO *et al.* 2009). However, in similar experiments we found that raising *dhc-1(or195^{ts})* mutants alone at the restrictive temperature (25°) without *dlc-1(RNAi)* did not typically result in the SYP protein foci phenotype (Fig. 2.1). In these experiments we did observe other expected *dhc-1* mutant phenotypes, including embryonic lethality and polyploid nuclei in the mitotic region of the gonad (not shown). A temperature-sensitive mutant of another component of the dynein complex, *dnc-1(or676)*, also did not display SYP foci in mutants raised at the restrictive temperature, despite also displaying embryonic lethality. Furthermore, *dnc-1(RNAi)* combined with *dhc-1(or195^{ts})* worms also did not display SYP foci when raised at the restrictive temperature (Fig. 2.1). In contrast, as has been previously reported, RNAi-mediated knockdown of DLC-1 alone at 25° resulted in formation of the SYP foci (BOHR *et al.* 2015) (Fig. 2.2, and discussed further below). These results indicate that the requirement for DLC-1 in meiotic progression and synapsis may be independent of its role in dynein motor activities.

2.4.2 SYP proteins form foci in a temperature sensitive manner with knockdown of DLC-1

While performing RNAi knockdown of DLC-1, we observed temperature-dependent differences in frequency of the SYP foci phenotype. When grown at 20°, 61% of gonads have SYP-2 foci, while growth at 25° results in 85.88% of gonads having SYP-2 foci (Fig. 2.2A and 2.2C). Interestingly, when grown at 16°, 0% of *dlc-1(RNAi)* gonads display the SYP foci phenotype (Fig. 2.2A and 2.2C). *htp-3(RNAi)* animals grown in parallel resulted in SYP-2 foci in 100% of gonads at all three temperatures, indicating that these results are unlikely to be due to temperature-dependent differences in RNAi efficiency of meiotic targets. Additionally, the higher the growth temperature the more severe the phenotype of *dlc-1* knockdown observed: *dlc-1(RNAi)* animals grown at 25° typically displayed longer regions of nuclei with SYP-2 foci (Fig. 2.2A), and regions that did not have SYP-2 foci appeared to have more diffuse SYP-2::GFP localization than *dlc-1(RNAi)* animals raised at 20°(Fig. 2.2B) . This diffuse localization of SYP-2::GFP in nuclei without foci could indicate increased inability to form normal SC structures at 25°, could be an intermediate before foci formation, or could indicate lower levels of protein or a lower amount of SC assembly onto chromatin. In any of these cases, this suggests a more severe phenotype of *dlc-1(RNAi)* at 25° of affected gonads, even in nuclei that do not display the foci phenotype.

2.4.3 SYPs form insoluble foci with knockdown of DLC-1

CE protein “polycomplexes” are often observed as normally transient foci in pre-meiotic nuclei that precede SYP protein loading into a more stable SC (GOLDSTEIN 2013; ROG AND DERNBURG 2015). In the absence or disruption of axial elements, such

as in *htp*-3 mutants, these polycomplexes are stabilized and remain for the rest of meiosis (GOODYER *et al.* 2008). The polycomplexes are dissolved by amphiphilic solvents such as 1,6-hexanediol, as is the normal SC that assembles onto chromosomes (ROG *et al.* 2017). In contrast, CE aggregates formed at elevated temperatures above 26.5° are resistant to dissolution (ROG *et al.* 2017). We confirmed that foci caused by *htp-3(RNAi)* were dispersed by 1,6-hexanediol in 100% of the gonads examined (Fig. 2.3). Additionally, heat-induced foci were less susceptible to 1,6-hexanediol, but we observed some dispersal. In our hands, adding 1,6-hexanediol caused dispersal of foci in 59.4% of gonads in *syp-2::gfp*(wgIs227) animals raised at 27°, and 22.9% of *syp-3::gfp(ok758; ieSi11)* animals raised at 27.5° (Fig. 2.S1). In contrast, 100% of SYP-2 foci in *dlc-1(RNAi)* animals grown at 25° were resistant to 1,6-hexanediol treatment, and thus are even less soluble than the heat induced aggregates. This indicates that there is a difference in the way the SYP foci form in *dlc-1(RNAi)* knockdown at 25° as compared to both normal SC assembly and the off-chromatin assembly of SC polycomplexes in the absence of HTP-3. We further verified that SYP-1 and SYP-2::GFP co-localized in foci induced by all conditions examined: *htp-3(RNAi)* animals, *dlc-1(RNAi)* animals, and in animals raised at 27.5°(Fig. 2.S2). Thus both SYP-1 and SYP-2 interact in SYP foci irrespective of the conditions causing them.

2.4.4 SYP-2 interacts with DLC-1 in vivo through a conserved binding motif

Dynein light chains in other organisms have been reported to interact with many different proteins via two consensus binding motifs (LO *et al.* 2001). These binding motifs are frequently found next to a coiled-coil domain in the target protein (RAPALI *et al.*

2011). We examined the protein sequences of axial and central elements of the *C. elegans* synaptonemal complex and discovered a potential binding motif (96-KMTQ-99) located next to a predicted coiled-coil domain (98-161) of SYP-2 (Fig. 2.4A) (SCHILD-PRUFERT *et al.* 2011). Interestingly, whereas the structure of CE proteins is conserved between organisms, the sequences of CE proteins are not well conserved (PAGE AND HAWLEY 2001; MACQUEEN *et al.* 2002). However, one of the CE proteins in both humans and yeast each contain a potential DLC-1 binding motif located next to a coiled-coil domain, implying that this motif may be important for the function of the CE proteins (Fig. 2.4A).

We therefore tested whether SYP-2 and DLC-1 interact *in vivo*, and whether the putative binding motif was required for any interaction. We used CRISPR-Cas9 to tag the endogenous SYP-2 with GFP [*syp-2(ck38)*, hereafter denoted as WT *syp-2::gfp*], and crossed this allele into a transgenic line expressing a FLAG-tagged DLC-1, with endogenous *dlc-1* deleted (WANG *et al.* 2016). We then performed anti-GFP immunoprecipitations followed by Western blot analyses probed with anti- FLAG. We observed specific co-immunoprecipitation of FLAG::DLC-1 with anti-GFP IP of SYP-2::GFP, indicating that these two proteins interact in vivo (Fig. 2.4B). This interaction was not observed in lysates from control animals that lacked one of the two tags.

To further determine if the identified consensus binding motif is important for this interaction, we used CRISPR-Cas9 to mutate the putative binding sequence from 96-KMTQ to 96-AMTA [*syp-2 (ck39)*, hereafter denoted as *syp-2::gfp(AMTA)*]. We crossed this allele into the transgenic line expressing FLAG::DLC-1 with endogenous *dlc-1* deleted and performed the same anti-GFP immunoprecipitation. A small amount of

FLAG::DLC-1 was observed to co-IP with the SYP-2::GFP(AMTA) mutant protein (Fig. 2.4B), however, less total SYP-2:GFP was immunoprecipitated from the *syp-2::gfp(*AMTA) lysates(Fig. 2.S4). However, the ratio of FLAG:DLC-1/SYP::GFP was lower in the mutant IP's (0.577 in *syp-2::gfp(AMTA)* as compared to 0.733 in WT *syp-2::gfp* (Table 2.4)) suggesting that the motif may contribute to the interaction of SYP-2 with DLC-1, but is not required; alternatively, it could suggest that mutation of only two residues in the binding motif is not enough to completely eliminate the interaction.

2.4.5 Mutation of the putative DLC-1 binding site in SYP-2 results in temperature sensitive meiotic defects

We next examined the phenotypic consequences of the *syp-2(AMTA)* mutation. Typically there is a short region where transient SYP polycomplexes are observed in a few pre-meiotic nuclei (GOLDSTEIN 2013; ROG AND DERNBURG 2015). In *syp-2::gfp(AMTA)* gonads, we observed a significant lengthening of this region when animals were raised at 20° as compared to WT *syp-2::gfp* animals (Fig. 2.5). Additionally, mutant *syp-2::gfp(AMTA)* animals raised at all temperatures displayed more proximal nuclei with chromosomes clustered together at the nuclear periphery, reminiscent of transition zone nuclei (Fig. 2.S3). There was also a 34% reduction of brood size in the *syp-2::gfp(AMTA)* compared to both WT *syp-2::gfp* and WT *syp-2* (N2 strain) at 16° and 20°. A more severe effect on brood size was observed in the *syp-2::gfp(AMTA)* strain at 25°, in which the mutant had a 77% reduction of brood size compared to the N2 (WT) strain (Fig. 2.6A). A slight but significant decrease in brood size was also observed in the WT *syp-2::gfp* strain at 25° as compared to N2, indicating a minor temperature sensitive consequence of the CRISPR mediated C-terminal

tagging of SYP-2 with GFP. However, the reduced brood size of the *syp-2::gfp(AMTA)* animals was dramatic when compared to both strains at this temperature.

Meiotic errors such as homolog pairing, synapsis errors, and/or non-disjunction in *C. elegans* can be readily detected by an increase in the frequency of males (Him phenotype) among hermaphrodite self-progeny, which results from non-disjunction of the X in meiosis. An additional measure of non-disjunction of the X chromosome is an increase of dumpy *(Dpy)* offspring, which is characteristic of an XXX karyotype (HODGKIN *et al.* 1979). *syp-2::gfp(AMTA)* animals have a statistically significant increase in the percentage of males over both WT *syp-2::gfp* and N2 that significantly increases when raised at 25°, but also increases, although not statistically significant, when increased from 16° to 20° (5.3% of the total *syp-2::gfp(AMTA)* brood at 16°, 7.02% at 20°, and 13.8% at 25° were males ($p=.1128$ and $p<.0001$ with each temperature increase, respectively)) (Fig. 2.6C). The *syp-2(AMTA)* strain also shows an increased percentage of Dpy offspring, further confirming an increase in X chromosome non-disjunction. Introduction of the GFP tag alone also causes a significant increase in male progeny as compared to N2 animals, but at a significantly lower level than the *syp-2::gfp (AMTA)* mutation (0.61% of the WT *syp-2::gfp brood* at 16°, 0.90% at 20°, and 4.5% at 25°). For comparison, X chromosome non-disjunction in WT animals hovers below 0.18% at all three temperatures measured. Additionally, the *syp-2::gfp(AMTA)* strain has a significant increase in embryonic lethality: approximately 10% of embryos never hatch when grown at 16° or 20°, but when the strain is grown at 25°, 64.3% of embryos never hatch (Fig. 2.6B). The increased embryonic lethality in the *syp-2::gfp(AMTA)* strain may be due to an overall increase in aneuploidy, as indicated by the increase in

male and Dpy offspring. Despite the *syp-2::gfp(AMTA)* line being fertile, the presence of these meiotic defects further supports that the potential DLC-1 interaction domain is important, but not completely essential to SYP-2 function.

2.5 Discussion

DLC-1 may work as a protein chaperone for SYP proteins at high temperatures

We found that although dynein may play an important role in chromosome movement during homolog pairing, disruption of the dynein motor complex does not appear to affect the subsequent ability of the SC to form and synapsis to occur between chromosomes. Instead, only specific loss of the dynein light chain DLC-1 results in the formation of SYP protein aggregates. Knock down of multiple other dynein complex components, alone or in combination, did not appear to dramatically affect SC assembly between chromosomes. This indicates that there is a dynein motor-independent function for DLC-1 that is required to help guide normal SC assembly onto chromatin, and to prevent aggregation of SYP proteins away from the chromosome axis. This function is temperature dependent, as foci formation upon loss of DLC-1 increases with increasing temperatures, with ~80% of ovaries exhibiting SYP aggregates at 25°C. In addition, SYP proteins that are properly assembled into an interhomolog SC have hydrophobic interactions that can be reversibly disrupted by 1,6-hexandiol. Similarly, SYP protein polycomplexes that spontaneously form when there is no lateral axis available for assembly (e.g. *htp-3* mutants or *htp-3(RNAi)*), can be disrupted by hexanediol (ROG *et al.* 2017). In contrast, foci formed in *dlc-1(RNAi)* animals are no longer disrupted by the amphiphilic solvent, implying that the foci that result from DLC-1

knockdown are not structurally similar to previously described polycomplexes. Instead, the temperature-dependent foci produced by loss of DLC-1 are more reminiscent of the aggregates that occur when animals are grown at temperatures above 26.5° (ROG *et al.* 2017). It was proposed that these heat-induced aggregates result from a change of protein structure into a partially denatured state (ROG *et al.* 2017); we hypothesize that the aggregates that are induced by DLC-1 depletion at 20° and 25° are similarly the result of a change in protein structure that is normally prevented by DLC-1. We further hypothesize that the temperature-sensitive requirement for DLC-1 to prevent SYP aggregation is due to its role as a type of chaperone required to guide SYP protein assembly in the earliest stages of meiosis, a role that is more essential as temperatures increase.

We show that SYP-2 and DLC-1 interact *in vivo* and surmise that this interaction is indicative of DLC's role as a chaperone specifically for SYP-2. As mentioned, there appears to be dynamic or temporary formation of small SYP protein foci that are likely transient polycomplexes formed as SYP protein synthesis initiates in pre-meiotic cells. As these proteins are prone to self-assembly, a mechanism likely exists to help prevent stable aggregate formation as axis formation and pairing requirements delay SC assembly on chromatin. We suggest that our results support a potential role for DLC-1 in this stabilization process, and in the absence of DLC-1, irreversible aggregation is favored over polycomplex formation as temperatures rise (Fig. 2.7). This is in line with numerous reports showing dynein light chain homologs acting as protein chaperones guiding protein-protein interactions, in addition to the canonical role of the light chain in

stabilizing folding and alpha-helix content of dynein intermediate chains in the dynein motor complex (reviewed in (RAPALI *et al.* 2011).

It has previously been shown that using the Auxin-inducible degredation (AID) system, degrading DHC-1 results in SYP foci (ZHANG *et al.* 2015). However, we noticed that both these foci, and *htp-3(RNAi)* induced polycomplexes all result in multiple, small foci in each nucleus, which may indicate they are more like the small SYP foci that normally appear in pre-meiotic nuclei, whereas *dlc-1(RNAi)* induced aggregates tend to be large, with one to two per nucleus. The DHC-1 degradation-induced foci may be the result of a delay in early meiosis resulting from delayed homolog pairing (WYNNE *et al.* 2012; ROG AND DERNBURG 2015). Our results do not rule out the proposed role for dynein motors in homolog pairing, only that DLC-1 has a separate, additional role in SC assembly.

The putative DLC-1 binding motif in SYP-2 is important, but not essential for SC function

We identified a potential DLC-1 interaction motif in SYP-2 and mutated it using CRISPR-directed mutagenesis. Mutation of the putative binding motif with just two amino acid substitutions results in low fertility at 25°, yet synapsis still occurs despite the mutations, indicating that this motif is not absolutely essential for the function of SYP-2. Additionally, co-immunoprecipitation experiments indicate that DLC-1 can still interact with the mutant SYP-2, albeit with potentially lower affinity. Dynein light chain, and even specifically *C. elegans* DLC-1, has been shown to bind to proteins without either canonical binding motif and can even bind to multiple sites within the same protein (DORSETT AND SCHEDL 2009; WANG *et al.* 2016). The potential DLC-1 interaction motif

may either not be important, contribute minimally to the interaction, or the mutations we created were insufficient to disrupt full DLC-1 binding to that part of SYP-2. Alternatively, DLC-1's interaction with SYP-2 could be indirect and/or interface with SYP-2 and other SYP proteins, such that its interaction with SYP-2 is altered but can still immunoprecipitate with SYP-2 in a multimeric complex.

In either case, changing just two amino acids in the motif (KMTQ→AMTA) causes significant meiotic defects with some temperature dependence in these phenotypes. The AMTA mutant *syp-2* animals display a small brood size, high embryonic lethality at 25°, and the progeny have a greatly increased incidence of both males and XXX animals. The increase in X chromosome segregation abnormalities indicates that there are chromosome segregation problems, and further imply that embryos that fail to hatch likely die because of defective meiosis and consequential aneuploidy. The phenotypes of the mutant *syp-2* animals also get significantly worse at 25°, further supporting that as temperature increases, so does the instability of SYP protein function. This further indicates that DLC-1 interaction with SYP-2 is to function as a protein chaperone in stressful conditions.

Window of SYP sensitivity

There appears to be a specific window in which SYP proteins can form aggregates, and outside of that window, they will remain assembled onto chromosomes. With short periods of growth at high temperatures, a small region of SYP aggregates is observed, with this region increasing as the time at high temperature increases; a subsequent shift down from a high temperature results in recovery of the ability for SYP proteins to assemble between chromosomes for all nuclei entering the transition zone

after the down shift, while more advanced nuclei that already formed aggregates do not recover (BILGIR *et al.* 2013). This indicates that there is a window around the end of the transition zone where a nucleus will never assemble SC between its chromosomes if SC formation has been prevented up until that time. As has previously been proposed by the Dernburg lab, post-translational modifications (e.g. phosphorylation and N-terminal acetylation of SYP proteins (GAO *et al.* 2016; NADARAJAN *et al.* 2017; SATO-CARLTON *et al.* 2018)) could affect how SYP proteins interact and phase separate, and there could be modifications that help to stabilize folding of SYP proteins that occur around the time synapsis is initiating (ROG *et al.* 2017). We have observed that male *C. elegans* do not need DLC-1 to synapse their chromosomes; this could indicate that males add stabilizing post-translational modifications earlier than hermaphrodites, or express other protein chaperone(s) to help SYP folding in warmer temperatures (chapter 3). Alternatively, it has been proposed that there is phase separation of the SYP proteins once they have assembled together (ROG *et al.* 2017); once the SYP proteins have separated and formed a stable central element, the conditions within this liquid crystal could keep SYP proteins folded and/or interacting correctly. This may be why the sensitive window is at synapsis initiation when proteins are not in the most favorable environment.

Dynein light chain in early meiosis

Dynein light chains are hub proteins that carry out many roles that are independent of the dynein motor (RAPALI *et al.* 2011). In fact, DLC-1 has several motor-independent roles in *C. elegans* meiosis that aid in meiotic progression. DLC-1 is needed to maintain the germline stem cell pool, by localizing FBF-2 to P-granules and

promoting its function of suppressing translation of meiotic mRNAs (WANG *et al.* 2016). DLC-1 then promotes entry into meiosis by binding to GLD-1, which aids in the repression of some of GLD-1's target germline stem cell genes (ELLENBECKER *et al.* 2019). Additionally, DLC-1 promotes meiotic entry by both aiding in localization to the nucleus, and in the function of the methyltransferase METT-10, which inhibits germline stem cell proliferation in sensitized backgrounds (DORSETT AND SCHEDL 2009). We have further shown that DLC-1 may act as a chaperone to help prevent inappropriate aggregation of SYP proteins before SC assembly is allowed, and this role is increasingly important with rising temperature. These findings help to further characterize the complicated, multi-faceted role of dynein light chain in protein interactions and meiosis.

2.6 Acknowledgements

We would like to thank S. Nadajaran and M. Colaiaocovo for generous protocol consultation for SYP-2 immunoprecipitation. We would also like to thank E. Voronina for the generous gift of the jmntSi13 [pME4.1] II; *dlc-1(tm3153)* strain, A. Dernburg for the generous gift of the anti-SYP-1 antibody, and A. Fire for the generous gift of the L4440 plasmid. We would like to thank S. L'Hernault and the members of the Kelly and Roger Deal labs for helpful experimental design suggestions. This research was partially funded by the National Institute of General Medical Sciences of the National Institutes of Health under Award Number F31GM123750.

2.7 Figures

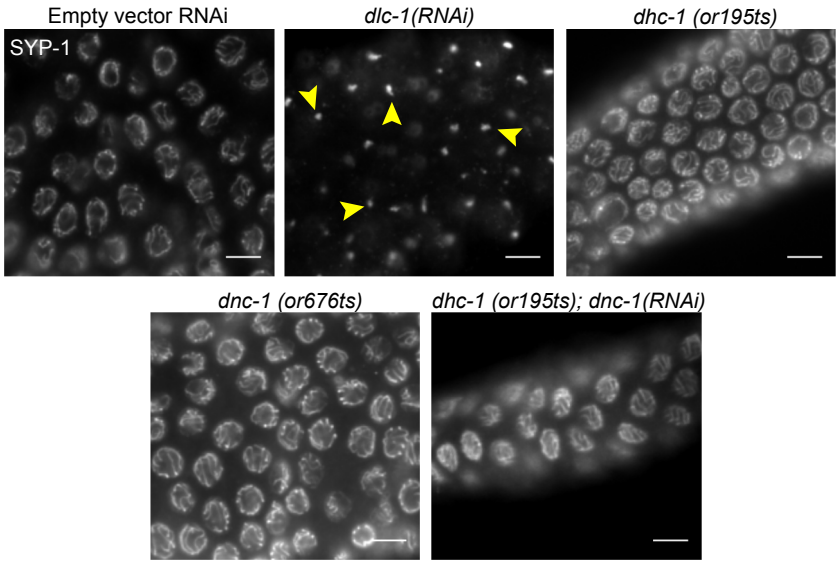

Figure 2.1. DLC-1 but not other dynein complex components are required for synapsis. Animals were raised at 25° for 24 hours before gonads were dissected, and whole mount fixed and probed with anti-SYP-1. All RNAi treated animals were raised on RNAi from larval stage L1. Images show early-pachytene region of ovary. WT N2 gonad treated with empty vector control RNAi for comparison (top left). Knockdown of *dlc-1(RNAi)* worm displays foci of SYP-1 in each nucleus (arrowheads; top middle), while both temperature sensitive mutants of *dhc-1(or195ts)*(top right) and *dnc-1(or676ts)* (bottom left) display normal synapsis. RNAi knockdown of *dnc-1* in a *dhc-1* temperature sensitive mutant displays normal synapsis of chromosomes (bottom right). Meiotic progression is depicted from left to right. Scale bars 5μm.

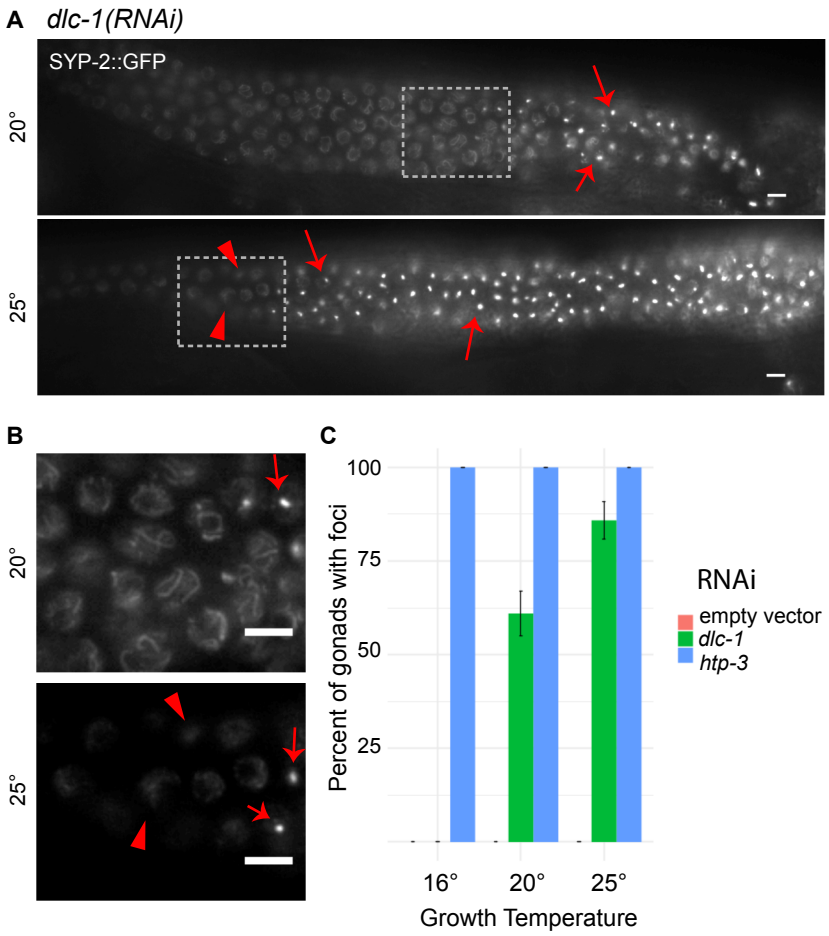

Figure 2.2. Synapsis defect in *dlc-1(RNAi)* is temperature sensitive. (A) Live GFP expression of SYP-2::EGFP using strain wgIs227; *syp-2(ok307)* V animals raised on *dlc-1* dsRNA-expressing bacteria from larval stage L1, and analyzed at 48 hours post-larval L4 stage. *dlc-1(RNAi)* animals raised at both temperatures display foci of SYP-2::GFP (arrows). Boxed portions of (A) shown at higher magnification in (B). Unaffected nuclei display normal SYP-2 loading in *dlc-1(RNAi)* at 20°, but show less structured, more diffuse localization in *dlc-1(RNAi)* at 25° (arrowheads). (C) Percentage of wgIs227; *syp-2(ok307)* V gonads with extended regions of SYP foci in *dlc-1(RNAi)* animals is 0% at 16° and increases as the temperature rises (n>100 total gonads scored at each temperature). The SYP foci phenotype is not temperature sensitive in

htp-3(RNAi) animals in which 100% of gonads display the phenotype at all temperatures assayed (n >60 total gonads scored at each temperature). Animals fed empty vector control never displayed the SYP foci phenotype at any of the three temperatures measured (n>60 total gonads scored at each temperature). Meiotic progression is displayed from left to right in all images. Scale bars 5μm.

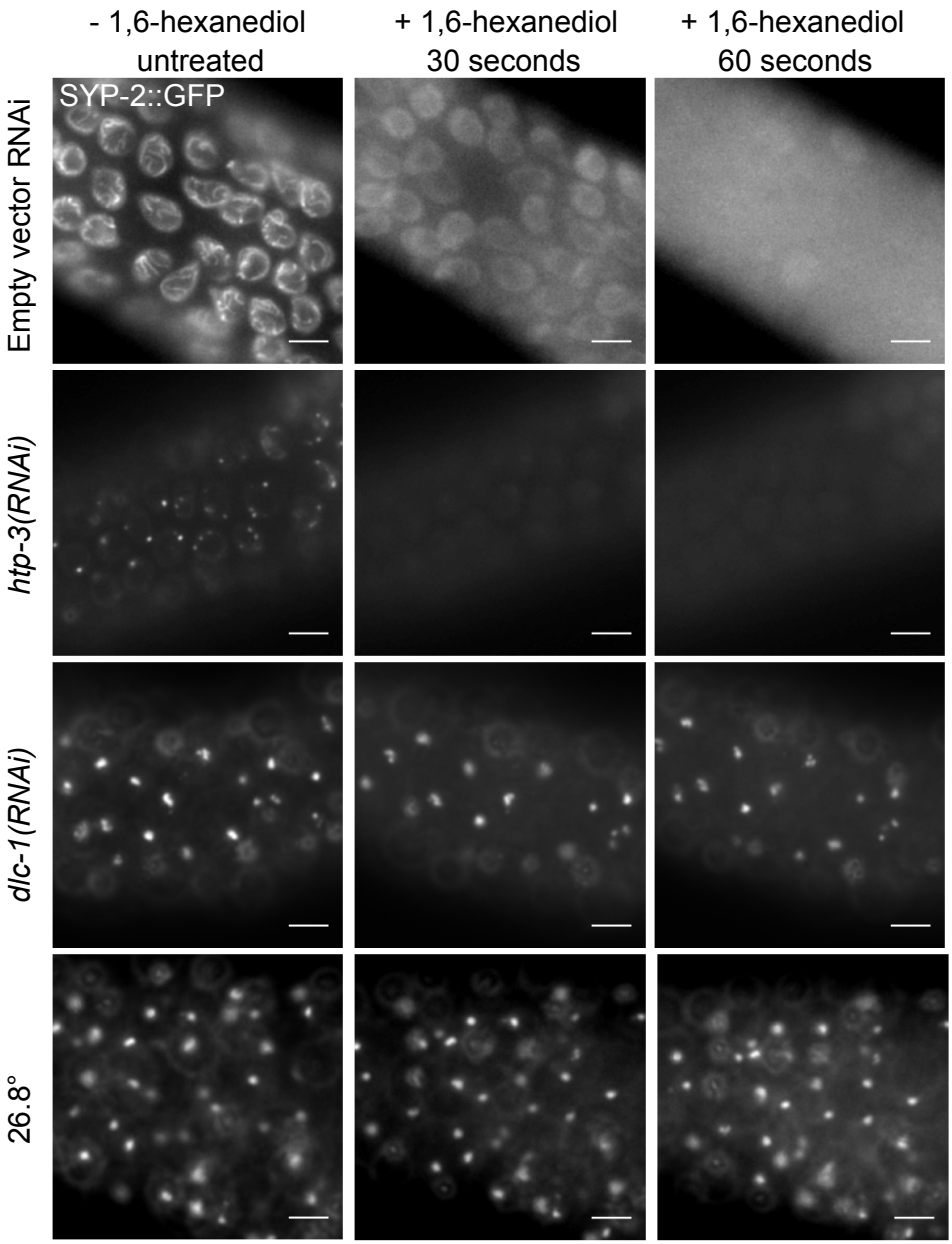

Figure 2.3. SYP foci formed with DLC-1 reduction or exposure to elevated temperature are resistant to hexanediol. Live GFP expression of wgIs227; *syp-2(ok307)* V age matched gonads treated with either empty vector control, *htp-3,* or *dlc-1* dsRNA expressing bacteria, or grown at a restrictive temperatures, with images taken immediately before exposure to 6.67% 1,6-hexanediol (first column), then 30 seconds

(second column) and 60 seconds (third column) after exposure. Animals fed empty vector dsRNA-expressing bacteria have a normal SC that dissolves with addition of hexanediol (top row). *htp-3(RNAi)* (second row) animals display SYP-2:GFP foci that dissolve within 30 seconds after addition of hexanediol. In contrast, *dlc-1(RNAi)* animals display SYP foci that do not dissolve after the addition of hexanediol (third row), similar to SYP foci formed in animals grown at 26.8° for 24 hours (bottom row). Scale bars 5μm.

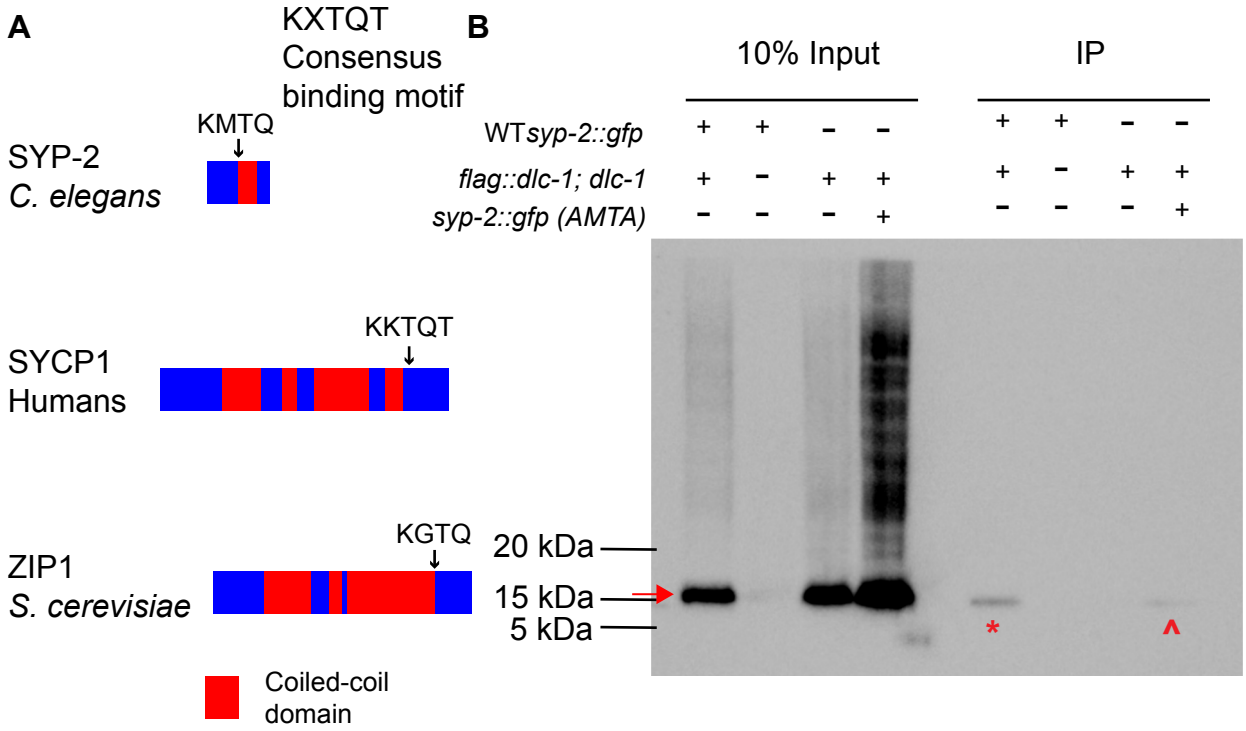

Figure 2.4. DLC-1 and SYP-2 interact in vivo. (A) DLC-1 orthologs in other species interact with a consensus binding motif (KXTQT) in other proteins, normally located in close proximity to a coiled-coil domain. *C. elegans* SYP-2 protein contains a similar motif (black arrow) located next to its coiled-coil domain (red block). A similar potential binding motif adjacent to a coiled-coil domain is found in CE proteins in both human and yeast. (B) Protein lysates from the indicated age matched strains were subjected to immunoprecipitation with anti-GFP antibody, followed by western blot analysis of the co-precipitates probed with anti-FLAG. FLAG::DLC-1 consistently migrates at approximately 15.5 kDa (red arrow). Immunoprecipitation of SYP-2::GFP results in co-precipitation of DLC-1::FLAG (asterisk). No immunoprecipitation was observed in the *dlc-1::flag; dlc-1* line alone, indicating there is no non-specific pull-down of FLAG. A smaller amount of FLAG::DLC-1 co-immunoprecipitates with SYP-2::GFP(AMTA)

(carrot) as compared to the amount of SYP-2::GFP pulled down (see Table 2.4), indicating the motif is important, but not essential for the interaction.

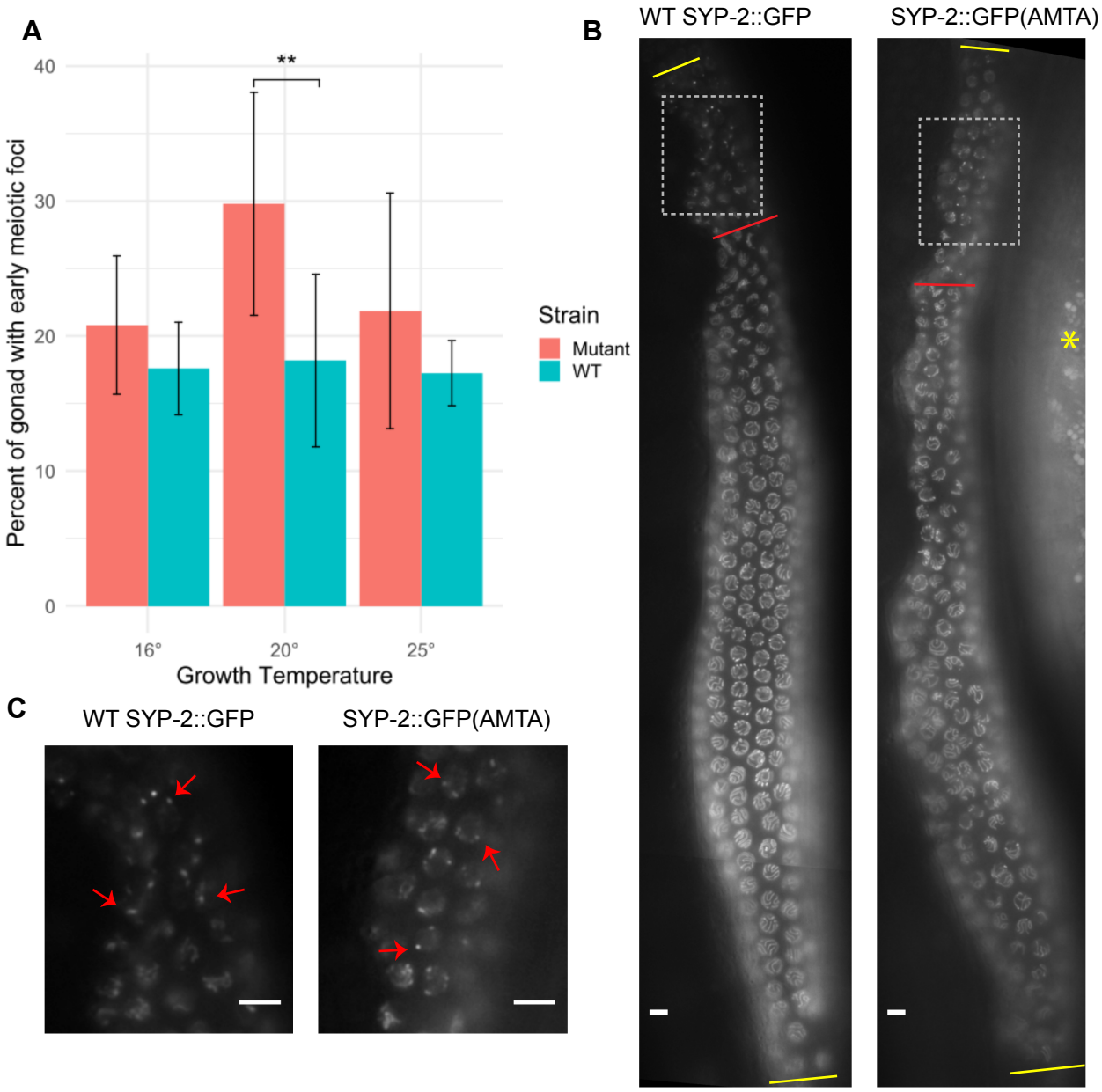

Figure 2.5. Mutation of the putative DLC-1 binding site in SYP-2 results in meiotic defects in the gonad. (A) *syp-2::gfp(AMTA)* gonads have a significantly larger percent of their gonads that have SYP-2::GFP foci at 20° than age matched WT *syp-2::*gfp. While *syp-2::gfp(AMTA)* gonads have larger percentages than WT at other temperatures, it is not significant. Statistical comparisons used Student's T test **p≤0.01.

Eight to nine WT *syp-2::gfp* gonads were measured at each temperature, and 12-13 *syp-2::gfp(AMTA)* gonads were measured at each temperature. (B) Live imaging of GFP in WT *syp-2::gfp* hermaphrodite and in *syp-2::gfp(AMTA)* hermaphrodite grown at 25°. Zone with foci were measured (from first yellow bar to red bar), and divided by total length of meiotic region (between yellow bars) to give data in A. In the *syp-2::gfp(AMTA)* image, there is autofluorescence from the gut on the right (red asterisk). Gray boxes indicate regions magnified in C (C) Magnified early meiotic SYP-2 foci (arrows) in both WT *syp-2::gfp* and *syp-2::gfp(AMTA).* Meiotic progression from top to bottom in all images. Scale bars 5μm.

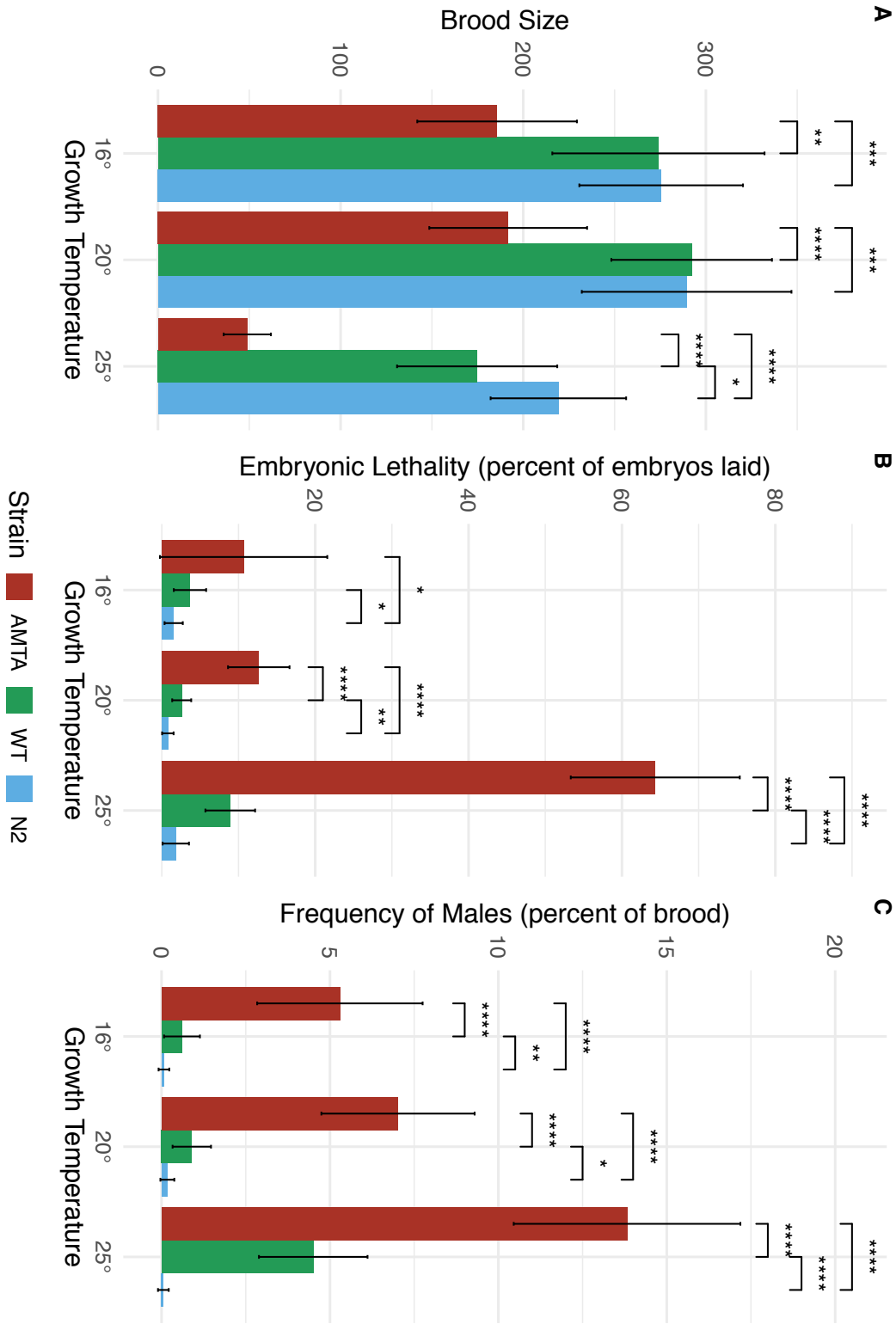

Figure 2.6. Mutation of the putative DLC-1 binding site in SYP-2 causes temperature-sensitive embryonic lethality and hallmarks of increased aneuploidy.

Nine to twelve WT *syp-2::gfp* (labeled WT in graph), N2, or *syp-2::gfp* (AMTA) animals were singled out for each temperature and their progeny statistics were recorded. (A) Brood Size Analysis. All progeny were counted until the animal no longer laid embryos for 24 hours. At all temperatures, the (AMTA) mutation had a significantly lower brood size than both WT and N2. WT *syp-2::gfp* animals had a slight but significantly lower brood size than N2 at 20° (B) Embryonic Lethality. Unhatched embryos were counted 24 hours after the adult was moved to the next plate. The (AMTA) mutation has a significantly higher embryonic lethality than N2 at all temperatures, and the embryonic lethality significantly increases at 25°, with 64% of embryos failing to hatch. (C) X chromosome nondisjunction was recorded as the percentage of the brood that was male or *Dpy* (indicating XXX genotype). At all temperatures, the (AMTA) mutation has a significantly higher rate of males than both WT and N2, with the amount of males at 25° significantly higher than both other temperatures ($p<0.0001$). One N2 animal grown at 16° was excluded from all analyses as it had an outlying brood size of 61. Student's T test was used for statistical checks. * $p\leq0.05$, ** $p\leq0.01$, *** $p\leq 0.001$, **** $p\leq 0.0001$

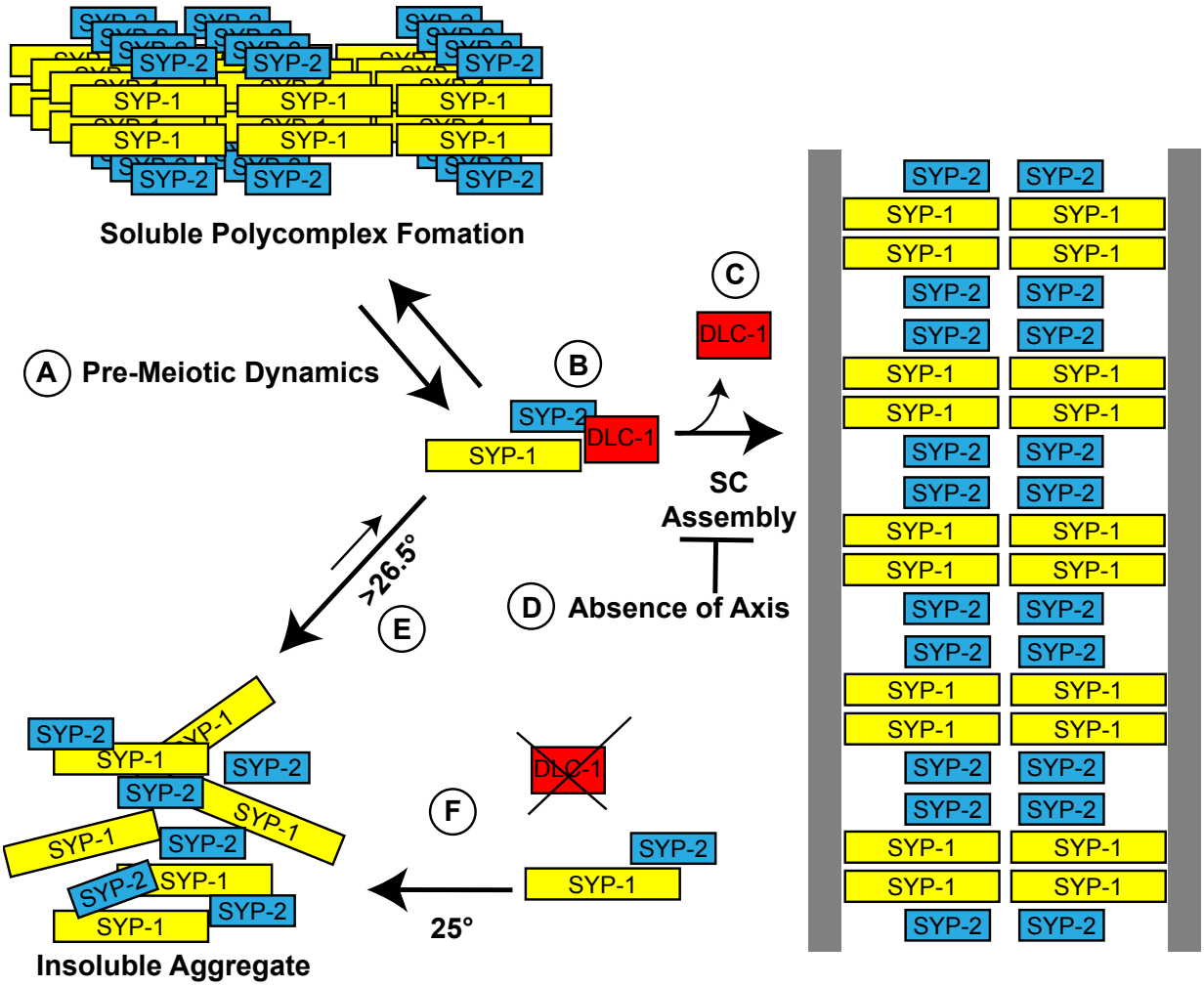

Figure 2.7. Model of DLC-1's role in pre-synapsis meiosis. (A) As meiosis begins, SYP proteins initially form small dynamic polycomplexes before the SC assembles onto paired homologs. (B) DLC-1 binding to SYP-2 helps to prevent temperature-dependent aggregation before synapsis initiates, (C) and disassociates during synapsis. (D) In the absence of axial components, assembly onto chromosomes is prevented, and polycomplexes are stabilized. (E) At temperatures higher than 26.5°, SYP proteins no longer fold correctly and form insoluble aggregates away from chromosomes even in the presence of DLC-1. (F) Without DLC-1, and more frequently at temperatures

approaching 25°, SYP proteins will no longer fold correctly and also form aggregates away from chromatin.

2.8 Tables

sgRNA name	Sequence
Dpy10 sgRNA	GCUACCAUAGGCACCACGAG
Syp2 guide 1 sgRNA	AUUUAUAACUUGUCAGCCCA
Syp2 guide 2 sgRNA	UUACGACAAACUUCUGGAUU
Syp2 guide 3 sgRNA	ACAAGAUCUGACAAUGGAGC
Syp2 guide 4 sgRNA	AAUGACACAAGAUCUGACAA

Table 2.1. sgRNA sequences used for transgenic strain construction. Syp2 guide 1 and 2 were used together in the same injection mix to generate ck38 and syp2 guide 3 and 4 were used together in the same injection mix to generate line ck39.

Name	Oligo HDR repair template sequence 5' to 3'
Dpy10 ssDNA	CACTTGAACTTCAATACGGCAAGATGAGAATGACTGGAAACCGTAC CGCaTgCGGTGCCTATGGTAGCGGAGCTTCACATGGCTTCAGACCA ACAGCCTAT
Syp-2::GFP gBlock®	CAATGATGTTCAGGCGGCTATAAAAATAATCAATAATGCAAAAATCA ACAACGATGGGTTCTCGGAAGATTTCTCTGCTCATTACGACAAACTT CTGGATCTCGTTGAAACGCTCGAGCCGTGGGCTGACAAGTTAGGA GGTGGAGGTGGAGCTATGAGTAAAGGAGAAGAACTTTTCACTGGA GTTGTCCCAATTCTTGTTGAATTAGATGGTGATGTTAATGGGCACAA ATTTTCTGTCAGTGGAGAGGGTGAGGGTGATGCAACATACGGAAAA CTTACCCTTAAATTTATTTGCACTACTGGAAAACTACCTGTTCCATG GGTAAGTTTAAACATATATATACTAACTAACCCTGATTATTTAAATTT TCAGCCAACACTTGTCACTACTTTCTGTTATGGTGTTCAATGCTTCT CGAGATACCCAGATCATATGAAACAGCATGACTTTTTCAAGAGTGC CATGCCCGAAGGTTATGTACAGGAAAGAACTATATTTTTCAAAGATG ACGGGAACTACAAGACACGTAAGTTTAAACAGTTCGGTACTAACTA ACCATACATATTTAAATTTTCAGGTGCTGAAGTCAAGTTTGAAGGTG ATACCCTTGTTAATAGAATCGAGTTAAAAGGTATTGATTTTAAAGAA GATGGAAACATTCTTGGACACAAATTGGAATACAACTATAACTCACA CAATGTATACATCATGGCGGACAAACAAAAGAATGGAATCAAAGTT GTAAGTTTAAACATGATTTTACTAACTAACTAATCTGATTTAAATTTT CAGAACTTCAAAATTAGACACAACATTGAAGATGGAAGCGTTCAACT AGCAGACCATTATCAACAAAATACTCCAATTGGCGATGGCCCTGTC CTTTTACCAGACAACCATTACCTGTCCACACAATCTGCCCTTTCGAA AGATCCCAACGAAAAGAGAGACCACATGGTCCTTCTTGAGTTTGTA ACAGCTGCTGGGATTACACATGGCATGGATGAACTATACAAAtaaatc atctgttgtattcaatttccttgttttattacatgacatgtatcattttaatgtttgtccatcgtattgcatgtattg ctttctcaaatatggg
Syp2 (AMTA) ssDNA	GGATGACGTTTCTGAAATTGAACACAAAATGATCAAGCAGGCGgctat gacagctGATCTGACAATGGAGCTCGCAAATTCAATCGAACGTATCGC AAATATGGCATTAGC

Table 2.2. Repair templates used for transgenic strain construction. Underlined, lowercase sequence indicates non-silent mutations. Uppercase, underlined letters indicate silent mutations to PAM sites. Dark green letters indicate *gfp* sequence, and blue letters indicate GGGGGA linker sequence. PAM site mutation for *syp-2::gfp(AMTA)* strain was not integrated into the genome as confirmed with strain sequencing.

Gene	Forward primer	Reverse primer
dlc-1	GGTACCCACGTAGGATCAGGTCACAA	GCGGCCGCCCGCATTCACAACCGTTATT

Table 2.3. Primers used to amplify regions of genes from genomic DNA to insert into L4440. Blue letters represent added restriction sequences (NotI and KpnI) for ease of addition into the multi-cloning site of the L4440 vector.

	Ratio of FLAG::DLC-1 to SYP-2::GFP pull down
WT *syp-2::gfp*	0.733
syp-2::gfp (AMTA)	0.577

Table 2.4. Less FLAG::DLC-1 pulls down with SYP-2::GFP(AMTA) than WT SYP-2::GFP. Band intensities for FLAG::DLC-1 in anti-GFP co-immunoprecipitation were calculated using ImageJ (Fig. 2.4) and divided by intensities of corresponding SYP-2::GFP bands that were immunoprecipitated (Fig. 2.S4).

2.9 Supplemental Material

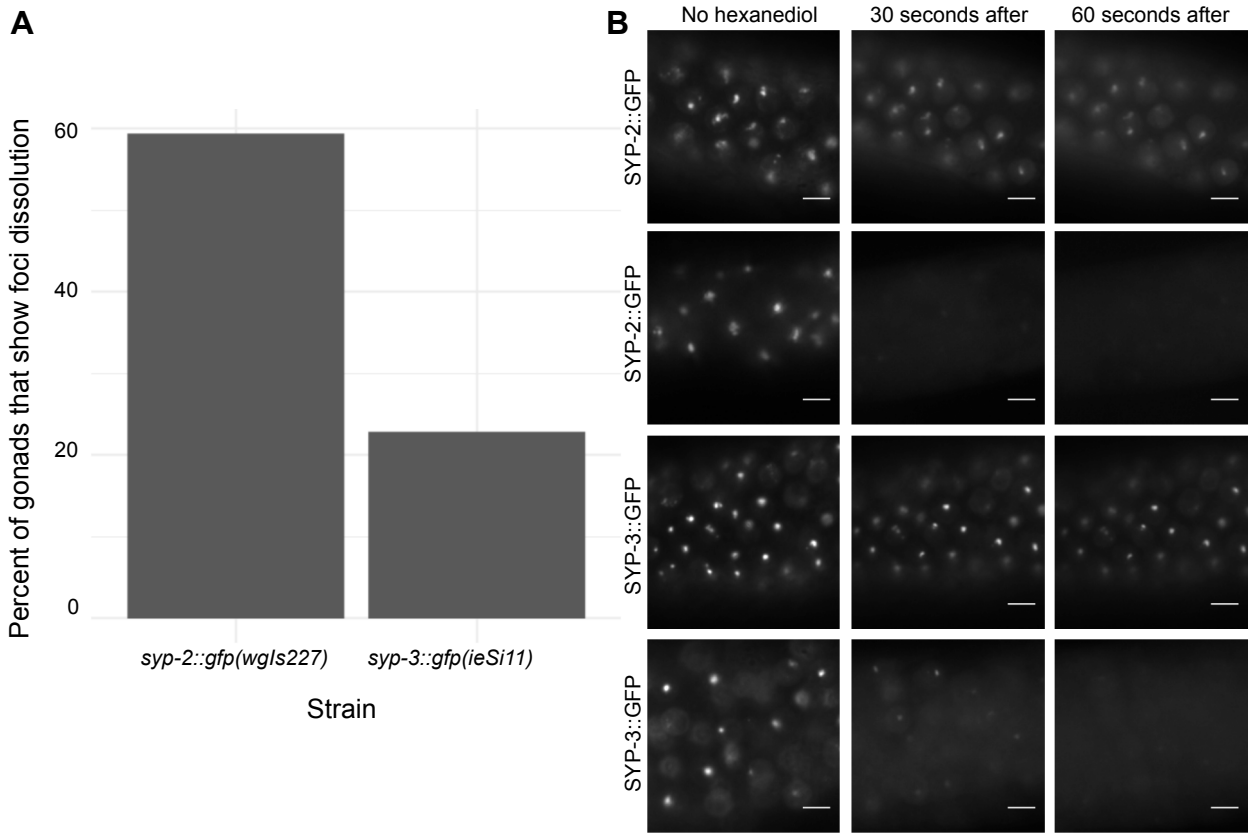

Supplemental Figure 2.S1. Heat induced foci are partially susceptible to 1,6-hexanediol. (A) In *syp-2::gfp(wgIs227); syp-2(ok307)* V gonads with heat-induced foci, 59.38% show dissolution of foci when exposed to 1,6-hexanediol (n=64), while only 22.86% of foci in *syp-3::gfp(ok758;ieSi11)* dissolve when exposed (n=35) (examples in B) (B) Live imaging of GFP in *wgIs227; syp-2(ok307)* V gonads (top two rows), and *syp-2::gfp(ok758;ieSi11)* gonads (bottom two rows); all animals grown at 27.5° for 24 hours starting at larval stage L4. Examples of *syp-2::gfp(wgIs227)* gonads with foci that do not dissolve with addition of 1,6-hexanediol (top row), and *syp-2::gfp(wgIs227)* gonads that show dissolution (second row). Examples of *syp-3::gfp(ok758;ieSi11)* that do not dissolve with exposure to 1,6-hexanediol (third row), and that do dissolve with exposure (bottom row). Scale bars 5μm.

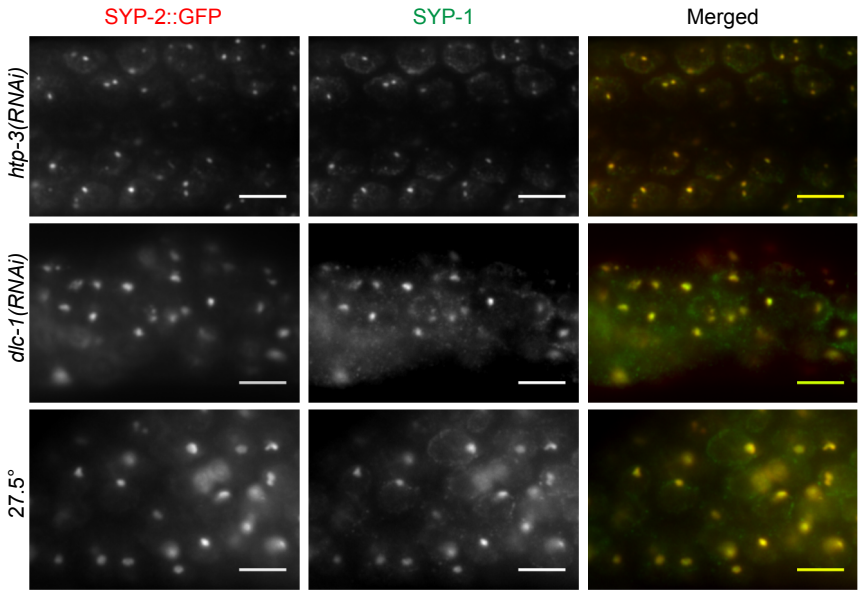

Supplemental Figure 2.S2. SYP-2 and SYP-1 co-localize in foci formed under various conditions. Whole mount fixed, age matched *wgIs227*; *syp-2(ok307)* V gonads were probed with anti-GFP and anti-SYP-1. All SYP-2::GFP foci overlap with all SYP-1 foci in *htp-3(RNAi)* animals raised at 25° (top row), *dlc-1(RNAi)* animals raised at 25° (middle), or animals raised at 27.5° (bottom). Meiotic progression depicted from left to right. Scale bars 5μm.

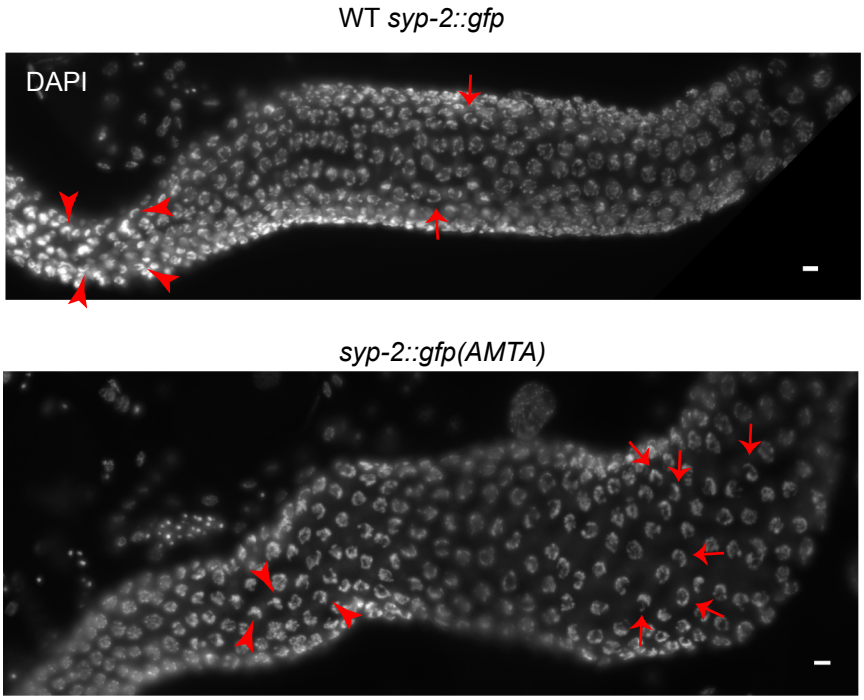

Supplemental Figure 2.S3. Mutation of putative binding site in SYP-2 results in meiotic defects. Whole mount fixed gonads of age matched animals probed with DAPI. Many nuclei in *syp-2::gfp(AMTA)* hermaphrodites show odd DNA conformation throughout gonad (arrows) reminiscent of clustering of transition zone nuclei (arrowheads). This is rarely observed in WT *syp-2::gfp* hermaphrodites (arrows). Meiotic progression from left to right in all images. Scale bars 5μm.

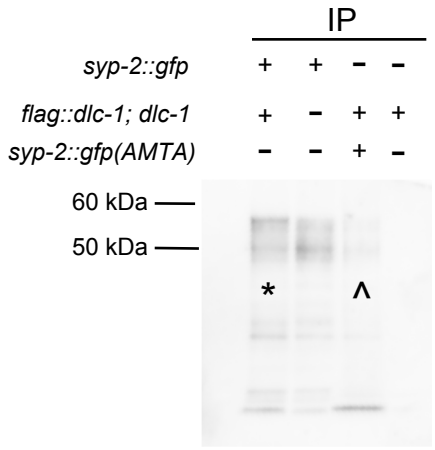

Supplemental Figure 2.S4. Anti-GFP IP less efficient in the mutant line. Protein lysates from the indicated age matched strains were subjected to immunoprecipitation with anti-GFP antibody, followed by western blot analysis of the precipitates probed with anti-GFP. SYP-2::GFP consistently migrates as a doublet at 50 kDa-55 kDa A lower amount of SYP-2::GFP(AMTA) (carrot) immunoprecipitated than WT SYP-2::GFP (asterisk).

CHAPTER 3: MULTIPLE SEX-SPECIFIC DIFFERENCES EXIST IN THE REGULATION OF SYNAPSIS IN *C. ELEGANS* MEIOSIS

Sara M. Fielder, Rieke Kempfer, and William G. Kelly

This work is under revision for the journal Genetics.

Sara Fielder performed experiments and data analysis for Figures 3.1, 3.3, 3.4 (except for row 4 of Figure 3.4, which was performed by Rieke Kempfer), 3.5- 3.8, and Supplementary figure 3.S1. WG Kelly performed experiments for Figures 3.2 and 3.S2. Model Figure 3.9 designed by Sara Fielder.

3.1 Abstract

Meiosis is a highly conserved sexual process, yet significant differences exist between males and females in meiotic regulation in many species. Meiotic progression in *C. elegans* males proceeds more rapidly than hermaphrodite meiosis, suggesting that hermaphrodite meiotic regulation may be more stringent than in males. We have identified multiple differences in the regulation of synapsis, including a difference that suggests the presence of a hermaphrodite-specific meiotic checkpoint that senses the proper initiation of synapsis. This checkpoint is detected by sex differences in the targeting of histone H3 lysine 9 dimethylation (H3K9me2) to unsynapsed chromatin. During oogenic meiosis in hermaphrodites, the failure to initiate synapsis leads to failure to target H3K9me2 enrichment on unsynapsed chromosomes. Loss of the pachytene checkpoint does not reintroduce H3K9me2 enrichment in hermaphrodites, indicating these checkpoints are separable. In contrast, widespread H3K9me2 enrichment occurs

as a result of loss of synapsis initiation in both male meiosis and during spermatogenic meiosis in larval XX hermaphrodites. Additionally, male synapsis is insensitive to loss of the dynein motor light chain DLC-1 and to elevated temperatures, whereas hermaphrodite synapsis is prevented by both conditions. We also show that loss of spindle assembly checkpoint proteins, which provide a kinetic barrier to meiotic progression and are required for DLC-1-dependent synapsis phenotypes in hermaphrodites, does not speed up the rate of synapsis in spermatogenic meiosis of larval hermaphrodites. These results indicate that meiosis proceeds more rapidly in males because males lack barriers to meiotic progression that is activated by defective synapsis initiation in hermaphrodites.

3.2 Introduction

Meiotic synapsis of homologous chromosomes is required in both oogenesis and spermatogenesis to prevent sterility and developmental defects caused by aneuploidies in the offspring. *C. elegans* has been developed as an excellent genetic model system for studying meiotic processes, aided by their transparent gonad in which an assembly line of germ cells progressing through sequential stages of meiotic prophase I is readily visible. Germline stem cells, which divide throughout the adult life of each animal, populate a distal mitotic region, and then move proximally and exit mitosis to enter the leptotene and zygotene stages of Meiosis I. In this region, called the “transition zone” (TZ), the chromosomes condense and cluster together at the nuclear periphery, yielding characteristic crescent shaped nuclei (reviewed in (LUI AND COLAIACOVO 2013)). This organization is mediated by Zinc finger In Meiosis (ZIM) proteins, each of which bind to specific DNA sequences, named “pairing centers”, on one end of one or two

chromosomes (described below), and help attach them to each other and to the nuclear envelope (PHILLIPS AND DERNBURG 2006; PHILLIPS *et al.* 2009). While pairing and homology are being established, lateral elements of the synaptonemal complex (HIM-3, HTP-3, etc) assemble onto chromosomes, and form an axis onto which central element (CE) components (e.g., SYP proteins) assemble (ZETKA *et al.* 1999; COUTEAU AND ZETKA 2005; GOODYER *et al.* 2008; KOHLER *et al.* 2017). The outer nuclear membrane protein ZYG-12 connects chromosomes to the motor complex dynein in the cytoplasm through binding to the inner nuclear membrane protein SUN-1 (PENKNER *et al.* 2007; SATO *et al.* 2009). This trans-nuclear membrane connection to cytoplasmic dynein motors is proposed to move chromosomes around the nuclear periphery during their search for their homologs (PENKNER *et al.* 2007; SATO *et al.* 2009; WYNNE *et al.* 2012; WOGLAR AND JANTSCH 2014).

Defects in or depletion of dynein motor components cause a decrease but not complete cessation of movements of chromosome ends around the nuclear periphery (WYNNE *et al.* 2012), and pairing takes longer to occur, increasing the TZ length (SATO *et al.* 2009). Less than half of nuclei will have an incorrectly paired chromosome II with a defect in the dynein complex, implying that dynein induced movements aid, but are not completely necessary for correct homolog pairing (SATO *et al.* 2009). As mentioned, in *C. elegans* one end of each chromosome is enriched for genetic elements that comprise pairing centers that aid in homolog identification and pairing (MACQUEEN *et al.* 2005; PHILLIPS *et al.* 2005; PHILLIPS AND DERNBURG 2006). ZIM proteins recognize and bind to these elements, and inter-ZIM protein interactions help to match up potential homologous chromosomes (MACQUEEN *et al.* 2005; PHILLIPS *et al.* 2005; PHILLIPS AND

DERNBURG 2006). Because some ZIM proteins can bind to more than one specific chromosome, the proposed role of the dynein motor is to provide forces to test the strength of interactions within each paired homolog set and pull apart incorrect matches. Once a match has survived this test, SYP proteins (SYP-1, -2, -3, and -4) form a dynamic, physical bridge that "zips" the homologs together starting near ZIM proteins and processing down the length of the condensed chromosomes (SCHILD-PRUFERT *et al.* 2011; ROG AND DERNBURG 2015; ROG *et al.* 2017). Depletion of dynein motor components has been reported to cause off-chromatin assembly of SYP proteins into "polycomplexes", as does deletion of a lateral element such as HTP-3 (SATO *et al.* 2009; ZHANG *et al.* 2015; ROG *et al.* 2017). The polycomplexes resulting from deletion of HTP-3 have a structural organization similar to that found in the chromosome-associated synaptonemal complex (ROG *et al.* 2017). Synapsis in hermaphrodites is also inherently temperature sensitive, as exposure to temperatures above 26.5° results in unrecoverable aggregation of SYP proteins into structures that are different from polycomplexes (BILGIR *et al.* 2013; ROG *et al.* 2017). Sequestration of SYP proteins into these polycomplexes and aggregates results in failure of meiosis in these nuclei.

As homologous chromosomes complete synapsis, they spread out within the nucleus and then enter the pachytene stage, where recombination occurs. In *C. elegans,* any chromosomes or chromosome segments that remain unsynapsed, such as the single male X, are targeted for enrichment of histone H3 lysine 9 dimethylation (H3K9me2)(BEAN *et al.* 2004). Related processes occur in mice and other organisms, called meiotic silencing of unsynapsed chromosomes (MSUC), with enrichment of repressive epigenetic marks on any chromosomes or segments that fail to completely

synapse (KHALIL *et al.* 2004; TURNER *et al.* 2005; TURNER *et al.* 2006)(reviewed in (TURNER 2007). Despite the enrichment of the heterochromatin mark, it is unclear whether genes on the enriched chromosomes are actually ”silenced”, but the H3K9me2 enrichment has been proposed to help “hide” the unsynapsed X chromosome from the synapsis checkpoint machinery in *C. elegans* males (CHECCHI AND ENGEBRECHT 2011). In this synapsis checkpoint, Pachytene Checkpoint Protein 2 (PCH-2) senses pairing proteins bound to unsynapsed chromatin during pachytene and activate the apoptosis pathway to prevent aneuploid, and thus defective, gametes from developing (BHALLA AND DERNBURG 2005) . Checkpoints in meiosis ensure that important processes have been completed before progressing into subsequent steps, and either prevent progression until that process is completed, or, if they are unable to be completed, sentence cells to apoptosis.

Although the final goal of meiosis –the generation of haploid gametes- is the same in males and females, there are significant differences in basal aspects of meiosis observed between spermatogenesis and oogenesis. An obvious difference is that completion of oogenic meiosis results in a single oocyte, whereas four equal sperm cells are produced from each germ cell in spermatogenesis. Another difference in mammals is that males have more stringent responses to errors in meiosis than females: defects in oocytes that lead to arrest and/or apoptosis in spermatogenesis can by-pass inspection during oogenesis and lead to an increased rate in aneuploidy in mammalian females as compared to mammalian male gametes (Reviewed in (MORELLI AND COHEN 2005)). However, not all organisms have increased stringency in male meiosis as compared to female meiosis. For example, female *Drosophila* synapse and

recombine their chromosomes but neither of these processes occur in males and spermatogenesis proceeds uninterrupted (MORGAN 1914). Interestingly, *C. elegans* males complete prophase nearly two and a half to three times faster than hermaphrodites, and it has been speculated that less stringent checkpoints in males may account for this difference (JARAMILLO-LAMBERT *et al.* 2007). There is substantial apoptosis during *C. elegans* oogenesis, but apoptosis is inhibited in spermatogenesis, even in cases where meiotic checkpoints are activated (GUMIENNY *et al.* 1999; GARTNER *et al.* 2000). Indeed, male germ cells attempt to repair any damage that would normally set off a checkpoint, yet do not eliminate germ cells that are ultimately unable to repair genomic defects during Prophase I (JARAMILLO-LAMBERT *et al.* 2010).

In this study, we identify and examine two additional differences in early meiotic prophase between spermatogenesis and oogenesis. First, we identify an apparent checkpoint, operating only in oogenesis, which senses the initiation of synapsis. This checkpoint is observed when examining the onset of H3K9me2 enrichment on unsynapsed chromatin: if synapsis initiation occurs normally or is only delayed, unsynapsed chromosomes become enriched with this modification. However, if synapsis initiation is not reached in hermaphrodite meiosis, H3K9me2 enrichment is not observed on any chromosomes. The proposed checkpoint appears to engage after pairing is complete but before the onset of synapsis: if synapsis even partially initiates on one or two sets of chromosomes, H3K9me2 enrichment is observed. In contrast, all chromosomes become enriched for H3K9me2 in male mutants lacking any synapsis initiation. Second, as previously reported (SATO *et al.* 2009; ZHANG *et al.* 2015), when dynein is depleted during leptotene/zygotene in oogenesis, SYP proteins associate into

polycomplexes unassociated with chromosomes. However, polycomplexes are not observed in male meiotic cells lacking dynein function. The connection between these processes is not currently understood, but may illustrate a novel and basal sex-specific difference in the stringency of meiotic genome quality control between the two sexes.

3.3 Methods

Strains

Strains used in this paper are AV307 (*syp-1*(me17) V/ nT1 (IV;V)), CA258 (*zim-2* (tm574)), N2 Bristol strain, CA1207 (*dhc-1* (ie28[*dhc-1*::degron::GFP]) I), CA1199 (*unc-119*(ed3) III; ieSi38[sun-1p::TIR1::mRuby::sun-1 3'UTR + Cbr-unc-119(+)] IV), wgls227 [syp-2::TY1::EGFP::3xFLAG(92C12) + unc-119(+)]; *syp-2*(ok307) V, *him-5*(e1467), *pch-2*(tm1458) II, *her-1*(e1518), *tra-2*(q276), and *rrf-3(pk1426)* I. The *syp-2:gfp (ck38)V* allele was generated using CRISPR-mediated GFP tagging of the endogenous locus (Fielder and Kelly, manuscript in preparation). All strains were grown at 20° on NGM plates unless noted otherwise noted. Large quantities of synchronized stages were obtained by adding bleach to a final concentration of 10% and incubating for 5-7 minutes to dissolve adults, followed by three washes with M9. Embryos obtained were rocked overnight at room temperature without food to allow hatching and synchronization of L1s. Some strains were provided by the CGC, which is funded by NIH Office of Research Infrastructure Programs (P40 OD010440).

RNA interference

RNAi knockdown of *htp-3* was achieved by feeding animals with HT115 bacterial cells transformed with an *htp-3* RNAi clone (F57C9.5) from Source BioScience (KAMATH *et al.* 2003). Knockdown of *dlc-1* was achieved by transforming the plasmid developed

in Chapter 2 into HT115 cells, and feeding the resulting bacteria to animals. Empty vector control RNAi was performed by feeding animals HT115 bacteria transformed with the empty vector RNAi plasmid L4440 (a generous gift from Andrew Fire).

For all RNAi knockdown experiments, animals were fed with dsRNA expressing bacteria starting from the L1 larval stage at 20° until 24 hours past the larval L4 stage, and were then shifted to 25° for 24 or 48 hours before examination by immunofluorescence, except where noted differently in Figure 3.2.

Immunofluorescence

Immunofluorescence was performed essentially as previously described (AHN *et al.* 2017), except animals were fixed with 1% final concentration of paraformaldehyde, then slides were frozen with coverslips for less than five minutes on a dry ice block followed by incubation in 100% ethanol at -20° for 2 minutes. Primary antibodies used were goat anti-SYP-1 (1:1500)(HARPER *et al.* 2011) guinea pig anti-HTP-3 (1:500)(MACQUEEN *et al.* 2005), guinea pig anti-ZIM-2 (1:200)(PHILLIPS AND DERNBURG 2006), rabbit anti-ZIM-1 (1:200)(PHILLIPS AND DERNBURG 2006), rabbit anti-ZIM-3 (1:200)(PHILLIPS AND DERNBURG 2006) (all generous gifts from Abby Dernburg), rabbit anti-MDF-1 (1:500), rabbit anti-MDF-2 (1:500)(ESSEX *et al.* 2009), rabbit anti-BUB-3 (1:500)(ESSEX *et al.* 2009), (generous gifts from Arshad Desai), and mouse anti-H3K9me2 (1:500) (Abcam ab1220). Secondary antibodies were used at 1:500 dilution: donkey anti-goat (Invitrogen A11055), donkey anti-rabbit (Invitrogen A21207), donkey anti-mouse (Invitrogen A21203), rabbit anti-guinea pig (ThermoFisher PA1-28595).

Auxin induction

Auxin induced degradation was performed essentially as previously described (ZHANG *et al.* 2015). A stock solution of 400mM auxin (Alfa Aesar #A10556) dissolved in ethanol was kept in a light proof tube at 4° for no more than a week. NGM media was prepared and cooled to approximately 50° before adding 1mM final concentration of auxin. Poured plates were kept in tin foil-lined containers to avoid exposing plates to light. OP50 bacteria were seeded onto auxin plates and grown at room temperature in a dark cabinet for 2 days before adding worms that were 24 hours past larval L4 stage for auxin induction. Auxin exposure to worms took place in a dark 20° incubator for 8 hours before analysis by immunofluorescence.

Hexanediol treatment

Animals treated with RNAi were dissected on poly-L-lysine coated slides in 1x egg buffer + 2.5mg/mL levamisole to immobilize animals. Slides were immediately live imaged for before pictures, and 2x volume of 10% 1,6-hexanediol (Acros Organics/Fisher Scientific 120650010) dissolved in 1x egg buffer for a final concentration of 6.67% was gently pipetted under the coverslip. Images were taken 30 seconds after addition of hexandeiol.

3.4 Results

3.4.1 H3K9me2 targeting to unsynapsed chromosomes differs between sexes

Dimethylation of histone H3 on lysine 9 (H3K9me2) is normally detectable at low levels by immunofluorescence in *C. elegans* pachytene stage germ cells, and is largely confined to the ends of the chromosomes (KELLY *et al.* 2002; REUBEN AND LIN 2002) (Fig. 3.1). However, this modification becomes enriched when one or more sets of homologs fail to synapse, and is also enriched at unsynapsed chromosomal segments (KELLY *et al.* 2002; BEAN *et al.* 2004). Examples include the asynapsed lone X chromosome in males (BEAN *et al.* 2004) (Fig. 3.1), or the two unsynapsed chromosome V's in *zim*-2 (Fig. 3.1). Additionally, *zim-1* mutant hermaphrodites that cannot pair or synapse multiple chromosome pairs (LG II and III) display as many as four chromosomes with high enrichment for H3K9me2 (data not shown). Thus when multiple chromosomes remain unsynapsed, they are targeted for H3K9me2 enrichment in hermaphrodite germ cells. Importantly, in these cases the remaining chromosomes still engage in normal synapsis and are not enriched in H3K9me2. We also investigated mutants that have a complete synapsis defect in all chromosomes, such as occurs in *syp-1* mutants. Surprisingly, in the complete absence of synapsis no enrichment of H3K9me2 was observed on any chromosomes in the pachytene region of *syp-1* hermaphrodite germ cells (adult hermaphrodite germ cells will be referred to as female germ cells for clarity; Fig. 3.1). The absence of H3K9me2 enrichment was also observed in other animals with complete synapsis defects, such as *syp-2* and *him-3* mutants; furthermore, the lack of H3K9me2 enrichment in chromatin was not due to dispersal of a limited signal, as H3K9me2 signal in *syp* mutants mid-gonad nuclei is over ten times lower than that of

zim-2 mutant nuclei (Table 3.1). As previously shown, mutants with complete asynapsis also display an extended region of condensed, crescent-shaped chromatin that is normally restricted to the transition zone, indicating that meiotic progression has stalled in these nuclei (MACQUEEN *et al.* 2002). Both of these pieces of information could indicate that meiosis in synapsis mutants is stalled due to activation of a checkpoint.

Unexpectedly, in contrast to what we observed in hermaphrodite germ cells, male *syp-1* mutants displayed widespread enrichment of H3K9me2 in germ cell chromatin on all chromosomes in pachytene nuclei (Fig. 3.1). The enrichment of H3K9me2 on all chromosomes in male germ cells further indicates that the absence of enrichment in hermaphrodite germ cells is not due to a more diffuse or diluted enrichment due to an increase in unsynapsed chromatin substrate. The difference in responses to the loss of synaptonemal components in males versus hermaphrodites is due to germline sex: *syp-1* larval L4 hermaphrodites, which undergo spermatogenesis before switching to oogenesis at the L4/adult molt, display widespread enrichment of H3K9me2 (Fig. 3.1). These results indicate that there is a differential regulation of H3K9me2 targeting to unsynapsed chromosomes during meiosis in male versus hermaphrodite germlines, and implies that males could be escaping a checkpoint that stalls meiosis in hermaphrodties.

In WT hermaphrodites, a widespread enrichment of H3K9me2 on chromatin normally begins in diplotene (KELLY *et al.* 2002; BESSLER *et al.* 2010) (Fig. 3.S1). This enrichment coincides temporally with the beginning of removal of SYP proteins in preparation for chromosome separation. This is also observed in *syp-1* hermaphrodites: at the bend of the gonad arm, when diplotene normally occurs, H3K9me2 enrichment is

observed (Fig. 3.S1). The H3K9me2 enrichment at the end of pachytene further implies that the absence of this mark earlier in meiotic progression is not due to a dispersal of the signal, nor to a defect in methyltransferase activity. These results imply that hermaphrodite germ cells have separable modes of H3K9me2 regulation: one that requires the initiation of synapsis and is absent in SC mutants, and one that occurs in diplotene that is unaffected by defective synapsis initiation.

3.4.2 PCH-2 is not required for adult hermaphrodite- specific prevention of H3K9me2 enrichment with disrupted synapsis

PCH-2, a homolog of yeast PCH2, is required for the selective apoptosis of cells with defective synapsis during hermaphrodite meiosis in *C. elegans* and is proposed to regulate the "pachytene checkpoint" in *C. elegans* (BHALLA AND DERNBURG 2005). PCH-2 is expressed before the onset of meiosis, and is required to restrain meiotic progression kinetics, with meiosis proceeding more rapidly in *pch*-2 mutants. PCH-2 is thus thought to provide a "kinetic barrier" to ensure meiotic quality control (DESHONG *et al.* 2014). In contrast to hermaphrodites, defects in *C. elegans* male synapsis do not induce apoptosis, and meiosis proceeds with faster kinetics in males versus hermaphrodites, suggesting that PCH-2's activity may not be required in males, and may be involved in the hermaphrodite specific regulation of H3K9 methylation (JARAMILLO-LAMBERT *et al.* 2007; DESHONG *et al.* 2014). Disabling a PCH-2 dependent checkpoint in hermaphrodites could thus allow the accumulation of H3K9me2 to occur in the complete absence of synapsis. We therefore knocked down *syp*-2 by GFP RNAi in a line expressing a CRISPR-generated *syp-2:gfp* in the presence or absence of the *pch-2 (tm1458)* mutation. No increased H3K9me2 enrichment was observed in the *pch-*

2(tm1458); syp-2:gfp(ck38) hermaphrodite germ cells relative to those in *syp-2:gfp(ck38)*, despite a clear disruption of synapsis by GFP RNAi (Fig. 3.2). With knockdown of HTP-3 in *pch-2*, there is occasional widespread enrichment of H3K9me2 in hermaphrodite germ cells, but this is mirrored by occasional widespread enrichment of H3K9me2 in hermaphrodite germ cells with knockdown of HTP-3 alone (Fig. 3.S2). Therefore, the pachytene checkpoint that is regulated by PCH-2 does not appear to be involved in the prevention of H3K9me2 accumulation in hermaphrodite mutants unable to initiate synapsis. PCH-2 loading onto the SC is only observed after synapsis has begun, thus its activity may be required after the initiation of synapsis and thus later than the sex-specific process we observe (DESHONG *et al.* 2014).

3.4.3 Initiation of synapsis is required for H3K9me2 enrichment of unsynapsed chromosomes in adult hermaphrodite meiosis

In some *htp-3(RNAi)* hermaphrodites we noticed that a few nuclei had small, faint SYP-1 tracks between one or two chromosomes, with the rest of SYP-1 in foci away from chromatin (Fig. 3.3, arrows). These nuclei had at least partially initiated synapsis, and also displayed enrichment of H3K9me2 on other chromosomes (Fig. 3.3, arrows). This contrasted with other nuclei in the same gonad that had no or extremely little synapsis and little H3K9me2 enrichment (Fig. 3.3, arrowheads). We further investigated the temporal dynamics of H3K9me2 targeting to unsynapsed chromatin by utilizing RNAi knockdown of dynein motor light chain 1 (DLC-1) in a temperature shift experiment. *dlc-1(RNAi*) animals grown at 25° form foci of synapsis proteins instead of normal SC tracks between chromosomes (SATO *et al.* 2009). Nuclei that entered meiosis during the period of temperature shift showed SYP-1 foci and low H3K9me2

enrichment (Fig. 3.3, arrowheads), as was observed in *syp-1* and other mutants with complete synapsis defects. In contrast, more proximal nuclei showed some SYP-1 loading onto chromatin, indicating these nuclei had partially entered meiosis at the onset of the temperature shift (Fig. 3.3, arrows). These proximal nuclei had very short SYP-1 tracks localized to one or two chromosomes, yet the rest of the chromosomes that lacked SYP-1 were highly enriched for H3K9me2, (Fig. 3.3, arrows). However, there do appear to be occasional instances where there is H3K9me2 enrichment when there is no obvious synapsis initiation; however, there could be a very small track of synapsis loading that looks like a polycomplex (Fig. 3.3). These results are generally consistent with a requirement for some level of synapsis initiation to occur before H3K9me2 enrichment on unsynapsed chromosomes can be triggered, and implies that the checkpoint stalling meiosis is near or at the time of synapsis initiation.

3.4.4 Dynein is not required for males to correctly pair and synapse chromosomes.

Dynein motors have been proposed to play an essential role in testing for proper pairing and the subsequent initiation of synapsis (SATO *et al.* 2009). Interestingly, as opposed to hermaphrodites exposed to RNAi in parallel, *dlc-1(RNAi)* males did not exhibit SYP-1 foci, and instead displayed grossly normal synapsis (Fig. 3.4). In contrast, *htp-3(RNAi)* animals form SYP-1 foci in the germlines of both sexes (Fig. 3.4), indicating this result is not a difference in RNAi efficiency in the two sexes. To address if the *dlc-1(RNAi)* phenotype is a germline sex or chromosome count specific phenotype, we also tested sex determination mutants: *her-1(e1518)* XO females, and *tra-2(q276)* XX males. SYP-1 foci were observed in *her-1 dlc-1(RNAi)* XO females (Fig. 3.4), while *tra-2 dlc-*

1(RNAi) XX males displayed grossly normal synapsis (Fig. 3.4). These results suggest that male germ cells, whether of karyotype XO or XX, can initiate synapsis despite a loss of DLC-1.

To further investigate the apparent lack of a requirement for dynein in male meiosis, we next investigated whether males require dynein heavy chain (DHC-1), another dynein complex protein, for synapsis. We utilized the auxin inducible degradation (AID) system targeting dynein heavy chain, DHC-1, adapted for use in *C. elegans* by the Dernburg lab (ZHANG *et al.* 2015). SYP-1 foci were observed in hermaphrodite germ cells after 8 hours of auxin-induced degradation (Fig. 3.4). In contrast, males grown on the same plates displayed grossly normal tracks of SYP-1 proteins (Fig. 3.4) instead of the foci observed in their hermaphrodite counterparts, further indicating that males do not need dynein in order to synapse their chromosomes.

As mentioned, dynein has been proposed to play a role in ensuring the correct pairing of homologs prior to synapsis onset. As dynein is not required for male synapsis, we next investigated whether these males were still able to correctly pair their chromosomes. It has been previously shown that hermaphrodites with depleted dynein have a pairing defect: by the end of meiosis, only 60% of hermaphrodites with depleted dynein correctly pair and synapse chromosome V (SATO *et al.* 2009). We performed immunofluorescence probing ZIM-2 on *dlc-1(RNAi)* males that had been grown at 25° for 24 hours. The region showing ZIM-2 foci was distributed into four zones (Fig. 3.5A) and pairing status of chromosome V was measured in each nucleus (Fig. 3.5B). These males have statistically the same rates of pairing as their empty vector RNAi counterparts at all four zones analyzed ($p=0.825$, $p=0.054$, $p=0.424$, and $p=0.424$,

respectively) (Fig. 3.5C), indicating that males do not need *dlc-1* in order to correctly pair their chromosomes. Further, as pairing can still occur in both *dlc-1(RNAi)* hermaphrodite and male germ cells, but H3K9me2 is not enriched in *dlc-1(RNAi)* hermaphrodites, this indicates that H3K9me2 enrichment of unsynapsed chromosomes normally is triggered after pairing has completed (SATO *et al.* 2009).

3.4.5 Male synapsis is not as sensitive to heat as hermaphrodite synapsis

As we identified several differences between males and hermaphrodites related to initiation of synapsis, we decided to investigate if the synaptonemal complex formed in males has similar characteristics as that formed in hermaphrodites. Previous electron-microscopic analyses revealed that the foci formed in *htp*-3 mutants have a similar structure, albeit unassociated with chromosomes, to synaptonemal complexes on synapsed chromosomes (ROG *et al.* 2017). They additionally showed that exposure to amphiphilic alcohols, such as 1,6-hexanediol, readily disperses both *htp-3* mutant foci as well as the correctly assembled synaptonemal complex (ROG *et al.* 2017). However, foci formed at higher temperatures (above 26.5°) do not dissolve when exposed to 1,6-hexanediol, implying a change in protein structure (BILGIR *et al.* 2013; ROG *et al.* 2017). Unexpectedly, male synaptonemal complexes are resistant to elevated temperatures, even to 27.5°, and these SYP tracks observed at elevated temperatures still dissolved with exposure to 1,6-hexandiol, similar to hermaphrodite synaptonemal complexes formed under standard growing temperatures (Fig. 3.6) (ROG *et al.* 2017). Additionally, larval stage L4 hermaphrodite germ cells, which produce sperm, also do not display SYP foci when raised at 27.5° and the SC formed was also readily dispersed by 1,6-hexandiol (Fig. 3.6). These results suggest that although there is not an obvious

structural difference in the SC in male and hermaphrodite germ cells once formed, the formation of the SC appears to have an inherent temperature sensitivity in hermaphrodite meiosis that is not observed in male germlines.

3.4.6 Spindle assembly checkpoint proteins in males.

Male meiosis in *C. elegans* has been shown to progress more rapidly than hermaphrodite meiosis (JARAMILLO-LAMBERT *et al.* 2007). In support of this, we noticed that males also appear to complete pairing faster than in hermaphrodites. Empty vector control RNAi males show 98% pairing in the second zone in which ZIM-2 appears (Fig. 3.5C). By comparison, WT adult hermaphrodites do not reach 90% pairing until zone three (SATO *et al.* 2009). Interestingly, it has been shown that meiotic progression speeds up, and the SYP foci phenotype in *dlc-1(RNAi)* hermaphrodites is suppressed in spindle assembly checkpoint (SAC) protein mutants. SYP-1 proteins do not form foci and synapsis is more rapid but appears to proceed normally in these mutants (*mdf-1*, *mdf-2*, and *bub-3*) when combined with *dlc-1(RNAi)* (BOHR *et al.* 2015). Expression data from public datasets also suggested that these proteins are expressed at lower levels in males than in adult hermaphrodites (GERSTEIN *et al.* 2010). To investigate this, we probed male and adult hermaphrodite germ cells by immunofluorescence using an anti-MDF-2 antibody (Fig. 3.7)(ESSEX *et al.* 2009). All three proteins were observed in both male and hermaphrodite germlines (Fig. 3.7 and data not shown), however, we observed a noticeable difference in MDF-2 localization in male versus hermaphrodite germ cells. Whereas MDF-2 is enriched at the nuclear periphery in and before the transition zone in hermaphrodites (Fig. 3.7), its distribution is strikingly more diffuse in male transition zone nuclei (Fig. 3.7). This could imply that MDF-2's function in males

differs from its function in hermaphrodite germ cells and may not be required for normal meiotic progression in males.

To further investigate the MDF proteins in male vs hermaphrodite germlines, we next examined the rate of synapsis in *mdf* mutants. It was previously shown that mutants in the SAC (*mdf-1* and *bub*-3) have faster completion of synapsis. As *mdf-2* mutants have an extended mitotic region, and MDF-2 has differential localization in males, our analysis differed slightly from that previously published (BOHR *et al.* 2015). In this analysis, we measured the meiotic region according to where SYP proteins begin forming small foci before synapsis occurs and where HTP-3 starts localizing to chromatin (Fig. 3.8A). This was divided into five regions, and the percent of nuclei that had complete synapsis (all stretches of HTP-3 have co-localizing SYP-1 tracks) was measured (Fig. 3.8A). We analyzed L4 hermaphrodites undergoing spermatogenesis, and there was no statistical significant difference in the percent synapsed in the first two zones of meiosis between N2 WT L4s and *mdf-2* L4s (Fig. 3.8B). Unexpectedly, there was a significantly lower percentage of complete synapsis in the third and fourth zone in *mdf-2* mutants as compared to N2, indicating a minor full synapsis defect ($p = 0.014$, and $p = 0.049$, respectively). However, a lack of significant difference in the first two zones of meiosis indicates that synapsis proceeds at the same rate in WT vs *mdf-2* spermatogenesis, further implying that MDF-2 does not function in the same way in male germ cells as in hermaphrodite germ cells. This further implies that there is a difference in the requirement for SAC function in male and hermaphrodite germ cells.

3.5 Discussion

A sex specific checkpoint at the initiation of synapsis

Chromosomes that are unable to complete synapsis are targeted for H3K9me2 enrichment during *C. elegans* meiosis (BEAN *et al.* 2004). Surprisingly, whereas the complete absence of synapsis in male meiosis yields H3K9me2 enrichment on *all* chromosomes, complete asynapsis in hermaphrodite germ cells fails to trigger H3K9me2 enrichment on *any* chromosome. We have shown that in contrast to situations where the initiation of synapsis is inhibited, hermaphrodite meiotic nuclei that are able to partially initiate synapsis can still trigger enrichment of H3K9me2 in pachytene stage of hermaphrodite meiosis. It thus appears that the signal for H3K9me2 enrichment of unsynapsed chromatin in oogenesis requires at least partial synapsis initiation. In contrast, unsynapsed chromatin in males can be targeted for H3K9me2 enrichment, despite a complete lack of synapsis. In the absence of synapsis initiation, hermaphrodite oogenesis cannot proceed to the stage where H3K9me2 enrichment is activated, whereas in males this arrest does not occur, or if there is an arrest, it occurs after H3K9 methylation targeting. We propose that the differential regulation of H3K9me2 enrichment is a consequence of a checkpoint that is only present in oogenic meiosis.

Although it is a reliable marker of asynapsed chromatin in *C. elegans,* the exact purpose of H3K9me2 enrichment and its regulation is poorly understood, as it is not essential for meiotic progression. H3K9me2 enrichment on the unpaired X chromosome in XO (sex transformed) females has been shown to shield it from activating meiotic checkpoints, but detection of asynapsis of homologs is not affected by loss of H3K9me2 (CHECCHI AND ENGEBRECHT 2011). Mutations in *met*-2, the H3K9 methyltransferase responsible for germline H3K9me2, have only minor meiotic defects (BESSLER *et al.*

2010). In addition, meiosis appears normal in *met-2* mutant XO males, suggesting that the addition of H3K9me2 to unsynapsed chromatin is not essential for meiotic progression (BESSLER *et al.* 2010). Despite its similarity to the Meiotic Silencing of Unpaired Chromatin (MSUC) process observed in other organisms, genes along unsynapsed chromosomes may not be repressed (Checchi and Engebrecht, 2011). It is thus not clear what consequences result from H3K9me2 enrichment, as it does not appear to target genomic regions *de novo* on unsynapsed X chromosomes in *him-8* mutant hermaphrodites, nor are there obvious transcriptional changes (GUO *et al.* 2015). The enrichment for H3K9me2 in unsynapsed chromatin may be a simple consequence of defects in SC assembly and meiotic chromatin reorganization. Indeed, a previous study reported an increase in scattered foci of H3K9me2 in *syp-1* hermaphrodite germ cell chromatin (LAMELZA AND BHALLA 2012). We observed occasional nuclei in partial synapsis inhibition RNAi that did not appear to have initiated synapsis but had enrichment of H3K9me2, but we cannot rule out that there was a small amount of synapsis initiation that is short enough to resemble a polycomplex. Although we did not consistently observe H3K9me2 enrichment in multiple SC mutants, the difference in results could reflect a difference in the fixation procedures, which in turn could reflect some aspect of chromatin reorganization. It should also be noted that although we generally do not observe H3K9me2 enrichment coinciding where SC proteins have loaded, we do not always observe H3K9me2 where SC proteins are absent. Reorganization of meiotic chromatin may randomly expose genomic regions that are already heritably marked by H3K9me2 in germ cell chromatin, but are normally less accessible to MET-2 activity after axis maturation and SC assembly initiates.

Alternatively, the increased enrichment of H3K9me2 may simply represent an alteration in chromatin structure that increases accessibility for the MET-2 methyltransferase only in males. However, it is unlikely that there is such a dramatic difference in chromatin accessibility between the sexes since *zim* mutants display enriched H3K9me2 on unsynapsed chromosomes in both sexes.

Increased methylation may be protective for the genome, as in the case of the un-partnered/unsynapsed X chromosome in XO hermaphrodites, and may mask its unsynapsed status and/or protect it from the activation of recombination checkpoints (CHECCHI AND ENGEBRECHT 2011). Importantly, MET-2 associates with the DNA repair protein SMRC-1 in mitotic and meiotic germ cells, and its activity is proposed to limit replication stress in germ cells (YANG *et al.* 2019). Loss of SMRC-1 leads to a generational depletion of H3K9me2 in germline chromatin, indicating it is required to heritably maintain MET-2-dependent H3K9me2. SMRC-1 is a worm homolog of SMARCAL1 and thus a member of the SWI/SNF family of ATP-dependent chromatin remodelers (YANG *et al.* 2019). The proposed checkpoint could act through SMRC-1 or other DNA damage sensing paths to recruit MET-2 to the exposed domains. Although there is no apparent difference in SMRC-1 presence or nuclear distribution in male versus hermaphrodite meiosis, its activity could be differentially regulated and this remains to be explored (YANG *et al.* 2019).

We therefore can only conclude that in hermaphrodite germ cells, the failure to initiate synapsis prevents meiotic progression to a stage in which H3K9me2 is targeted to unsynapsed chromatin, whatever the role of that targeting may be. In contrast, H3K9me2 targeting proceeds unimpeded in males, despite complete synaptic failure.

Our interpretation of these results is that hermaphrodite meiosis requires passage of a post-pairing checkpoint that is absent in males. Interestingly, apoptosis does not occur in *C. elegans* male germ cells (GUMIENNY *et al.* 1999; GARTNER *et al.* 2000), yet even in hermaphrodite germlines, activation of the newly proposed checkpoint may not induce apoptosis. Indeed, in *syp-1* hermaphrodites where the checkpoint appears to be activated, all apoptosis observed is accounted for by both the PCH-2-dependent checkpoint and by the DNA damage-checkpoint (BHALLA AND DERNBURG 2005).

This newly proposed checkpoint is distinct from the PCH-2-dependent pachytene checkpoint as (a) we found no obvious difference in H3K9me2 enrichment (or lack thereof) when either HTP-3 or SYP-2 is depleted in the presence or absence of PCH-2, and (b) this proposed checkpoint takes place before the PCH-2 checkpoint. The PCH-2-dependent checkpoint senses the unsynapsed pairing centers remaining after other chromosomes have synapsed, and stalls meiosis in the pachytene stage (Fig. 3.9) (BHALLA AND DERNBURG 2005). Indeed, H3K9me2 enrichment on unsynapsed chromosomes is observed when either the DNA damage or pachytene checkpoints are activated, indicating that activation of these checkpoints does not preclude activation of MET-2 targeting to unsynapsed chromatin, suggesting they act downstream of H3K9me2 enrichment (LAMELZA AND BHALLA 2012). The proposed checkpoint senses failure to initiate *any* synapsis, leading to the stalling of meiosis in the leptotene/zygotene stage of prophase I (Fig. 3.9). As we cannot currently separate the checkpoint from the absence of synapsis, it is unclear what the consequences of not having this proposed checkpoint are; it may even not be essential to ensure proper meiotic progression, as one of the only phenotypes measured so far is initiation of

H3K9me2 enrichment. However, as meiotic progression is stalled, a potential benefit of this proposed checkpoint would be that it delays further steps (e.g., redistribution of chromosomes throughout the nucleus from a clustered configuration) that could interfere with proper synapsis and allows further time for nuclei to finish pairing and begin synapsis if conditions are not ideal.

Male synapsis is insensitive to high temperatures, unlike hermaphrodite synapsis

As has been shown previously, hermaphrodite SYP proteins form foci when grown at elevated temperatures (BILGIR *et al.* 2013). However, SYP aggregates do not form in either males or larval stage L4 hermaphrodites undergoing spermatogenesis when grown at an elevated temperature. This indicates that there is some process during synapsis initiation in hermaphrodite meiosis that is temperature sensitive, but this process is not apparent in spermatogenesis. The temperature sensitivity of this process in adult hermaphrodites could be the result of improper protein folding at this higher temperature, or this could be a mechanism to halt meiosis in an unfavorable environment. The temperature dependent component in hermaphrodite meiosis could be required for a signal once pairing has been established to initiate synapsis, or a protein that post-translationally modifies SYPs to allow assembly onto chromatin. Whatever the case, this process or protein is not necessary for synapsis initiation in spermatogenesis. *C. elegans* males typically result from non-disjunction of the X chromosome during hermaphrodite meiosis, and non-disjunction, and therefore males, occurs more frequently when hermaphrodite *C. elegans* are grown at higher temperatures. As males occur more frequently in a stressful condition like high temperature, and in higher temperatures the generation time for *C. elegans* compresses

down to approximately 48 hours, it could be evolutionarily advantageous for male *C. elegans* to complete meiosis quickly and more robustly at elevated temperatures.

Males mimic spindle assembly checkpoint mutants

While hermaphrodites require DLC-1 to synapse their chromosomes, males have grossly normal synapsis even with depletion of DLC-1. Males complete pairing and synapsis faster than hermaphrodites and even correctly pair their chromosomes without DLC-1. Male meiosis mimics spindle assembly checkpoint (SAC) mutant hermaphrodites, as these mutants also suppress the *dlc-1(RNAi)* phenotype and show an increased speed of synapsis completion. It has been hypothesized that the SAC proteins act to block or slow synapsis in early prophase I to allow more time for chromosomes to correctly pair (BOHR *et al.* 2015).

C. elegans males have an inherent problem in meiosis in that they have a single X chromosome with an exposed and unmatched pairing center. The spindle assembly checkpoint (SAC) complex is required for the pachytene checkpoint (BOHR *et al.* 2015), in which PCH-2 senses any unpaired pairing centers. This checkpoint could be triggered in every male meiotic nucleus because of the unpaired and unsynapsed X chromosome. Thus it is beneficial for males to not have a working pachytene checkpoint to keep meiosis from stalling because of their usual XO status. MDF-2, a component of the SAC, has a different localization in early male meiosis compared to hermaphrodites, as it is no longer concentrated near pairing chromosome ends and this could impede the function of the SAC. Without all of the SAC components, nuclei will be unable to sense that synapsis has not completed for all chromosome sets and therefore would not stall meiosis in males. Synapsis could complete more quickly in males without a fully

functioning SAC complex to delay this step. While males do not undergo meiotic apoptosis in response to checkpoint activation, they still stall meiosis in response to DNA damage checkpoint activation (GUMIENNY *et al.* 1999; GARTNER *et al.* 2000; JARAMILLO-LAMBERT *et al.* 2010). Therefore dismantling checkpoints that will unnecessarily hinder all meiotic progression both speeds up meiosis and conserves energy for male *C. elegans,* allowing them to produce more sperm and hence more progeny. Males complete prophase I two and a half to three times faster than hermaphrodites (JARAMILLO-LAMBERT *et al.* 2007); the absence of a step designed to slow meiotic progression likely contributes to the accelerated speed of meiosis observed in male *C. elegans*.

Parallels in C. elegans meiosis and mammalian meiosis

Mammals, like *C. elegans*, have differences in phenotypes related to SAC function in males versus hermaphrodites. Male mammals have a more stringent SAC response to problems in meiosis, such as to Robertsonian fusions, including arresting meiosis at meiotic metaphase (EAKER *et al.* 2001), while hermaphrodites do not show evidence for metaphase arrest (CHMATAL *et al.* 2014). In mammals, the reduction in stringency in hermaphrodites appears to be linked to the large size of oocytes, with the resulting dilution of the SAC proteins in the larger volume restricting the ability of the SAC to prevent the transition to anaphase (Kyogoku and Kitajima 2017). Similarly, lower levels of expression and/or a change of localization of any of these SAC proteins in *C. elegans* males could lead to a lower local concentration of these proteins as in mammalian oocytes, and therefore to less activity.

Spermatogenesis in mammals appears to be more greatly affected by several defects in meiotic processes, which usually result in meiotic arrest at early stages of prophase I (reviewed in (MORELLI AND COHEN 2005)), and infertility or greatly reduced fertility in males. However, these same mutations in oogenesis in mammals results in arrest at a later stage of prophase I, and several mutations still result in fertile females. This general reduction of stringency for oogenesis checkpoints in mammals is opposite to what we have observed in *C. elegans* spermatogenesis. We have shown that male *C. elegans* pair and synapse their chromosomes faster, do not require DLC-1 to synapse or pair their chromosomes, and are able to synapse chromosomes when raised at high temperatures, all or any of which may or may not be linked to a novel checkpoint that senses the initiation of synapsis. All of these differences may ultimately result from sex chromosome evolution in a hermaphroditic species with the stress-induced generation of XO males. *C. elegans* males therefore may be able to give further insight into other ways that meiotic checkpoints can be escaped by one sex but not the other, and how these differences evolve.

3.6 Figures

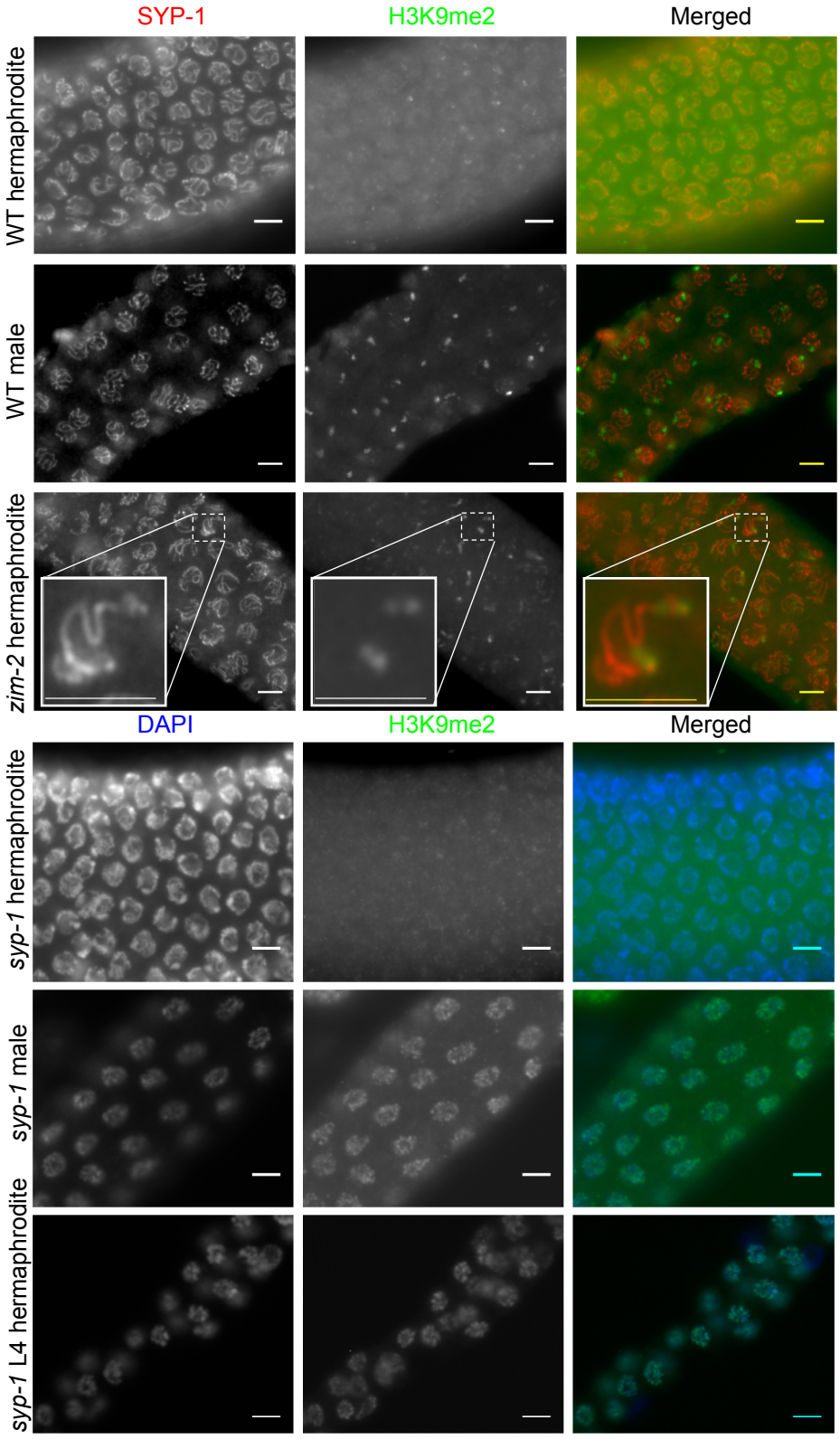
SYP-1
H3K9me2
Merged
WT hermaphrodite
WT male
zim-2 hermaphrodite
DAPI
H3K9me2
Merged
syp-1 hermaphrodite
syp-1 male
syp-1 L4 hermaphrodite

Figure 3.1. Germline sex-specific H3K9me2 enrichment in response to meiotic synapsis defects. Whole mount fixed gonads were probed with anti-SYP-1 and anti-H3K9me2 (top 3 rows) and/or counterstained with DAPI (bottom 3 rows, with meiosis progressing from left to right in all images). Chromatin in WT hermaphrodite synapsis have low levels of H3K9me2 (top row), while male germ cells have the unsynapsed, single X chromosome that is highly enriched for H3K9me2 (second row). *zim-2* hermaphrodites have defective pairing and synapsis of LG Vs, and display two chromosomes that accumulate high levels of H3K9me2 (third row, insets). *syp-1* hermaphrodite germ cells cannot initiate synapsis and have low levels of H3K9me2 (fourth row), whereas *syp-1* male germ cells exhibit widespread H3K9me2 (fifth row). *syp-1* L4 hermaphrodites undergoing spermatogenesis also display widespread H3K9me2 (bottom row). Scale bars 5 μm.

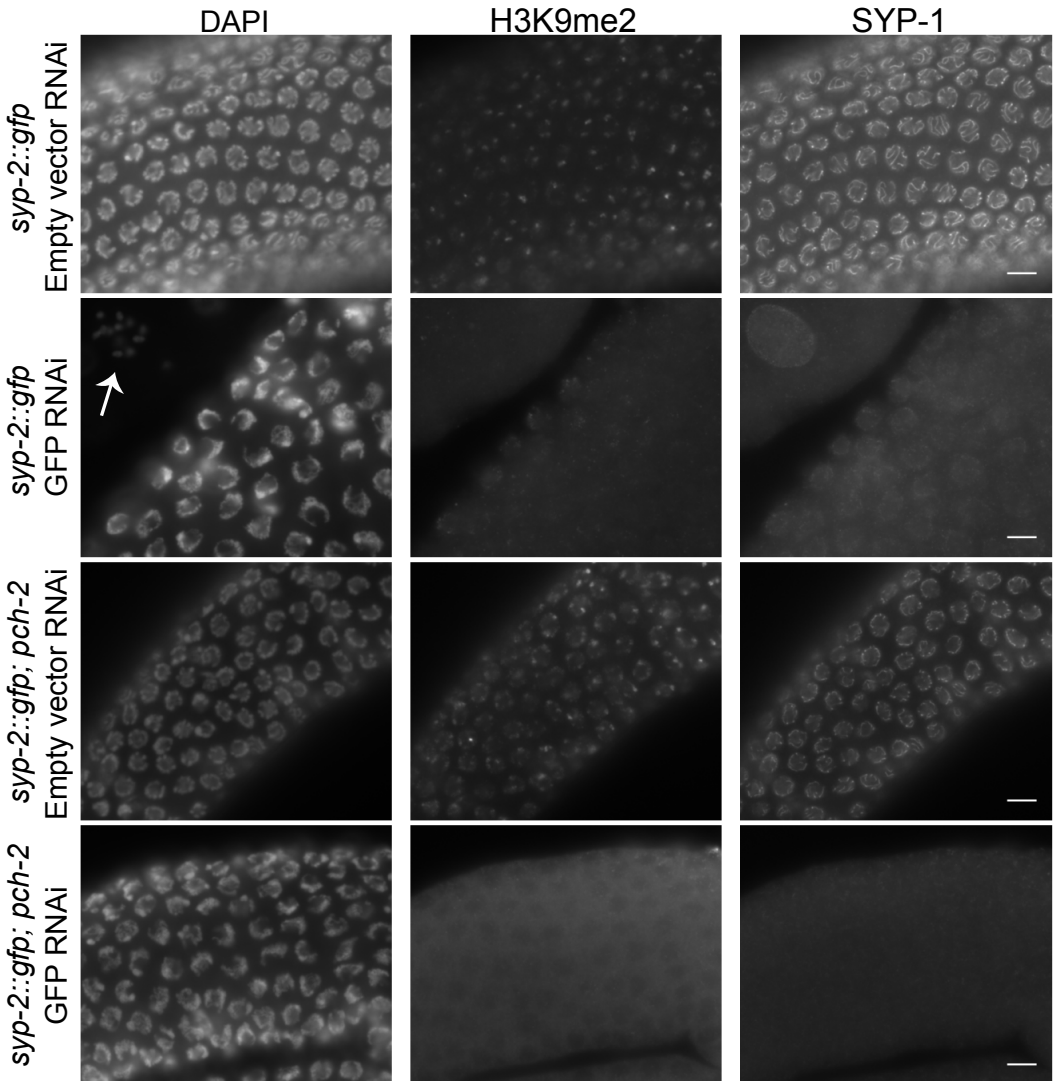

Figure 3.2. *pch-2* hermaphrodites do not have widespread enrichment of H3K9me2 with absence of synapsis. Whole mount dissected fixed *syp-2::gfp(ck38)* or *syp-2::gfp(ck38); pch-2* gonads probed with anti-H3K9me2, anti-SYP-1, and DAPI. The tagged SYP-2::GFP line gives H3K9me2 enrichment around the telomeres (top row), while knockdown of SYP-2::GFP eliminates much of H3K9me2 (second row). Knockdown of SYP-2::GFP results in increase of DAPI bodies in oocytes (arrow). Deletion of *pch-2* does not result in a change in H3K9me2 patterning in empty vector control RNAi (third row). Deletion of *pch-2* also has low H3K9me2 when SYP-2::GFP is knocked down (bottom row).

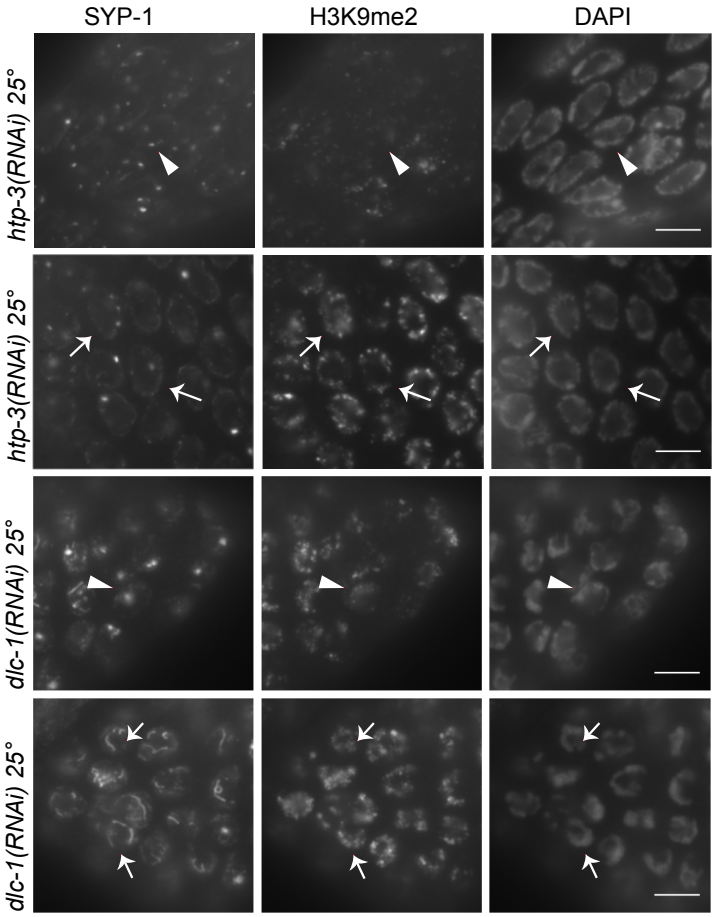

Figure 3.3. Partial initiation of synapsis is sufficient to trigger widespread H3K9me2 enrichment in hermaphrodite germ cells. Whole mount dissected fixed gonads were probed with anti-SYP-1, anti-H3K9me2, and DAPI. In *htp-3(RNAi)* animals, if SYP-1 proteins are mostly confined to foci (top row, arrowheads), there is little H3K9me2 present. However, in some cases where a small amount of SYP-1 protein has localized to chromatin in *htp-3(RNAi)* animals, there is widespread H3K9me2 enrichment (second row, arrows). Similarly, in *dlc-1(RNAi)* animals, if a nucleus has SYP-1 present only in foci away from chromatin, there is low H3K9me2 (third row, arrowheads), while nuclei that have some, but incomplete synapsis have enrichment of H3K9me2 (bottom row, arrows). Scale bar 5 μm.

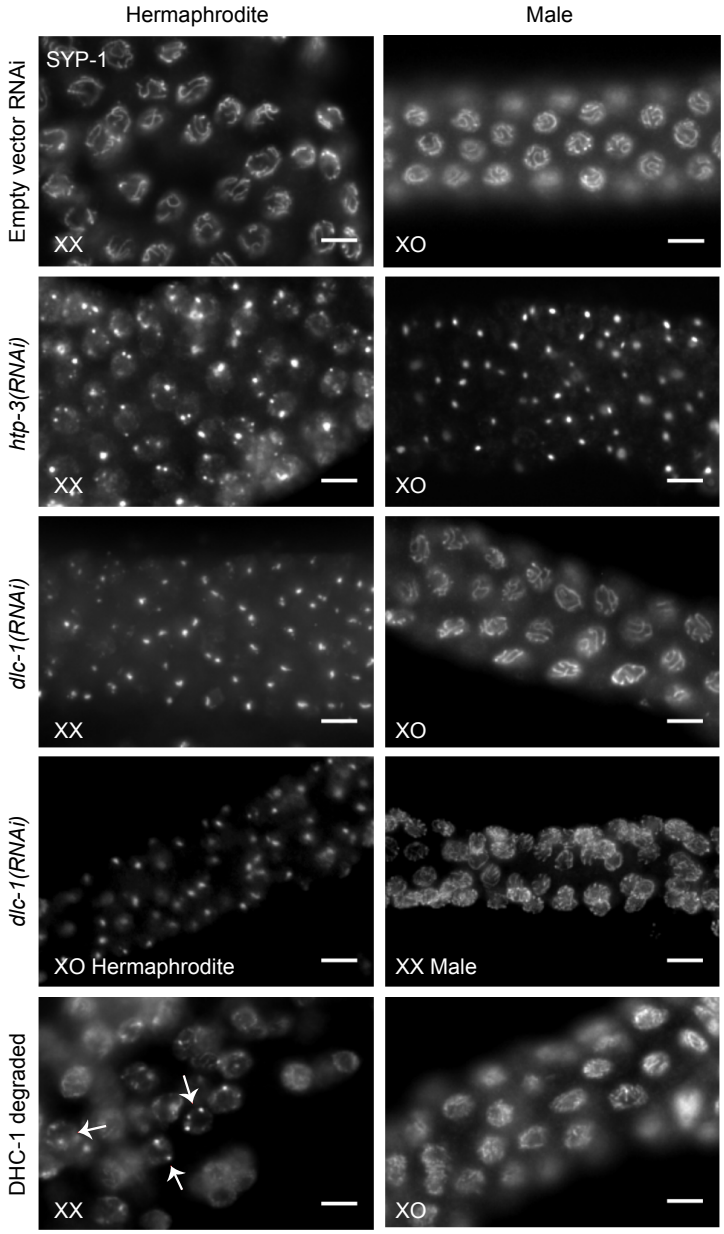

Figure 3.4. Dynein depletion dramatically affects adult hermaphrodites, but not male synapsis. Whole mount dissected fixed gonads probed with anti SYP-1 are show, with meiotic progression from left to right. WT empty vector RNAi XX hermaphrodites and XO males normally show SYP-1 tracks in between chromosomes (top row). Both *htp-3(RNAi)* XX hermaphrodites and XO males have SYP-1 foci formed away from chromatin (second row). *dlc-1(RNAi)* XX hermaphrodites also form SYP-1 foci away

from chromatin, however, *dlc-1(RNAi)* XO males have grossly normal SYP-1 tracks (third row). Depleting DLC-1 in sex determination mutant *her-1(e1518)* XO females display SYP-1 foci, while *tra-2(q278)* XX males have grossly normal synapsis like their male counterparts (fourth row). *dhc-1(ie28)* I; ieSi38 IV animals exposed to 1mM auxin for eight hours at 20° to degrade DHC-1 resulted in XX hermaphrodites that had incidences of SYP-1 foci (arrows), while all XO males analyzed had grossly normal SYP-1 tracks (bottom row). Scale bar 5 μm.

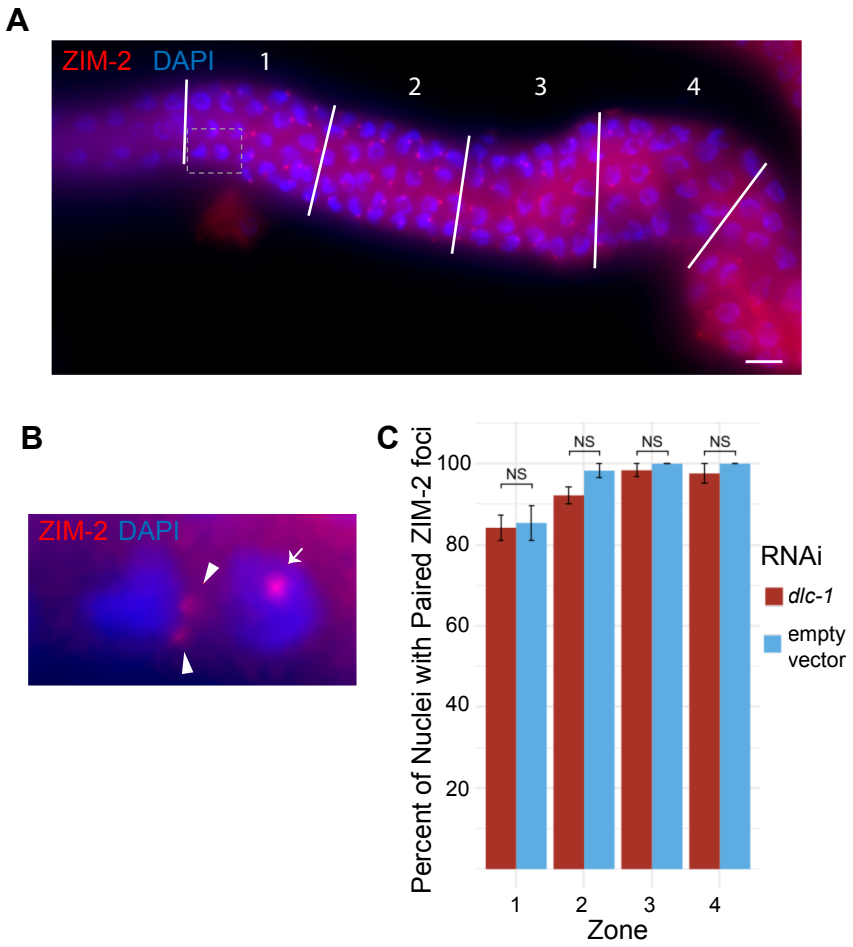

Figure 3.5. Pairing rates remain unchanged in *dlc-1(RNAi)* males. (A) Whole mount fixed male gonad treated with empty vector RNAi and probed with anti ZIM-2 (red) and DAPI (blue), shown as an example of how the region containing ZIM-2 foci of each gonad was measured, then divided into four equal length zones and each nucleus scored for pairing status of ZIM-2. Dotted box represents portion blown up in panel B. (B) Zoom in of a two nuclei from zone 1, with a nucleus with unpaired, two ZIM-2 foci (arrowheads), and a nucleus with paired, one ZIM-2 focus (arrow) chromosome V. Meiotic progression is depicted from left to right. Scale bar 5 μm. (C) Knockdown of *dlc-1* in N2 males does not change the pairing rates (8 males measured) as compared to empty vector RNAi treated N2 control in males (6 animals measured). No significance

based on in any of the four zones was found using student's T test ($p=0.825$, $p=0.054$, $p=0.424$, and $p=0.424$, respectively). Error bars represent SEM.

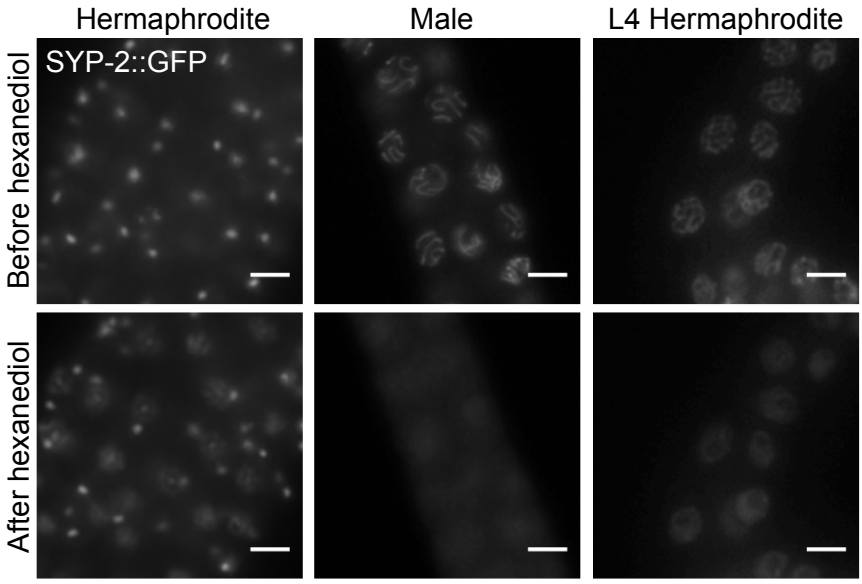

Figure 3.6. Synaptonemal complex stability is unaffected by increased temperature in male germ cells. Live imaging of extruded gonads of wgIs227 (*syp-2::gfp); syp-2(ok307)* V animals. Animals were raised at 27.5° for 24 hours before imaging, starting incubation at larval stage L4 for hermaphrodite and males. Growth at high temperature results in SYP-2 foci in adult hermaphrodites, but males and L4 hermaphrodites, which undergo spermatogenesis, display grossly normal SYP-2 assembly between chromosomes (top row). 30 seconds after addition of 1,6-hexanediol, hermaphrodite SYP-2 foci do not dissolve, but both male and L4 hermaphrodite SC dissociates off of chromosomes to produce a haze around the nucleus of SYP-2. Scale bar 5 μm.

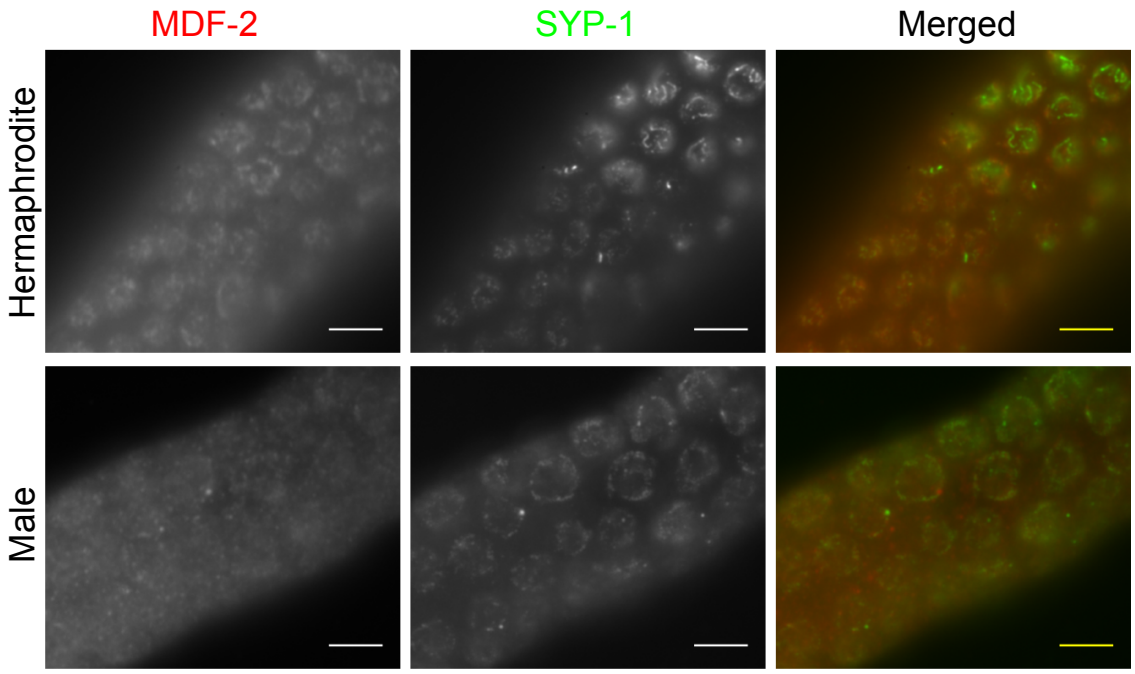

Figure 3.7. MDF-2 localization in early meiosis changes in males. (A) Whole mount fixed gonads of N2 young adults probed with anti SYP-1 (green) and anti MDF-2 (red) are shown with meiotic progression from left to right. MDF-2 localizes to the nuclear periphery during early meiosis before chromosomes begin synapsing in hermaphrodites (top row). However, males have more diffuse localization of MDF-2 before chromosomes begin synapsing (bottom row). Scale bars 5 μm.

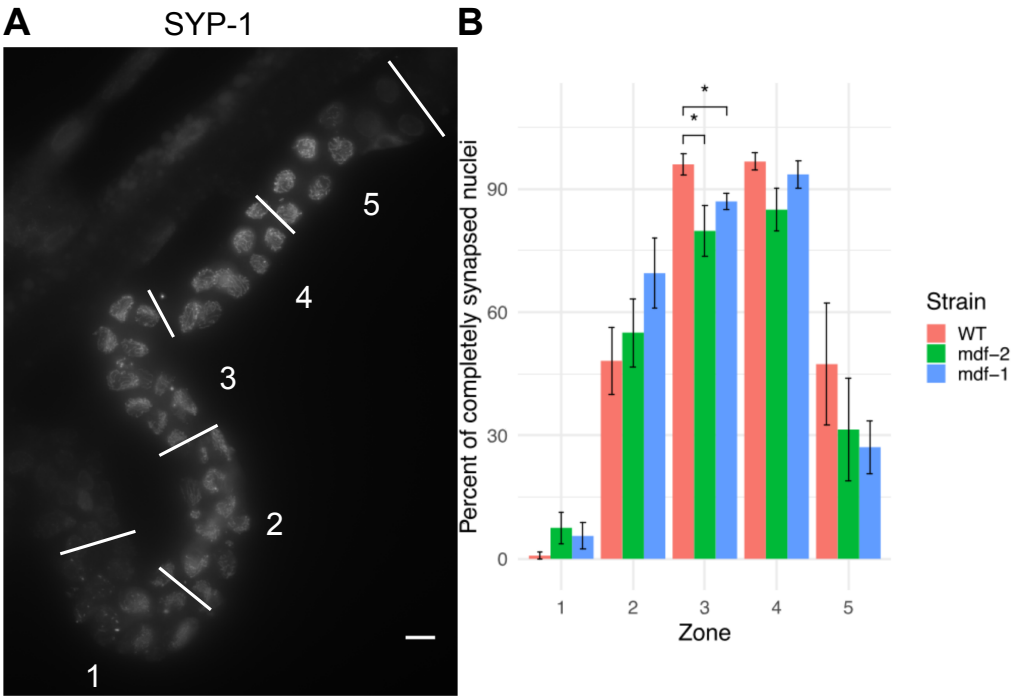

Figure 3.8. Loss of MDF-2 or MDF-1 does not increase rate of synapsis in male germ cells. (A) Whole mount fixed larval stage L4 hermaphrodite *mdf-2(av16) unc-17(e245)* IV gonad probed with anti SYP-1. Shown as an example of how the meiotic region of the gonad was measured starting at initial HTP-3 localization and SYP-1 foci until the end of pachytene; this region was divided into five equal length regions, and percent of nuclei synapsed (i.e. nuclei that all regions of HTP-3 tracks co-localized with SYP-1 tracks) was measured for each region. Scale bar 5 μm. Images stitched using Grid/Collection plugin for ImageJ developed by Preibisch et al., 2009. (B) There is no statistical difference in the rate of synapsis between *mdf-2* spermatogenic larval stage L4 hermaphrodites (8 animals) and WT L4 hermaphrodites (7 animals) in the first two zones (p=0.119, and p=0.704). *mdf-2* L4 animals have a full synapsis defect in zones three and four, where they have a significantly lower rate of synapsis than WT (p=0.0135, and p= 0.049). Error bars represent SEM. Statistical significance tested using student's T-test.

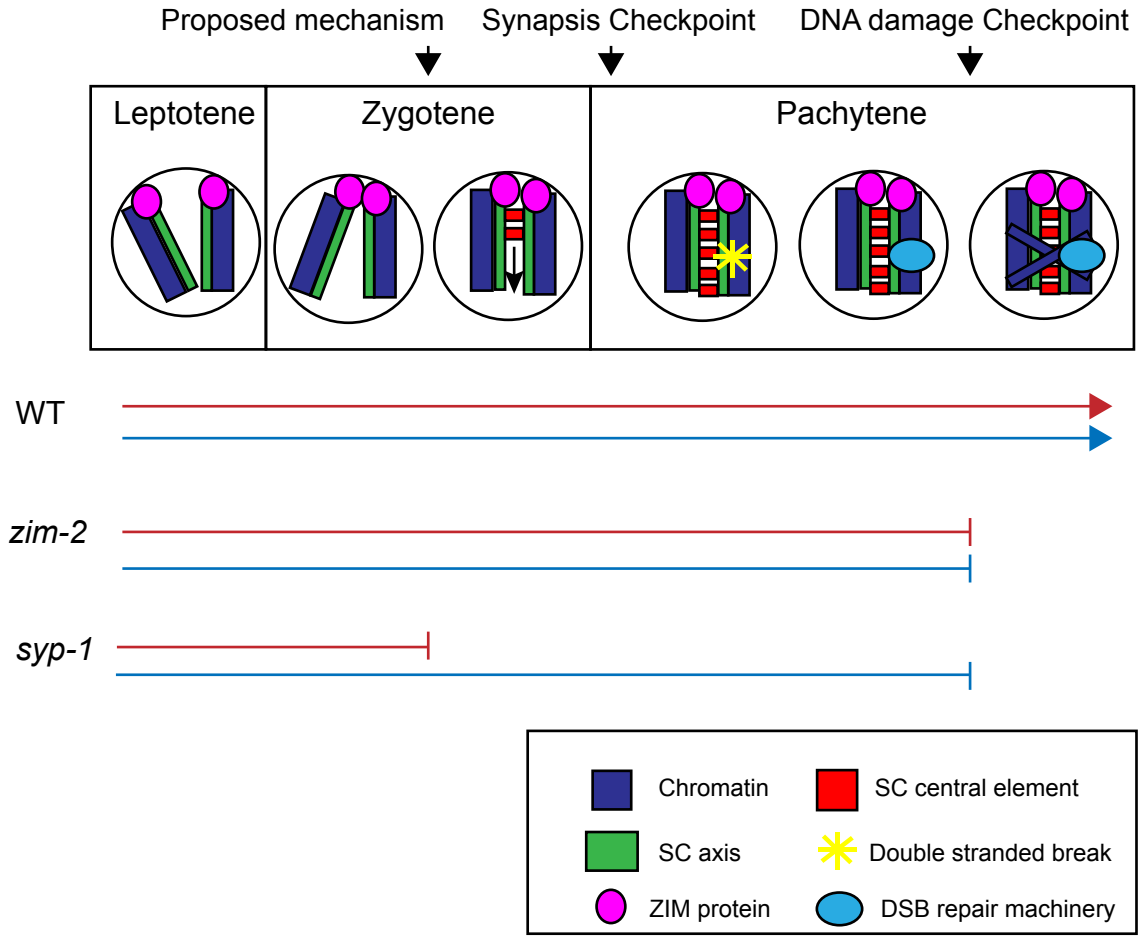

Figure 3.9. Timing of the newly proposed mechanism. Diagram showing the timeline of the checkpoints in *C. elegans* meiosis, and how far different hermaphrodites (red lines) or male (blue lines) mutants will progress in meiosis until stalling. The proposed mechanism takes place after the synaptonemal complex axis assembles onto chromosomes, and pairing of at least one set of chromosomes have synapsed. The proposed mechanism senses the initiation of synapsis, and stalls meiosis in *syp-1* hermaphrodites (red line). However, we propose that the mechanism does not exist in males, and *syp-1* males will instead stall meiosis in response to the DNA damage checkpoint. Figure inspired by (MORELLI AND COHEN 2005).

3.7 Tables

Strain	Mid-gonad average	Proximal average
zim-2	153,819.48	223,786.82
syp-2	14,751.80	371,315.52
syp-1	3,171.76	171,766.12

Table 3.1 *zim-2* has over ten times as high total amount of H3K9me2 in each nucleus as in a synapsis mutant. Average quantification of amount of H3K9me2 signal in each nucleus using ImageJ in adult hermaphrodite gonads. *zim-2* mutants have over ten times as much H3K9me2 as either *syp* mutant mid-gonad (the normal region for pachytene). This indicates that there isn't a dilution of H3K9me2 signal across all chromosomes when synapsis isn't able to initiate.

3.8 Supplemental Figures

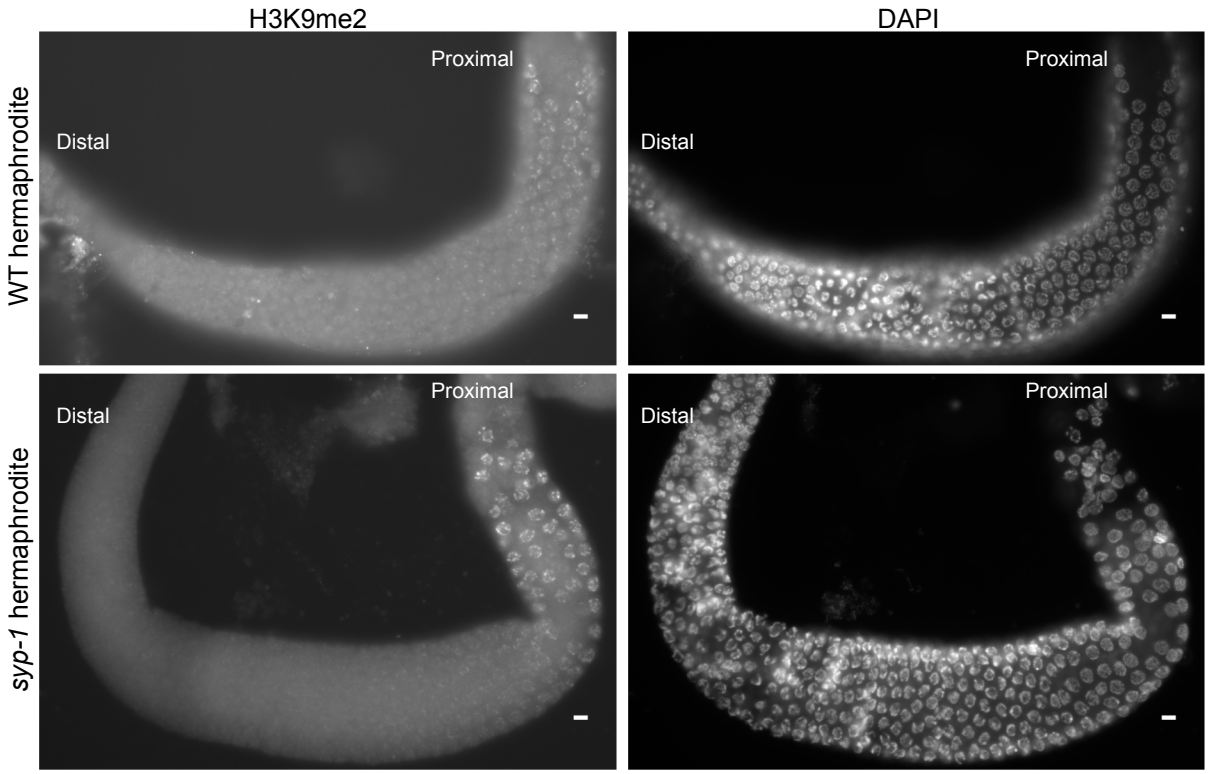

Figure 3.S1. Both WT and *syp-1* hermaphrodites have widespread enrichment of H3K9me2 in late pachytene, early diplotene. Whole mount fixed gonads probed with DAPI and anti H3K9me2, with meiotic progression from left to right. WT hermahrodites have low levels of H3K9me2 throughout prophase I, until late pachytene when there is widespread enrichment (top row). *syp-1* hermaphrodites also show low levels of H3K9me2 until late pachytene, when they also display widespread enrichment (bottom row). Both images were cropped and used for Figure 1. Scale bars 5 μm.

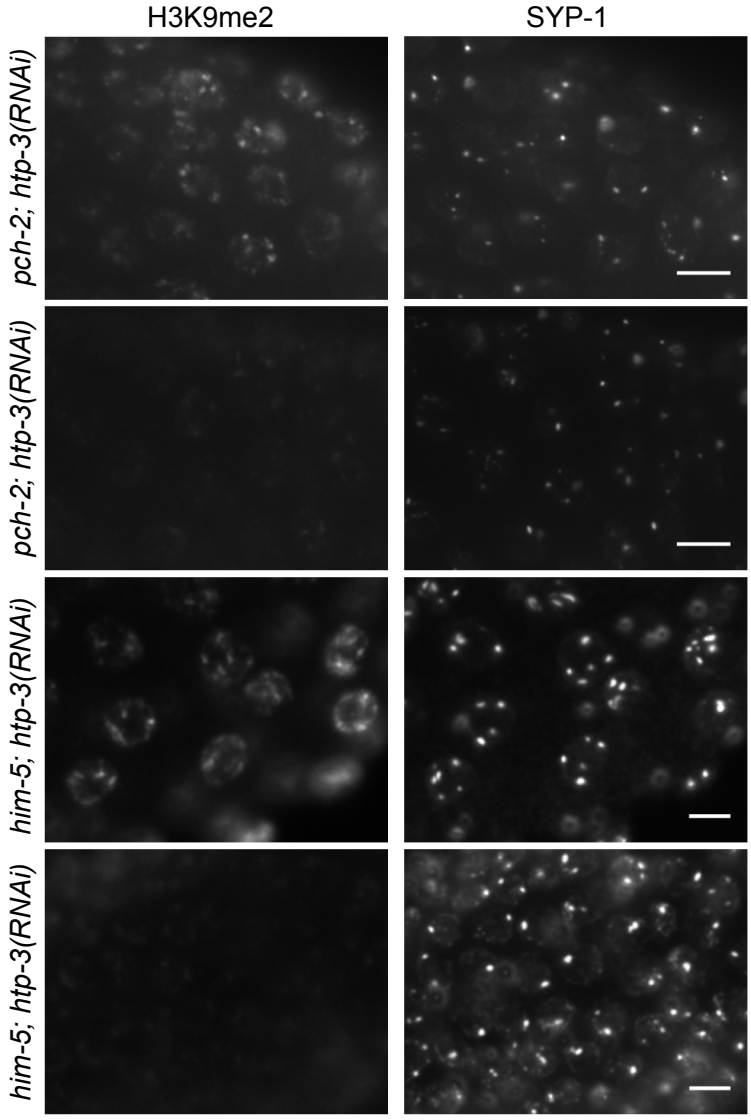

Figure 3.S2. H3K9me2 stays low with depletion of HTP-3 with occasional exceptions in hermaphrodties. Whole mount fixed gonads of either *pch-2* or *him-5* hermaphrodites probed with anti-SYP-1 and anti-H3K9me2 grown with *htp-3* RNAi. *pch-2* hermaphrodites with HTP-3 knockdown display SYP-1 polycomplexes, and occasional widespread enrichment of H3K9me2 (top row), while most gonads show low H3K9me2 when SYP-1 is in polycomplexes (second row). However, this also occurs with knockdown of HTP-3 in hermaphrodites with normal PCH-2 function: occasional widespread enrichment of H3K9me2 with SYP-1 in polycomplexes (third row), with most

gonads displaying low H3K9me2 when SYP-1 is in polycomplexes (bottom row). Scale bars 5 μm.

Chapter 4. Discussion and Future Directions

4.1 Summary of Dissertation

This dissertation has examined early prophase I in *C. elegans*, and has identified a sex-specific mechanism that senses meiotic synapsis initiation, differences in the way males conduct meiotic synapsis as compared to hermaphrodites, and a novel motor independent role for Dynein Light Chain 1 (DLC-1) in meiotic synapsis.

My research has led to the identification of a mechanism in early hermaphrodite meiosis that senses the initiation of synapsis, and stalls meiosis in response to a delay in synapsis initiation. This mechanism does not operate in males or sexually transformed female germ cells, and thus appears to be specific to female meiosis. Thus far, the only readout of this mechanism is failure to enrich chromosomes with H3K9me2 when synapsis in absent in hermaphrodites, commonly known as meiotic silencing of unsynapsed chromatin (MSUC) that also occurs in other organisms (reviewed in (TURNER 2007)). We conclude it is a mechanism sensing initiation of synapsis instead of sensing the failure to complete synapsis because even a small amount of synapsis initiation, such as when DLC-1 is partially knocked down or as occurs in individual ZIM mutants, unsynapsed hermaphrodite chromosomes will display widespread enrichment of H3K9me2. This mechanism does not appear to lead to apoptosis like other meiotic checkpoints, as elevated apoptosis levels in *syp* mutants can be completely eliminated by disabling meiotic checkpoints that act in later stages (BHALLA AND DERNBURG 2005).

Hermaphrodite *C. elegans* are commonly studied because of the ease of culture maintenance due to their self-production and because they undergo oogenesis for

multiple days at standard growth temperatures. XO male *C. elegans* are largely understudied because of this. As early prophase I has similar goals in both male and hermaphrodite meiosis, it could easily be presumed that they have the same requirements and consequently overlook interesting new mechanisms. In chapter 3, this dissertation attempts to address this gap by re-examining mechanisms in males that were originally identified in hermaphrodite meiosis, such as temperature sensitivity of synapsis, and the requirement of dynein in meiosis. I have observed that male CE assembly is not as temperature sensitive as adult hermaphrodite synapsis, as they are still able to form CE above 27.8°, while hermaphrodites form aggregates and arrest meiosis at 26.5° (BILGIR *et al.* 2013). This hints that there could be a temperature sensing or temperature sensitive regulator of SYP protein folding that is present in hermaphrodite meiosis, but not in males. Alternatively, this could indicate that males have an additional stabilizing protein chaperone that hermaphrodites do not. Males also do not require DLC-1 to synapse or correctly pair their chromosomes, even though *dlc-1(RNAi); dhc-1* hermaphrodites display a reduction of correct pairing and SYP protein aggregates (chapter 2)(SATO *et al.* 2009).

Dynein light chain is a hub protein, which interacts with many proteins to aid in stabilizing their structure, their ability to bind to other proteins, and the binding of those proteins to their ligands (reviewed in (RAPALI *et al.* 2011)). Previously, the need for DLC-1 in synapsis was presumed to be solely its role in the dynein motor complex aiding in chromosome movement and homolog pairing (SATO *et al.* 2009). In chapter 2, while investigating differences in meiosis between the sexes, I discovered an unexpected additional role for DLC-1 in SYP folding. With knockdown of DLC-1, SYP proteins form

insoluble aggregates unassociated with chromosomes in a manner suggesting that they are folded incorrectly. SYP-2 has a putative binding motif located next to its coiled-coil domain, and we demonstrate that SYP-2 and DLC-1 physically interact *in vivo.* Elimination of the putative binding motif reduces the interaction of SYP-2 and DLC-1, and results in a high incidence of male (Him) phenotype, a lower brood size, and embryonic lethality assumed to be due to aneuploidy. The role of DLC-1 appears to be temperature sensitive, as the aggregate phenotype in absence of DLC-1 is more frequent and more severe at 25°, and mutation of the putative binding motif also has more severe phenotypes at higher temperatures. This suggests that DLC-1 plays a protein chaperone-like role for SYP proteins when growth temperatures are above 16°.

4.2 A screen for components in the synapsis initiation "checkpoint"

The next step for studying the synapsis initiation sensing mechanism is to identify components of the mechanism. Performing an RNAi screen in *syp* mutants, starting with meiotic kinases, could identify components of this mechanism. As this mechanism could be a novel checkpoint, a kinase could be involved. Any knockdown that results in widespread H3K9me2 on unsynapsed chromosomes in *syp* hermaphrodites, and/or elimination of the extended transition zone clustering of DNA would indicate that a gene is involved stalling meiosis in response to a delay in synapsis initiation. Alternatively, if no meiotic kinases are involved, a screen of genes expressed in adult hermaphrodite germlines but not in male germlines would be the next step, as males appear to lack this mechanism. Identifying components of this mechanism, and subsequent study of their roles, can give insight into whether this mechanism we have uncovered is in fact a checkpoint.

Recently, a crossover surveillance mechanism was identified that I hypothesize occurs shortly after the checkpoint-like mechanism proposed in chapter 3. In mutants that are unable to form double-stranded breaks on one chromosome (i.e. a *him-5* mutant that cannot form double-stranded breaks on the X chromosome), SUN-1 is phosphorylated at Serine 12 (S12) in the transition zone (TZ), as occurs in WT meiosis (PENKNER *et al.* 2009; MACHOVINA *et al.* 2016). However, unlike WT these mutants have an unexpected "dead zone" shortly after the TZ where the phosphorylated S12, S8 and S43 epitopes are transiently lost in the early pachytene region (MACHOVINA *et al.* 2016). Eventually S12 phosphorylation returns, but this indicates that meiosis stalls if there are individual chromosomes that do not contain double-stranded breaks. The disappearance of the Ser12P epitope is not understood, but is thought to be either protein dynamics or dephosphorylation to signal delay. However, as this "dead zone" phenotype is not observed in mutants unable to synapse their chromosomes, this surveillance mechanism does not appear to be reached or is unable to be activated in synapsis mutants (PENKNER *et al.* 2009; WOGLAR *et al.* 2013). This does not exclude the possibility that players in this crossover surveillance mechanism are involved in the proposed synapsis initiation checkpoint; thus, once players in either have been identified, should be tested for their role in the other mechanism.

4.3 Post-translational modification of axial elements and the synapsis initiation failure response

In mouse male meiosis, MSUC requires phosphorylation of axial components HORMAD1 and HORMAD2 (FUKUDA et al. 2012). The phosphorylated form of HORMAD1 is only observed on unsynapsed chromosomes, and the inability of

phosphorylated HORMAD1 to localize to chromosome axes leads to failure to load MSUC components ATR and γH2AX (FUKUDA *et al.* 2012). So far, no studies have looked at post-translational modifications of axial components in *C. elegans*; thus, it is possible that hermaphrodites that cannot initiate synapsis, block phosphorylation of an axial component, which in turn blocks enrichment of H3K9me2 on unsynapsed chromosomes. Identification of post-translational modifications of axial elements and creation of phospho-dead and phospho-mimic mutants of these sites would determine the functions of these mutations, and whether or not they influence H3K9me2 targeting in synapsis and/or pairing mutants.

4.4 Male *C. elegans* evolution favors less stringent meiosis

Males may have eliminated the novel proposed checkpoint in chapter 3 because as the sex-delimited XO mechanism evolved, they would encounter checkpoints that are triggered by pairing and synapsis failure of the lone X. Although the enrichment of H3K9me2 has been proposed to hide the unpaired and unsynapsed male X from checkpoints, it could be beneficial for males to eliminate them entirely (CHECCHI AND ENGEBRECHT 2011). Bypass of the proposed synapsis initiation sensing mechanism proposed in chapter 3 is not necessary for males to complete meiosis, as they have five other sets of chromosomes that will initiate synapsis. However it is possible that a component in the synapsis initiation checkpoint has an additional role in other checkpoints that would hinder male meiosis, such as a secondary role in sensing whether all chromosomes have synapsed. Additionally, reduction of the stringency of meiosis in general would be beneficial to males to ensure their unpaired chromosome can go through meiosis. In this case, evolving to bypass a mechanism for a single

particular chromosome would be significantly more difficult to achieve compared to eliminating a process that altogether does not affect the quality of meiosis. I observed that males have differently localized MDF-2. As this protein is required for the synapsis checkpoint, elimination of MDF-2 function may prevent the synapsis checkpoint from recognizing their unpaired X chromosome and coincidentally eliminate their reliance on DLC-1 to synapse their chromosomes. However, further study would be required to determine if this change in localization actually affects the function of MDF-2 (chapter 3)(BOHR *et al.* 2015). Even with a faster initiation and completion of synapsis, males still largely correctly pair their chromosomes and produce euploid and high-quality sperm, despite having fewer stringent tests as hermaphrodites for correctness.

C. elegans males occur more frequently when there is stress in the environment (e.g. heat stress, alcohol) and therefore may have to live and propagate in a more stressful environment. A slightly higher rate of mutation in a stressful environment is more beneficial as this leads to a faster evolution rate for the population. Stringent checkpoints could eliminate some of these mutations, and therefore slow the rate of evolution. Therefore, less stringent checkpoints can be beneficial to a *C. elegans* population under stress.

Additionally, spermatogenesis may not have as intense checks for meiotic checkpoints because of the hermaphroditic nature of *C. elegans*. As *C. elegans* hermaphrodites go through spermatogenesis during their last larval stage before switching to oogenesis in adulthood, sperm is the limiting factor for the total number of progeny any single hermaphrodite can have. So in that case, it may be evolutionarily advantageous for spermatogenesis to complete as quickly as possible to produce the

greatest number of sperm possible. Indeed, it has been demonstrated that male prophase I proceeds 2.5 to 3 times faster than in adult hermaphrodites (JARAMILLO-LAMBERT *et al.* 2007). Removing checks for robust systems and inhibition steps (such as inhibition of synapsis until the dynein movement creates tension) could speed up spermatogenesis, which is what is observed in males, and therefore increases the total number of sperm produced in a limited amount of time.

4.5 Dynein light chain's myriad of functions

The work presented in chapter 2 adds to the many roles of dynein light chain, not only in *C. elegans* meiosis, but also in eukaryotic cells in general. Light chains were first identified to function in the dynein motor, but it has become increasingly obvious that perhaps the main function of the light chain is to aid in protein interactions and even in protein folding. In fact, the light chain's role in the dynein complex is to aid in the interaction of dynein intermediate chains. There is growing evidence that DLC-1 has several motor-dependent and independent roles in *C. elegans* meiosis, and this dissertation adds another to the role to the list (DORSETT AND SCHEDL 2009; WANG *et al.* 2016; ELLENBECKER *et al.* 2019). The multitude of functions even at similar times within the same cell in meiosis, such as aiding in chromosome movements as well as providing folding support for synapsis proteins, implies that DLC-1 could be performing multiple roles simultaneously in other tissues (SATO *et al.* 2009; WYNNE *et al.* 2012).

4.6 Ability of males to complete synapsis without DLC-1

The unexpected result that males do not require DLC-1 to pair or synapse their chromosomes (chapter 3), especially as we demonstrate that DLC-1 appears to act

similarly to a protein chaperone for SYP proteins, can add to the understanding of why and how dynein light chains interact with other proteins. One possible reason males do not need DLC-1 is that male meiosis occurs much faster than hermaphrodites and there are fewer checkpoints to delay immediate assembly of SYPs into the synaptonemal complex; thus, the role of DLC-1 as a chaperone during such dynamics is less important (JARAMILLO-LAMBERT *et al.* 2007). Another possible reason could be differential post-translational modifications of SYP proteins in males as compared to hermaphrodites. A future direction of study would be to identify differential modifications of SYP proteins between males and adult hermaphrodites. This could reveal stabilizing modifications that exist in males that allow them to not need DLC-1 as a chaperone, and to be unaffected by growth in high temperatures.

4.7 Future directions for study of interactions of DLC-1 with SYP proteins

I demonstrated that interaction of DLC-1 with SYP-2 decreases, but is not abolished by mutation of two residues in the putative binding motif (chapter 2). Further study is necessary to determine exactly how DLC-1 interacts with SYP-2. The protein GLD-1 interacts with DLC-1 during early meiosis, and mutation of some of the binding motif is not enough to completely abolish interaction *in vitro*; thus, it is possible that our mutation of only two residues in the binding motif was not enough to completely abolish DLC-1's ability to interact with that motif (DORSETT AND SCHEDL 2009). Complete mutation of all four residues in the putative binding motif would be a good starting point to determine how DLC-1 interacts with SYP-2. If this mutation still does not completely abolish this interaction, different portions of SYP-2 could be made *in vitro* and tested for interaction with DLC-1. Other proteins, such as FBF-2, have been demonstrated to

interact with DLC-1 in multiple locations, so it is possible that is also the case for SYP-2 (WANG *et al.* 2016).

For further study of the role of DLC-1 in meiotic synapsis, *in vitro* experiments to test DLC-1's ability to interact with the other individual SYP proteins should be conducted, regardless of the results mentioned above. The ability of DLC-1 to interact with other SYP proteins could indicate that DLC-1 interacts with SYP heterodimers to aid in folding of both SYP-2 and another of the SYP proteins. Additionally, none of the other SYP proteins have obvious light chain binding residues, so this would give insight into what other protein structures and/or motifs that DLC-1 binds to.

4.8 Future study required into CRL4 and DLC-1 similarities

A recent study identified that mutants in the Cullen RING E3 ubiquitin ligase 4 (CRL4) complex also form SYP protein aggregates that are both temperature dependent and resistant to 1,6-hexanediol, similar to the *dlc-1(RNAi)* induced aggregates identified in chapter 2 (ALLEVA *et al.* 2019). However, there is no indication that SYP-1, -2, -3, or -4 proteins are ubiquitinated (ALLEVA *et al.* 2019). At the time of publication, SYP-5 and SYP-6 had not yet been identified, and therefore were not tested in this study. It is possible that either or both of these two proteins are ubiquitnated by CRL4. However, the authors hypothesize that the CSN/Cop9 Signalosome deneddylates the CRL4 complex, which then ubiquitinates another component that stabilizes folding of SYP proteins (BROCKWAY *et al.* 2014; ALLEVA *et al.* 2019). Further study to determine whether DLC-1 is this component, or whether DLC-1 instead regulates the CRL4 and/or the CSN/Cop9, or whether these are independent modes of SYP protein stabilization is needed. Interestingly, the aggregate formation in CRL4

mutants is prevented by elimination of double stranded breaks (i.e. in *spo-11* mutants)(ALLEVA *et al.* 2019). This also needs to be investigated in *dlc-1(RNAi)* animals. This model that double-stranded breaks are required for aggregates to form could indicate that after initiation of breaks, proteins interacting with the SC could change, or that there are modifications that enable misfolding/aggregation of SYP proteins.

4.9 MPK-1 as a potential player in early meiosis

It has recently been shown that temperature sensitive and loss of function mutants of MPK-1, a map kinase, display SYP foci when raised at 25° (NADARAJAN et al. 2016). Interestingly, it is mentioned that the *mpk-1* null mutant shows these foci more frequently at 25° than at 20°. SYP-2 was shown to be phosphorylated at S25 by MPK-1, but phospho-dead and phosphomimetic mutants do not show SYP foci. However, the temperature these phosphorylation mutants were grown at is unclear. If they were grown at 20°, it is possible that either of these two grown at 25° could then show a higher frequency of SYP foci (NADARAJAN et al. 2016). This could be an interesting future direction for study, as this phenotype shows temperature sensitive effects, similar to the DLC-1 phenotype. An interesting experiment would be to determine whether these SYP foci in *mpk-1* mutants are aggregates or foci, using an amphiphilic solvent. Aggregates could indicate that MPK-1 helps to stabilize SYP-2 folding similar to DLC-1, or phosphorylation of SYP-2 by MPK-1 could stabilize SYP-2 folding once synapsis has been established. Polycomplexes could indicate that MPK-1 regulates other portions of meiosis, and that its absence stalls meiotic progression at an early stage. Alternatively, if *mpk-1* SYP foci are polycomplexes, this could be a potential target of study for other differences in males, and/or study for SC control and dynamics.

4.10 Future direction of study of SYP-2 in late meiosis

Preliminary data indicates that *syp-2(AMTA)* may not have as many nuclei as expected in diplotene with a higher than normal number of DAPI bodies as expected from the 60% embryonic lethality of this strain (W.G. Kelly, unpublished). The number of DAPI bodies is a common indicator of aneuploidy when there are more than 6 in *C. elegans*. This could indicate that this mutation affects an additional role of SYP-2 in late prophase I, potentially having to do with crossover repair, or with transcription that causes embryonic lethality. For example, it has been shown that constitutive phosphorylation of SYP-2 leads to defects in SC disassembly in diplotene on the long arms of bivalents, and these mutants have high levels of embryonic lethality (NADARAJAN *et al.* 2016). In the *syp-2(AMTA)* mutants, there could be similar issues of SYP disassembly from long arms of bivalents, accounting for the rest of the observed embryonic lethality. Alternatively, if disassembly of CE components from these arms is not observed, RNA-seq, and/or TRAP-seq could be used to examine whether there is mis-regulation of transcription and/or translation in these *syp-2(AMTA)* mutants.

4.11 Final Conclusions

Work presented in this dissertation has identified differences in the way male *C. elegans* conduct meiosis, and indicate a novel checkpoint that assesses whether synapsis has initiated in female meiosis is absent in males. Studying and comparing male versus hermaphrodite meiosis in *C. elegans* can help identify further sex-specific meiotic components and mechanisms. Sex-specific differences in conserved meiotic processes could give insight into how the mechanisms related to gamete-dependent

differences in human aneuploidies arise. Also, understanding the ways in which checkpoints are bypassed in human meiosis could give insight into fertility problems.

This dissertation also expands on the role of the dynein light chain in meiotic synapsis, and builds on the work on motor independent roles for the light chain. Getting more information on how dynein light chains interact with proteins, especially as it is a widely expressed and highly conserved protein, could be informative for human disease models, and potentially provide foundations for future therapeutic targets and/or treatments.

REFERENCES

Ahn, J. H., A. Rechtsteiner, S. Strome and W. G. Kelly, 2017 Correction: A Conserved Nuclear Cyclophilin Is Required for Both RNA Polymerase II Elongation and Co-transcriptional Splicing in Caenorhabditis elegans. PLoS Genet 13**:** e1006821.

Alleva, B., S. Clausen, E. Koury, A. Hefel and S. Smolikove, 2019 CRL4 regulates recombination and synaptonemal complex aggregation in the Caenorhabditis elegans germline. PLoS Genet 15**:** e1008486.

Alpi, A., P. Pasierbek, A. Gartner and J. Loidl, 2003 Genetic and cytological characterization of the recombination protein RAD-51 in Caenorhabditis elegans. Chromosoma 112**:** 6-16.

Bean, C. J., C. E. Schaner and W. G. Kelly, 2004 Meiotic pairing and imprinted X chromatin assembly in Caenorhabditis elegans. Nat Genet 36**:** 100-105.

Bessler, J. B., E. C. Andersen and A. M. Villeneuve, 2010 Differential localization and independent acquisition of the H3K9me2 and H3K9me3 chromatin modifications in the Caenorhabditis elegans adult germ line. PLoS Genet 6**:** e1000830.

Bhalla, N., and A. F. Dernburg, 2005 A conserved checkpoint monitors meiotic chromosome synapsis in Caenorhabditis elegans. Science 310**:** 1683-1686.

Bilgir, C., C. R. Dombecki, P. F. Chen, A. M. Villeneuve and K. Nabeshima, 2013 Assembly of the Synaptonemal Complex is a Highly Temperature-Sensitive Process that is Supported by PGL-1 during Caenorhabditis elegans Meiosis. G3 (Bethesda).

Bohr, T., G. Ashley, E. Eggleston, K. Firestone and N. Bhalla, 2016 Synaptonemal Complex Components Are Required for Meiotic Checkpoint Function in Caenorhabditis elegans. Genetics 204**:** 987-997.

Bohr, T., C. R. Nelson, E. Klee and N. Bhalla, 2015 Spindle assembly checkpoint proteins regulate and monitor meiotic synapsis in C. elegans. J Cell Biol 211**:** 233-242.

Brockway, H., N. Balukoff, M. Dean, B. Alleva and S. Smolikove, 2014 The CSN/COP9 signalosome regulates synaptonemal complex assembly during meiotic prophase I of Caenorhabditis elegans. PLoS Genet 10**:** e1004757.

Checchi, P. M., and J. Engebrecht, 2011 Caenorhabditis elegans histone methyltransferase MET-2 shields the male X chromosome from checkpoint machinery and mediates meiotic sex chromosome inactivation. PLoS Genet 7**:** e1002267.

Chmatal, L., S. I. Gabriel, G. P. Mitsainas, J. Martinez-Vargas, J. Ventura *et al.*, 2014 Centromere strength provides the cell biological basis for meiotic drive and karyotype evolution in mice. Curr Biol 24**:** 2295-2300.

Colaiacovo, M. P., A. J. MacQueen, E. Martinez-Perez, K. McDonald, A. Adamo *et al.*, 2003 Synaptonemal complex assembly in C. elegans is dispensable for loading strand-exchange proteins but critical for proper completion of recombination. Dev Cell 5**:** 463-474.

Couteau, F., K. Nabeshima, A. Villeneuve and M. Zetka, 2004 A component of C. elegans meiotic chromosome axes at the interface of homolog alignment, synapsis, nuclear reorganization, and recombination. Curr Biol 14**:** 585-592.

Couteau, F., and M. Zetka, 2005 HTP-1 coordinates synaptonemal complex assembly with homolog alignment during meiosis in C. elegans. Genes Dev 19**:** 2744-2756.

Dernburg, A. F., K. McDonald, G. Moulder, R. Barstead, M. Dresser *et al.*, 1998 Meiotic recombination in C. elegans initiates by a conserved mechanism and is dispensable for homologous chromosome synapsis. Cell 94**:** 387-398.

Deshong, A. J., A. L. Ye, P. Lamelza and N. Bhalla, 2014 A quality control mechanism coordinates meiotic prophase events to promote crossover assurance. PLoS Genet 10**:** e1004291.

Dombecki, C. R., A. C. Chiang, H. J. Kang, C. Bilgir, N. A. Stefanski *et al.*, 2011 The chromodomain protein MRG-1 facilitates SC-independent homologous pairing during meiosis in Caenorhabditis elegans. Dev Cell 21**:** 1092-1103.

Dorsett, M., and T. Schedl, 2009 A role for dynein in the inhibition of germ cell proliferative fate. Mol Cell Biol 29**:** 6128-6139.

Eaker, S., A. Pyle, J. Cobb and M. A. Handel, 2001 Evidence for meiotic spindle checkpoint from analysis of spermatocytes from Robertsonian-chromosome heterozygous mice. J Cell Sci 114**:** 2953-2965.

Ellenbecker, M., E. Osterli, X. Wang, N. J. Day, E. Baumgarten *et al.*, 2019 Dynein Light Chain DLC-1 Facilitates the Function of the Germline Cell Fate Regulator GLD-1 in Caenorhabditis elegans. Genetics 211**:** 665-681.

Essex, A., A. Dammermann, L. Lewellyn, K. Oegema and A. Desai, 2009 Systematic analysis in Caenorhabditis elegans reveals that the spindle checkpoint is composed of two largely independent branches. Mol Biol Cell 20**:** 1252-1267.

Fukuda, T., F. Pratto, J. C. Schimenti, J. M. Turner, R. D. Camerini-Otero *et al.*, 2012 Phosphorylation of chromosome core components may serve as axis marks for the status of chromosomal events during mammalian meiosis. PLoS Genet 8**:** e1002485.

Gao, J., C. Barroso, P. Zhang, H. M. Kim, S. Li *et al.*, 2016 N-terminal acetylation promotes synaptonemal complex assembly in C. elegans. Genes Dev 30**:** 2404-2416.

Gartner, A., S. Milstein, S. Ahmed, J. Hodgkin and M. O. Hengartner, 2000 A conserved checkpoint pathway mediates DNA damage--induced apoptosis and cell cycle arrest in C. elegans. Mol Cell 5**:** 435-443.

Gerstein, M. B., Z. J. Lu, E. L. Van Nostrand, C. Cheng, B. I. Arshinoff *et al.*, 2010 Integrative analysis of the Caenorhabditis elegans genome by the modENCODE project. Science 330**:** 1775-1787.

Goldstein, P., 2013 Multiple synaptonemal complexes (polycomplexes) in wild-type hermaphroditic Caenorhabditis elegans and their absence in males. Russian Journal of Nematology 21**:** 73-81.

Goodyer, W., S. Kaitna, F. Couteau, J. D. Ward, S. J. Boulton *et al.*, 2008 HTP-3 links DSB formation with homolog pairing and crossing over during C. elegans meiosis. Dev Cell 14**:** 263-274.

Gumienny, T. L., E. Lambie, E. Hartwieg, H. R. Horvitz and M. O. Hengartner, 1999 Genetic control of programmed cell death in the Caenorhabditis elegans hermaphrodite germline. Development 126**:** 1011-1022.

Guo, Y., B. Yang, Y. Li, X. Xu and E. M. Maine, 2015 Enrichment of H3K9me2 on Unsynapsed Chromatin in Caenorhabditis elegans Does Not Target de Novo Sites. G3 (Bethesda) 5**:** 1865-1878.

Gyuricza, M. R., K. B. Manheimer, V. Apte, B. Krishnan, E. F. Joyce *et al.*, 2016 Dynamic and Stable Cohesins Regulate Synaptonemal Complex Assembly and Chromosome Segregation. Curr Biol 26**:** 1688-1698.

Harper, N. C., R. Rillo, S. Jover-Gil, Z. J. Assaf, N. Bhalla *et al.*, 2011 Pairing centers recruit a Polo-like kinase to orchestrate meiotic chromosome dynamics in C. elegans. Dev Cell 21**:** 934-947.

Hodgkin, J., H. R. Horvitz and S. Brenner, 1979 Nondisjunction Mutants of the Nematode CAENORHABDITIS ELEGANS. Genetics 91**:** 67-94.

Hofmann, E. R., S. Milstein, S. J. Boulton, M. Ye, J. J. Hofmann *et al.*, 2002 Caenorhabditis elegans HUS-1 is a DNA damage checkpoint protein required for genome stability and EGL-1-mediated apoptosis. Curr Biol 12**:** 1908-1918.

Hurlock, M. E., I. Cavka, L. E. Kursel, J. Haversat, M. Wooten *et al.*, 2020 Identification of novel synaptonemal complex components in C. elegans. J Cell Biol 219.

Jaramillo-Lambert, A., M. Ellefson, A. M. Villeneuve and J. Engebrecht, 2007 Differential timing of S phases, X chromosome replication, and meiotic prophase in the C. elegans germ line. Dev Biol 308**:** 206-221.

Jaramillo-Lambert, A., and J. Engebrecht, 2010 A single unpaired and transcriptionally silenced X chromosome locally precludes checkpoint signaling in the Caenorhabditis elegans germ line. Genetics 184**:** 613-628.

Jaramillo-Lambert, A., Y. Harigaya, J. Vitt, A. Villeneuve and J. Engebrecht, 2010 Meiotic errors activate checkpoints that improve gamete quality without triggering apoptosis in male germ cells. Curr Biol 20**:** 2078-2089.

Kamath, R. S., A. G. Fraser, Y. Dong, G. Poulin, R. Durbin *et al.*, 2003 Systematic functional analysis of the Caenorhabditis elegans genome using RNAi. Nature 421**:** 231-237.

Kelly, W. G., C. E. Schaner, A. F. Dernburg, M. H. Lee, S. K. Kim *et al.*, 2002 X-chromosome silencing in the germline of C. elegans. Development 129**:** 479-492.

Khalil, A. M., F. Z. Boyar and D. J. Driscoll, 2004 Dynamic histone modifications mark sex chromosome inactivation and reactivation during mammalian spermatogenesis. Proc Natl Acad Sci U S A 101**:** 16583-16587.

Kim, Y., N. Kostow and A. F. Dernburg, 2015 The Chromosome Axis Mediates Feedback Control of CHK-2 to Ensure Crossover Formation in C. elegans. Dev Cell 35**:** 247-261.

Kim, Y., S. C. Rosenberg, C. L. Kugel, N. Kostow, O. Rog *et al.*, 2014 The chromosome axis controls meiotic events through a hierarchical assembly of HORMA domain proteins. Dev Cell 31**:** 487-502.

Kohler, S., M. Wojcik, K. Xu and A. F. Dernburg, 2017 Superresolution microscopy reveals the three-dimensional organization of meiotic chromosome axes in intact Caenorhabditis elegans tissue. Proc Natl Acad Sci U S A 114**:** E4734-E4743.

Kurahashi, H., H. Kogo, M. Tsutsumi, H. Inagaki and T. Ohye, 2012 Failure of homologous synapsis and sex-specific reproduction problems. Front Genet 3**:** 112.

Kyogoku, H., and T. S. Kitajima, 2017 Large Cytoplasm Is Linked to the Error-Prone Nature of Oocytes. Dev Cell 41**:** 287-298 e284.

Labella, S., A. Woglar, V. Jantsch and M. Zetka, 2011 Polo kinases establish links between meiotic chromosomes and cytoskeletal forces essential for homolog pairing. Dev Cell 21**:** 948-958.

Lamelza, P., and N. Bhalla, 2012 Histone methyltransferases MES-4 and MET-1 promote meiotic checkpoint activation in Caenorhabditis elegans. PLoS Genet 8**:** e1003089.

Lo, K. W., S. Naisbitt, J. S. Fan, M. Sheng and M. Zhang, 2001 The 8-kDa dynein light chain binds to its targets via a conserved (K/R)XTQT motif. J Biol Chem 276**:** 14059-14066.

Lui, D. Y., and M. P. Colaiacovo, 2013 Meiotic development in Caenorhabditis elegans. Adv Exp Med Biol 757**:** 133-170.

Luo, X., Z. Tang, J. Rizo and H. Yu, 2002 The Mad2 spindle checkpoint protein undergoes similar major conformational changes upon binding to either Mad1 or Cdc20. Mol Cell 9**:** 59-71.

Machovina, T. S., R. Mainpal, A. Daryabeigi, O. McGovern, D. Paouneskou *et al.*, 2016 A Surveillance System Ensures Crossover Formation in C. elegans. Curr Biol 26**:** 2873-2884.

MacQueen, A. J., M. P. Colaiacovo, K. McDonald and A. M. Villeneuve, 2002 Synapsis-dependent and -independent mechanisms stabilize homolog pairing during meiotic prophase in C. elegans. Genes Dev 16**:** 2428-2442.

MacQueen, A. J., C. M. Phillips, N. Bhalla, P. Weiser, A. M. Villeneuve *et al.*, 2005 Chromosome sites play dual roles to establish homologous synapsis during meiosis in C. elegans. Cell 123**:** 1037-1050.

MacQueen, A. J., and A. M. Villeneuve, 2001 Nuclear reorganization and homologous chromosome pairing during meiotic prophase require C. elegans chk-2. Genes Dev 15**:** 1674-1687.

Makokha, M., M. Hare, M. Li, T. Hays and E. Barbar, 2002 Interactions of cytoplasmic dynein light chains Tctex-1 and LC8 with the intermediate chain IC74. Biochemistry 41**:** 4302-4311.

Malone, C. J., L. Misner, N. Le Bot, M. C. Tsai, J. M. Campbell *et al.*, 2003 The C. elegans hook protein, ZYG-12, mediates the essential attachment between the centrosome and nucleus. Cell 115**:** 825-836.

Martinez-Perez, E., and A. M. Villeneuve, 2005 HTP-1-dependent constraints coordinate homolog pairing and synapsis and promote chiasma formation during C. elegans meiosis. Genes Dev 19**:** 2727-2743.

McKim, K. S., A. M. Howell and A. M. Rose, 1988 The effects of translocations on recombination frequency in Caenorhabditis elegans. Genetics 120**:** 987-1001.

Mei, F., P. F. Chen, C. R. Dombecki, I. Aljabban and K. Nabeshima, 2015 A Defective Meiotic Outcome of a Failure in Homologous Pairing and Synapsis Is Masked by Meiotic Quality Control. PLoS One 10**:** e0134871.

Minn, I. L., M. M. Rolls, W. Hanna-Rose and C. J. Malone, 2009 SUN-1 and ZYG-12, mediators of centrosome-nucleus attachment, are a functional SUN/KASH pair in Caenorhabditis elegans. Mol Biol Cell 20**:** 4586-4595.

Mlynarczyk-Evans, S., and A. M. Villeneuve, 2017 Time-Course Analysis of Early Meiotic Prophase Events Informs Mechanisms of Homolog Pairing and Synapsis in Caenorhabditis elegans. Genetics 207**:** 103-114.

Morelli, M. A., and P. E. Cohen, 2005 Not all germ cells are created equal: aspects of sexual dimorphism in mammalian meiosis. Reproduction 130**:** 761-781.

Morgan, T. H., 1914 No Crossing over in the Male of Drosophila of Genes in the Second and Third Pairs of Chromosomes. Biological Bulletin 26**:** 195-204.

Nadarajan, S., T. J. Lambert, E. Altendorfer, J. Gao, M. D. Blower *et al.*, 2017 Polo-like kinase-dependent phosphorylation of the synaptonemal complex protein SYP-4 regulates double-strand break formation through a negative feedback loop. Elife 6.

Nadarajan, S., F. Mohideen, Y. B. Tzur, N. Ferrandiz, O. Crawley *et al.*, 2016 The MAP kinase pathway coordinates crossover designation with disassembly of synaptonemal complex proteins during meiosis. Elife 5**:** e12039.

Nojima, H., 2006 Protein kinases that regulate chromosome stability and their downstream targets. Genome Dyn 1**:** 131-148.

Nyarko, A., M. Hare, T. S. Hays and E. Barbar, 2004 The intermediate chain of cytoplasmic dynein is partially disordered and gains structure upon binding to light-chain LC8. Biochemistry 43**:** 15595-15603.

Page, S. L., and R. S. Hawley, 2001 c(3)G encodes a Drosophila synaptonemal complex protein. Genes Dev 15**:** 3130-3143.

Pattabiraman, D., B. Roelens, A. Woglar and A. M. Villeneuve, 2017 Meiotic recombination modulates the structure and dynamics of the synaptonemal complex during C. elegans meiosis. PLoS Genet 13**:** e1006670.

Penkner, A., L. Tang, M. Novatchkova, M. Ladurner, A. Fridkin *et al.*, 2007 The nuclear envelope protein Matefin/SUN-1 is required for homologous pairing in C. elegans meiosis. Dev Cell 12**:** 873-885.

Penkner, A. M., A. Fridkin, J. Gloggnitzer, A. Baudrimont, T. Machacek *et al.*, 2009 Meiotic chromosome homology search involves modifications of the nuclear envelope protein Matefin/SUN-1. Cell 139**:** 920-933.

Phillips, C. M., and A. F. Dernburg, 2006 A family of zinc-finger proteins is required for chromosome-specific pairing and synapsis during meiosis in C. elegans. Dev Cell 11**:** 817-829.

Phillips, C. M., X. Meng, L. Zhang, J. H. Chretien, F. D. Urnov *et al.*, 2009 Identification of chromosome sequence motifs that mediate meiotic pairing and synapsis in C. elegans. Nat Cell Biol 11**:** 934-942.

Phillips, C. M., C. Wong, N. Bhalla, P. M. Carlton, P. Weiser *et al.*, 2005 HIM-8 binds to the X chromosome pairing center and mediates chromosome-specific meiotic synapsis. Cell 123**:** 1051-1063.

Rapali, P., A. Szenes, L. Radnai, A. Bakos, G. Pal *et al.*, 2011 DYNLL/LC8: a light chain subunit of the dynein motor complex and beyond. FEBS J 278**:** 2980-2996.

Reuben, M., and R. Lin, 2002 Germline X chromosomes exhibit contrasting patterns of histone H3 methylation in Caenorhabditis elegans. Dev Biol 245**:** 71-82.

Rodriguez-Crespo, I., B. Yelamos, F. Roncal, J. P. Albar, P. R. Ortiz de Montellano *et al.*, 2001 Identification of novel cellular proteins that bind to the LC8 dynein light chain using a pepscan technique. FEBS Lett 503**:** 135-141.

Rog, O., and A. F. Dernburg, 2015 Direct Visualization Reveals Kinetics of Meiotic Chromosome Synapsis. Cell Rep.

Rog, O., S. Kohler and A. F. Dernburg, 2017 The synaptonemal complex has liquid crystalline properties and spatially regulates meiotic recombination factors. Elife 6.

Sato, A., B. Isaac, C. M. Phillips, R. Rillo, P. M. Carlton *et al.*, 2009 Cytoskeletal forces span the nuclear envelope to coordinate meiotic chromosome pairing and synapsis. Cell 139**:** 907-919.

Sato-Carlton, A., C. Nakamura-Tabuchi, S. K. Chartrand, T. Uchino and P. M. Carlton, 2018 Phosphorylation of the synaptonemal complex protein SYP-1 promotes meiotic chromosome segregation. J Cell Biol 217**:** 555-570.

Schild-Prufert, K., T. T. Saito, S. Smolikov, Y. Gu, M. Hincapie *et al.*, 2011 Organization of the synaptonemal complex during meiosis in Caenorhabditis elegans. Genetics 189**:** 411-421.

Severson, A. F., L. Ling, V. van Zuylen and B. J. Meyer, 2009 The axial element protein HTP-3 promotes cohesin loading and meiotic axis assembly in C. elegans to implement the meiotic program of chromosome segregation. Genes Dev 23**:** 1763-1778.

Sironi, L., M. Mapelli, S. Knapp, A. De Antoni, K. T. Jeang *et al.*, 2002 Crystal structure of the tetrameric Mad1-Mad2 core complex: implications of a 'safety belt' binding mechanism for the spindle checkpoint. EMBO J 21**:** 2496-2506.

Smolikov, S., A. Eizinger, K. Schild-Prufert, A. Hurlburt, K. McDonald *et al.*, 2007 SYP-3 restricts synaptonemal complex assembly to bridge paired chromosome axes during meiosis in Caenorhabditis elegans. Genetics 176**:** 2015-2025.

Smolikov, S., K. Schild-Prufert and M. P. Colaiacovo, 2009 A yeast two-hybrid screen for SYP-3 interactors identifies SYP-4, a component required for synaptonemal complex assembly and chiasma formation in Caenorhabditis elegans meiosis. PLoS Genet 5**:** e1000669.

Takanami, T., S. Sato, T. Ishihara, I. Katsura, H. Takahashi *et al.*, 1998 Characterization of a Caenorhabditis elegans recA-like gene Ce-rdh-1 involved in meiotic recombination. DNA Res 5**:** 373-377.

Turner, J. M., 2007 Meiotic sex chromosome inactivation. Development 134**:** 1823-1831.

Turner, J. M., S. K. Mahadevaiah, P. J. Ellis, M. J. Mitchell and P. S. Burgoyne, 2006 Pachytene asynapsis drives meiotic sex chromosome inactivation and leads to substantial postmeiotic repression in spermatids. Dev Cell 10**:** 521-529.

Turner, J. M., S. K. Mahadevaiah, O. Fernandez-Capetillo, A. Nussenzweig, X. Xu *et al.*, 2005 Silencing of unsynapsed meiotic chromosomes in the mouse. Nat Genet 37**:** 41-47.

Volkmer, E., and L. M. Karnitz, 1999 Human homologs of Schizosaccharomyces pombe rad1, hus1, and rad9 form a DNA damage-responsive protein complex. J Biol Chem 274**:** 567-570.

Wagner, W., E. Fodor, A. Ginsburg and J. A. Hammer, 3rd, 2006 The binding of DYNLL2 to myosin Va requires alternatively spliced exon B and stabilizes a portion of the myosin's coiled-coil domain. Biochemistry 45**:** 11564-11577.

Wang, X., J. R. Olson, D. Rasoloson, M. Ellenbecker, J. Bailey *et al.*, 2016 Dynein light chain DLC-1 promotes localization and function of the PUF protein FBF-2 in germline progenitor cells. Development 143**:** 4643-4653.

Woglar, A., A. Daryabeigi, A. Adamo, C. Habacher, T. Machacek *et al.*, 2013 Matefin/SUN-1 phosphorylation is part of a surveillance mechanism to coordinate chromosome synapsis and recombination with meiotic progression and chromosome movement. PLoS Genet 9**:** e1003335.

Woglar, A., and V. Jantsch, 2014 Chromosome movement in meiosis I prophase of Caenorhabditis elegans. Chromosoma 123**:** 15-24.

Wynne, D. J., O. Rog, P. M. Carlton and A. F. Dernburg, 2012 Dynein-dependent processive chromosome motions promote homologous pairing in C. elegans meiosis. J Cell Biol 196**:** 47-64.

Yang, B., X. Xu, L. Russell, M. T. Sullenberger, J. L. Yanowitz *et al.*, 2019 A DNA repair protein and histone methyltransferase interact to promote genome stability in the Caenorhabditis elegans germ line. PLoS Genet 15**:** e1007992.

Zetka, M. C., I. Kawasaki, S. Strome and F. Muller, 1999 Synapsis and chiasma formation in Caenorhabditis elegans require HIM-3, a meiotic chromosome core component that functions in chromosome segregation. Genes Dev 13**:** 2258-2270.

Zhang, L., J. D. Ward, Z. Cheng and A. F. Dernburg, 2015 The auxin-inducible degradation (AID) system enables versatile conditional protein depletion in C. elegans. Development 142**:** 4374-4384.